1966

Fatigue behavior of simple span and continuous composite beams, December 1966 (68-11)

J. H. Daniels

LEHIGH UNIVERSITY INSTITUTE OF RESEARCH

Shear Connector Design for Highway Bridges

FATIGUE BEHAVIOR OF CONTINUOUS COMPOSITE BEAMS

by
J. Hartley Daniels
John W. Fisher

Fritz Engineering Laboratory Report No. 324.1

FATIGUE BEHAVIOR OF CONTINUOUS COMPOSITE BEAMS

by

J. Hartley Daniels

and

John W. Fisher

This work has been carried out as part of an investigation sponsored jointly by the New York Department of Public Works, the Department of Commerce - Bureau of Public Roads, Nelson Stud Division of Gregory Industries, Inc., KSM Products Division of Omark Industries Inc., Tru-Weld Division of Tru-Fit Screw Products Inc., and Lehigh University.

December 1966

Fritz Engineering Laboratory
Department of Civil Engineering
Lehigh University
Bethlehem, Pennsylvania

Fritz Engineering Laboratory Report No. 324.1

TABLE OF CONTENTS

ABSTRACT

The provisions of the current (1966) AASHO Bridge Design Specifications for composite steel-concrete bridge beams was based on static tests and allows the omission of shear connectors in the negative moment regions of continuous composite beams with continuous longitudinal slab reinforcement. A recent study, reported in Refs. 1 and 5 has evaluated the fatigue strength of shear connectors on the basis of modified pushout tests and has suggested a design criteria which would assume adequate static and fatigue strength of shear connectors in composite beams. This study also suggested that shear connectors were required in the negative moment regions of continuous composite beams with continuous longitudinal reinforcement.

To evaluate the stud design recommendations in Refs. 1 and 5, four 2-span, full size continuous beams were designed and tested under static and fatigue loading. The major variables considered were

(1) The effect of shear connectors in the negative moment regions, and (2) The effect of increased amounts of longitudinal reinforcement in the negative moment region.

The results of the fatigue tests are presented in this report. A subsequent report will present the static test results.

It is concluded that shear connectors are required in the negative moment regions of continuous composite beams with continuous longitudinal slab reinforcement. In addition, the study indicated an increased amount of longitudinal reinforcement is required in the negative moment region, over that currently allowed by the AASHO Specifications, to improve interaction and to control slab cracking.

The fatigue tests also brought out several additional variables which require further study. They are discussed at the end of this report.

1. INTRODUCTION

A recently developed procedure for the design of the shear connectors in composite steel and concrete bridge members, considers their performance under working loads and their ability to develop the flexural strength of the member.[1] The results of previous fatigue tests of composite beams[2,3,4] and a fatigue test program which involved several factorial experiments on stud and channel shear connectors,[5] were used to develop a design criteria which would assure adequate fatigue strength of the shear connection.

The analysis of the laboratory fatigue tests of pushout specimens reported in Ref.5, showed that minimum stress was only significant for the case of stress reversal and that a conservative estimate of the fatigue life could be made by considering only the range of shear. A comparison of the data with results of simple beam tests, indicated that the lower limit of the beam tests overlapped the upper limit of dispersion for the pushout tests. Because the pushout tests provided a lower bound of fatigue strength, it was satisfactory to consider the mean S-N curve for the design of stud shear connectors.[1,5] On this basis, a suitable design value can be obtained for any desired fatigue life.

For simple span beams, it was shown in Refs.1 and 5 that the

range of shear stress throughout the span varies from zero to a maximum value at the supports to near full reversal at midspan. At any section along the span, the full range of shear, that is, the difference between the maximum shears in both directions must be resisted by the connectors. The tests of simple beams reported in Refs.2 and 3, confirmed this design approach.

The design criteria proposed in Refs.1 and 5 also proposed that connectors be provided throughout the length of continuous beams. This was considered necessary because in negative moment regions with continuous reinforcement, tensile forces would exist that must be carried by connectors along the beam length.

Placing the shear connectors in the negative moment regions was suggested to assist in maintaining flexural conformance throughout a beam. This would also prevent the sudden transition from a composite to a non-composite section when they were omitted. Their placement was also suggested to minimize the large differentials in slip deformation that might otherwise occur which could lead to fatigue failure of connectors adjacent to the negative moment region. However, the behavior of continuous composite beams was not known as no fatigue tests had been conducted.

Current designs normally omit connectors in the negative moment regions of continuous composite beams. The current design procedure[6]

for shear connectors for composite steel and concrete beams, is based on the static properties of connectors.[7] The studies made in Ref.7 noted that in the negative moment regions only the slab reinforcement can act compositely with the steel beams. It was also concluded that because there was no significant difference in the distribution of strains and moments for composite beams with or without connectors in the negative moment region, that no special provisions were needed for the design of continuous composite beams. Hence, the specifications only noted that in the negative moment regions, the slab reinforcement may be considered as contributing to the moment resisting capacity of the section if connectors were used. If connectors were only provided in the positive moment regions, the steel beams must be designed to resist the full negative moment.

Since shear connector design was very conservative because of the static criteria used, no apparent difficulties were encountered. Fatigue tests of beams designed using the criteria suggested in Ref.7 had shown that an adequate fatigue strength was provided for simple beams and it was assumed to hold for continuous beams. Bridge engineers recognized that the design procedure was conservative. Because of this, the factor of safety was reduced in the currently used specification.[6] However, as noted in Ref.5, it is not possible to arbitrarly reduce the factor of safety because the fatigue behavior may become critical.

Because of the divergence in views, it was considered desirable to evaluate the performance of continuous composite beams which had shear connectors proportioned by the criteria suggested in Refs.1 and 5. Both the fatigue behavior and static behavior needed further consideration and evaluation to ascertain the applicability of the suggested design concepts to continuous composite beams.

To provide information on the fatigue and static strength of continuous composite beams with shear connectors throughout their length, comparative fatigue tests on four two-span continuous beams were conducted. Two of these specimens were identical except one had connectors in the negative moment region and the other had the connectors omitted as commonly done in current designs. Both of these specimens had the same amount of longitudinal slab reinforcement. The amount of reinforcement was made equal to the amount which would be placed in bridge decks of similar proportions. The two other continuous beam specimens had substantially more longitudinal reinforcement in their negative moment regions.

These tests were all intended to provide information on the behavior of continuous composite beams and to provide verification of the applicability of the design criteria proposed in Refs. 1 and 5. Only the results of the fatigue studies are discussed in this report. After the fatigue testing was completed, the continuous beams were all

tested statically to destruction. The results of these static ultimate load test will be the subject of a subsequent report.[14]

2. REVIEW OF PREVIOUS STUDIES ON CONTINUOUS BEAMS

A detailed review of fatigue studies on mechanical shear connectors, is given in Refs. 1, 2 and 3 and will not be repeated here. These tests were on bare studs, pushout specimens and simple span beams. Viest, Fountain and Siess[7] discussed the negative moment regions of continuous composite beams in some detail. This discussion was based on the static behavior of two composite model bridges that were reported by Siess and Viest.[8] These models differed in that one had shear connectors throughout the beam while the second had shear connectors in the positive moment regions only. From these studies, it was concluded that (1) in the negative moment regions, only the slab reinforcement can act compositely with the steel sections, (2) in beams with shear connectors throughout the beam, the slab reinforcement was fully effective; when connectors were omitted from the negative moment region the slab reinforcement was only partly effective, and (3) the action of both of these continuous composite bridges was about the same as the distributions of strains and also moments in both the negative and positive moment regions was nearly the same.

Based on these studies, it was concluded that the use of an elastic analysis in conjunction with the usual load distribution factors is justified, and no special provisions are needed for the design of continuous composite bridges.[7]

Slutter and Driscoll[9] summarized the behavior of a single continuous composite beam tested statically to its ultimate load. It was noted that the theoretical plastic collapse load was exceeded in the test even though the member had inadequate shear connection throughout its length. This test also indicated that on the basis of static tests alone, there was not a great deal of need for shear connectors in the negative moment region of continuous composite beams. It was concluded that although the feasibility of the plastic design of continuous composite members cannot be fully evaluated on the basis of one test, it appeared that members in which the negative plastic hinge forms first could be designed by plastic analysis. Beams forming positive plastic hinges first have not been tested. More recently, Barnard and Johnson[10] presented the results of a study on the plastic behavior of continuous composite beams. It was shown that simple plastic theory gave a good estimate of the flexural strength of the beams tested, provided that various types of secondary failure could be prevented by appropriate detailing.

These preliminary studies were followed up by further studies designed to provide more information on these secondary failures.[11] In particular, the effects of cracking and transverse bending of the slab and the behavior of the longitudinal reinforcement over the supports was examined. This study indicated that simple plastic theory can be

used for the design of continuous composite beams and that full use can be made of the tensile strength of longitudinal reinforcement in the slab.

All of these studies were to ascertain the static behavior of continuous composite beams. No information was available on the fatigue behavior of continuous composite beams.

3. DESCRIPTION OF TEST SPECIMENS

The four continuous beam test specimens were each 50'-10" long. Each of the beams had two equal spans of 25'-0" between bearings. Symmetrical concentrated loads were placed 10'-0" from the exterior support in each span. The four beams each consisted of a reinforced concrete slab 60-in wide and 6-in thick connected to a 21W62 steel beam by pairs of 3/4-in stud shear connectors 4-in high. The rolled beams were all supplied from the same heat of A36 steel. Details of the composite beams are shown in Figs. 1 and 2.

Design Criteria

The design of the composite beams was based on the moment of inertia method. The concrete slab was transformed to an equivalent area of steel. A modular ratio of 10 was assumed in the design. Since the designs of the four beams were based on the fatigue or static criteria suggested by Ref. 1, the flexural stresses were allowed to exceed the AASHO specified allowables when necessary. Table 1 summarizes the design stresses for the steel beams. A small spreading of shear connectors over the support of beam CC-2F was made however, so that the tensile stress in the beam flange adjacent to a stud shear connector did not exceed the specification value.[6]

The concrete slabs for all four beam specimens were designed

to be of the same width and thickness. The reinforcement for each beam was designed in accordance with the AASHO Bridge Specification.[6] The transverse reinforcing steel was designed assuming that a 5'-0" center-to-center spacing of beams was being used and loaded with an H20-S16 truck. The longitudinal distribution reinforcing steel was the same in the positive moment regions of all beams and in the negative moment regions of beams CC-1F and CC-2F. In these two beams it was made continuous for the entire beam length. The amount of longitudinal steel used for beams CC-1F and CC-2F was that specified by AASHO. It was taken as 0.67% of the required transverse reinforcement and was equal to 0.61% of the cross-sectional area of the concrete slab. The negative moment regions of beams CC-3S and CC-4S had substantially more longitudinal reinforcing steel. In CC-4S, the amount of longitudinal steel was increased until the ultimate plastic strength at the negative moment section was equal to the ultimate plastic strength of the positive moment regions based on handbook values. In the remaining beam CC-3S, the longitudinal reinforcement was proportioned so that the strength of the negative moment region was approximately midway between the other two cases. The reinforcing steel area is summarized in Fig. 2 and the relationship between negative moment capacity and the area of steel is summarized in Fig. 3. Curve (a) shows the relationship based on assumed section properties. This curve was used to proportion negative reinforcing steel in beams CC-3S and CC-4S. Curve (b) shows

the same relationship based on measured properties.

The shear connectors for all four beams were designed according to the criteria proposed in Ref. 1. For beams CC-1F and CC-2F, all connectors were proportioned to sustain 2,000,000 cycles of load. The two beams differed only in that connectors were not provided in the negative moment region of beam CC-1F. For beams CC-3S and CC-4S, the connectors were proportioned on the basis of the static strength requirements suggested in Ref. 1. As a result, during the fatigue loading, only a portion of the connectors were subjected to shear forces near the design level recommended for 500,000 cycles of loading. Table 1 summarizes the shear connector design and indicates the critical regions in beams CC-3S and CC-4S.

Design Details and Fabrication

The details of the steel beams are shown in Fig. 4. Each of the four beams was cut from nominal length 57ft rolled sections by a local fabricating shop. The excess pieces were marked and delivered to the laboratory after all shear connectors were installed to provide material for tension tests of the steel section and of the studs. Bearing plates were fitted and welded to the beams by the fabricating shop. The bearing plates at the center supports of CC-1F and CC-2F, were cut short to eliminate welds near the region of high tensile stresses. Web stiffners and additional short bearing plates in the region of the center

supports of beams CC-3S and CC-4S, were installed in the laboratory to stiffen that region and to prevent premature failure of the beams during the static ultimate load tests.

All 3/4-in studs were placed in pairs except for the studs in the negative moment region of beam CC-2F. Single studs were staggered throughout that region as shown in Fig. 4. Before the studs were welded to the test beams, the stud welding equipment was calibrated by welding several studs to the excess lengths that were cut off. The quality of the welds were verified using the welding and inspection procedure outlined in Ref. 12. Two different lots of 3/4-in x 4-in studs were installed. They were supplied by two manufacturers. Beams CC-1F and CC-4S had lot A studs, and beams CC-2F and CC-3S had lot B studs. This choice was randomly made.

The placement of reinforcing bars is shown in Figures 1 and 2. The section views shown on Fig. 2 are referenced on Fig. 1. The lapped No. 4 bars in CC-1F and CC-2F were welded to provide continuous longitudinal reinforcement throughout. No welding was done in beams CC-3S and CC-4S.

The transverse reinforcement in all beams was provided by No. 5 bars bent into rectangular hoops. In beams CC-1F and CC-2F, these bars were placed at 6-in centers throughout the beam. For beams CC-3S and CC-4S, a variable spacing was used as indicated in Fig. 1. Obser-

vation of the test results of beams CC-1F and CC-2F had indicated that it was not necessary to provide such a large amount of transverse reinforcing steel in most of the positive and negative moment regions. However, a closer spacing was used under load points and at the center support to provide for cross bending of the slab at these points.

To assist in moving these large test specimens in the laboratory, 1½-in pipe sleeves were cast into the slabs approximately 13ft on each side of the interior support. They penetrated the full depth of the slab and were located 10-in on each side of the centerline of the beam. The lifting points were selected so that the concrete tensile stresses were minimized during fabrication and erection.

Construction

Construction of the composite continuous T- beams began with the erection of a pair of structural steel beams on supports bolted to the dynamic test bed. The beams were spaced 5ft, 2-in apart and fastened to the supports by clamps.

Plywood forms for the slabs of the two T- beams were suspended from the beams. A two-inch timber spacer was used to separate the slabs of the two T- beams along their length. Figure 5 shows the formwork and reinforcement prior to casting the slabs of beams CC-3S and CC-4S.

The concrete for the slabs was provided by a transit-mixed concrete proportioned for a 28-day compressive strength of 3000 psi. Beams CC-1F and CC-2F were constructed first. The concrete placement for these two beams began at the exterior supports of each span and progressed simultaneously toward the interior supports. Placement was stopped 6ft on each side of the interior support for these two beams. The remaining 12ft was placed a week later to allow time for installation of strain gages on the reinforcement in that region. Beams CC-3S and CC-4S were constructed at a later date and the concrete placement began at one exterior support and progressed toward the other end as shown in Fig. 6. Consolidation was accomplished by internal vibration along the slab as placement progressed. The final finish was obtained by hand troweling. From 16 to 32 test cylinders were poured with each placement.

The concrete in the slabs of all beams was moist-cured for seven days with the exposed surface covered with wet burlap and a polyethylene sheet. The forms for each pair of test specimens were removed approximately 14 days after casting and the specimens were allowed to cure under dry conditions until at least 28 days had elapsed.

4. PROPERTIES OF TEST BEAMS

A detailed test program was conducted to determine the physical characteristics of the materials used in the T- beams. Also, the physical dimensions were obtained to help ascertain the section properties of the composite beams.

Rolled Steel Beams

The four rolled steel beams were made of structural carbon steel meeting the requirements of ASTM A36 - 63T. The beams were all nominally 57ft in length and furnished from the same heat. The mill report is given in Table 2.

Mechanical properties of the structural steel were determined from tests of tensile coupons cut from a 2ft piece of the beam that had been flame cut from the original 57ft length. The coupons were tested in tension at a speed of 0.025-in per minute up to the onset of strain hardening and then at a speed of 0.50-in per minute to fracture. In all tests, the yield point, static yield level and ultimate load were recorded. The modulus of elasticity and the strain hardening modulus were determined from a stress-strain curve which was plotted automatically during the test. The mean values and standard deviation of the yield point, static yield stress, and the ultimate strength are listed in Table 3. The modulus of elasticity and the strain hardening modulus are also given.

Reinforcing Bars

The mechanical properties of the No. 4, 6 and 7 deformed longitudinal reinforcing bars were determined by tension tests of 3ft lengths of reinforcement. In the case of beams CC-1F and CC-2F, the No. 4 test specimens were cut from a relatively unstressed portion of the slab following the beam tests. For beams CC-3S and CC-4S, extra lengths of No. 6 and 7 bars were supplied with the main reinforcement and were used for the tension tests. The deformed bars were of intermediate grade conforming to ASTM A15. The average yield points and ultimate strengths are given in Table 3.

Stud Shear Connectors

The stud shear connectors were made from a low carbon steel. They were supplied by two manufacturers. The properties of the studs were determined from tensile tests on full sized studs. These studs had been welded to a short length of the 21WF62 steel section after proper welds were obtained as noted earlier. A 4-in x 4-in square of the beam flange containing a stud was cut out and the unit tested in a special test jig. The average yield points and ultimate strengths are also summarized in Table 3.

Slab Concrete

The concrete placed in the slabs of all four beams was made of Type 1 portland cement, crushed gravel and natural bank sand. Two

mix designs were used - both for a 3000 psi design. The first mix was used for beams CC-1F and CC-2F. The second mix was used for beams CC-3S and CC-4S. Standard 6-in by 12-in cylinders were made during the casting of the slabs. These cylinders were tested at the age of 28 days and at the beginning of each fatigue test. The 28 day cylinders were all moist cured. The other cylinders were dry cured under approximately the same curing conditions as the slabs.

The compressive strengths, splitting strengths and moduli of elasticity are given in Table 4. It was because of the high concrete strength obtained from the first mix design that a second mix design was used for beams CC-3S and CC-4S to ensure a lower strength concrete.

Cross-Section Properties

Cross-section properties of the 21W62 rolled steel beams are given in Table 5. The properties are based on measured dimensions and are compared with standard handbook values.

The section properties of the composite sections in the positive moment regions were computed on the following assumptions:

(1) The effective width of the slab was taken as the full 5ft width, and

(2) the modulus of elasticity of the concrete

was equal to that determined from 28 day cylinder test results.

The section properties of the composite sections in the negative moment regions were computed based on the steel beam and the area of the longitudinal reinforcing steel. It was assumed that the concrete slab was cracked throughout its depth.

Table 6 gives the moments of inertia and the distance of the neutral axis from the bottom of the beam for each test specimen.

5. INSTRUMENTATION AND TESTING PROCEDURE

Instrumentation

The instrumentation for beams CC-1F and CC-2F was essentially the same. The instrumentation for beams CC-3S and CC-4S was also essentially the same but differed from beams CC-1F and CC-2F. Figures 7, 8 and 9 summarize the instrumentation used on the four test beams. A combination of electrical resistance strain gages, dial gages and level bars was used.

Figure 7 shows the location of the electrical resistance strain gages which were used to determine the flexural strains in the steel beams and in the concrete slabs. For beams CC-1F and CC-2F, these strain gages were placed on the underside of both the top and bottom flanges of the steel beam as well as on both sides of the web. They were located at 6 sections along the beam as shown in Fig. 7. Strain gages were also placed on the top surface of the concrete slab at sections 1 and 6 in the positive moment regions. These gages were used to ascertain the transverse distribution of the strain during the conduct of the fatigue test.

In addition, electrical resistance strain gages were also attached to the top surface of all the longitudinal No. 4 bars over the interior support. They were located on a line midway between

sections 3 and 4 as shown in Fig. 7. These gages were waterproofed and wrapped before the concrete was placed. The wrapping broke bond over a length of about 2-in. The lead wires were passed through the bottom of the wood form during construction.

For beams CC-3S and CC-4S electrical resistance strain gages were placed on the underside of the top and bottom flanges of the steel beam at sections 1, 3, 5 and 7. This is shown in Fig. 7. No strain gages were placed on the webs or concrete slabs of beams CC-3S and CC-4S. However, electrical resistance strain gages were attached to the top surface of some of the longitudinal reinforcement over the interior support of beams CC-3S and CC-4S. These gages were located at section 4 shown in Fig. 7. They were placed on 8-No. 6 bars in beam CC-3S and 12-No. 7 bars in beam CC-4S. The strain gages were evenly divided between top and bottom bars and were distributed across the slab width.

Mechanical strain gage points were placed at sections 2, 4 and 6 of beams CC-3S and CC-4S. Four 1/16" diameter holes spaced 8" apart were drilled in the top and bottom flange tips on both sides of the steel beam at each section, as shown in Fig. 7. This allowed four sets of strain measurements to be taken at each section, each set comprising three strain measurements. A mechanical strain gage with a gage length of 8" and an accuracy of 0.001-in was used. Gage points were used at these sections so that reliable strain

measurements could be made up to ultimate capacity of the beams during the static tests which followed the fatigue testing.

Electrical resistance strain gages were also placed on the underside of the top flanges near some of the stud connectors. These strain gages were used to help detect connector failure and their use and development is discussed in some detail in Refs. 2 and 3. Figure 8 summarizes the location of the stud shear connectors that had strain gages attached opposite them and shows the relative locations of the stud and the strain gage.

Figure 9 shows the locations of the dial gages that were used to measure slip and deflection. Dial gages (0.001-in) were placed under the beams at the load points to measure vertical deflection. These gage readings were used to adjust the maximum dynamic load level at the beginning and throughout the duration of each beam test. Dial gages (0.001-in) were also used to measure slip at each end of the four continuous beams and at various sections along the beam spans. For beam CC-1F, the dial gages shown in Fig. 9 between sections 2 and 5 were installed midway through the fatigue test when it became apparent that slip data in this region was desirable. All other slip gages on the four test beams were installed at the beginning of each beam test.

For beams CC-3S and CC-4S, a large compression dynamometer was used at the interior support to measure the center reaction. The dynamometer is shown in Fig. 10. This reaction was used together with the known loads to determine bending moments along the beam. A check was thus provided on the bending moments computed from the strain measurements on the steel beam.

A 40 power microscope was used to measure the width of cracks in the slab in the negative moment region of CC-3S. Crack widths during the other three beam tests were estimated. In addition, the crack patterns were photographed following each beam test.

Test Procedure

Each two span continuous beam was supported at three points resulting in two 25-ft spans. Load was applied to each span by hydraulic jacks located 10-ft from each exterior support. The load was distributed across the width of the concrete slab by a 4-ft loading beam. The test set up is shown schematically in Fig. 11.

The interior support of CC-1F and CC-2F consisted of a bearing plate free to rotate on a fixed support assembly. Longitudinal and lateral stability was thus provided at this point. For beams CC-3S and CC-4S the interior support was replaced by a bearing plate resting on the compression dynamometer shown in Fig. 10.

To ensure stability at this point, a fixed assembly of beams and plates was mounted on either side of the dynamometer. Grooved plates were fitted to the web stiffeners to maintain longitudinal stability and butt plates were fitted to the edges of the bottom flange of the 21WF62 to provide lateral stability. A small clearance was provided at all points between these plates and the test beam so that during testing the entire support was being provided by the compression dynamometer.

The bearing plate at the interior support of beams CC-1F and CC-2F was 9" long by 2" thick. A 6" by 2" bearing plate was used at the interior support of beams CC-3S and CC-4S. A small amount yielding was observed in beam CC-1F at the edges of the bearing plate due to a high stress concentration resulting from flexure over the bearing plate. To prevent this, lead shims from $\frac{1}{4}$" to $\frac{3}{8}$" thick were placed between the interior bearing plates and the beams on subsequent tests. During the fatigue tests, the lead deformed to a rounded surface thus providing even bearing of the beams.

The exterior supports of all continuous beams was provided by bearing plates mounted on high rocker plates. End braces were provided over each rocker support to provide lateral stability and to prevent excessive transverse vibration of the beams during the fatigue tests.

Since the bottom flanges of the continuous beams were not perpendicular to the plane of the web, steel and copper shims were placed over the exterior bearing plates when necessary. Additional shims were used to bring the three supports to the same elevation. From $\frac{1}{4}$" to $^3/4$" of shims were used at the exterior supports for this purpose.

Fatigue testing of beams CC-1F, CC-2F, CC-3S and CC-4S, was started 35, 71, 39 and 45 days respectively, after the concrete slabs were cast. Initially, each beam was loaded statically to the maximum load to be applied during the fatigue testing. The load was applied in increments of 10 kips up to a maximum of 60 kips at each load point for beams CC-1F, CC-2F and CC-3S, and to 70 kips for beam CC-4S. Readings were taken from all gages at each load increment. The maximum load to be applied during the fatigue tests was governed by the deflection obtained under the maximum static load. The maximum dynamic test load was determined such that the smallest deflection obtained under one of the load points was equal to the deflection of that load point at the maximum static load. The deflection of the other load point thus exceeded the static load deflection by small amounts. All beams were loaded at the rate of 250 cycles per minute. Frequent checks were made of the deflections during the initial stages of the test, and adjustments to the dynamic load were made. Since the bending stiffness of each span was changing because of bond failure

and other causes, the deflections gradually changed and eventually equalized early in the test. Frequent static tests from zero to maximum load were run so that adjustments in the dynamic load could be made.

The maximum dynamic load was always less than the maximum static load because of the dynamic effect. For beams CC-1F and CC-2F the dynamic load correction was usually from 1 to 2.5 kips at each load point. Just prior to installing the clamp in the east span of CC-1F, the dynamic load correction was approximately 6.5 kips. In all the beam tests the higher value was associated with the initial 10 to 20 percent of the total number of cycles applied to the beam, except for beam CC-1F where it was reached midway through the test.

The minimum dynamic load varied from 3.5 to 7.5 kips for beams CC-1F and CC-2F and from 2.0 to 4.0 kips for beams CC-3S and CC-4S. In this case the lower values tended to be associated with the initial stages of the test. The minimum load was the smallest that could be applied without separation of the beam and loading jack throughout the fatigue testing period. Hence the loading cycle was nearly zero to maximum throughout all the tests, based on static load levels.

The applied dynamic loading placed all connectors in beams CC-1F and CC-2F at the design shear level suggested in Ref. 1 for

2,000,000 cycles of load. Because beams CC-3S and CC-4S were designed on the basis of static strength considerations, only certain regions of these beams were loaded to the fatigue strength levels suggested in Ref. 1 for 500,000 cycles. For beam CC-3S only the studs in the negative moment region were at or slightly in excess of the suggested design level. For beam CC-4S only the connectors in the positive moment region were at or slightly above the suggested design level. (See Table 1)

Beam CC-1F had no connectors in the negative moment region and it was apparent that connectors were failing after 500,000 cycles. This was observed to be more serious in the east span so that the resulting loss of stiffness caused a large difference in the deflections of the two spans at approximately 1,100,000 cycles. If the test were to continue, some means of preventing the large differences in stiffness was necessary. Because of this observed behavior, a clamp was installed in the east span approximately at the inflection point so that greater frictional resistance could be developed between the slab and the steel beam. Figure 12 shows the clamp in place. The upper figure shows the steel plate on the top of the slab. The lower figure shows the lower steel plate attached to the steel beam. (Same detail on both sides). Two one-inch bolts

provided the clamping force. After approximately 300,000 cycles of additional load, the two spans had similar stiffness characteristics and the clamp was removed.

After completion of each fatigue test, all four continuous beams were then tested to their static ultimate strength. The results of this series of tests will be reported later.[14] After the static strength tests were completed, the concrete slab was removed from the steel beam near the exterior supports, throughout the negative moment region, and from the positive moment regions near the points of contraflexure. Photographs were made of the connector failures and cracked connectors at that time. Also each connector in these regions was bent 45% with a sledge to ascertain whether or not fatigue cracks were present. Several connectors fractured during this process. The visual inspection was used as a check and verification of the information obtained from the electrical resistance strain gages under the studs. If a connector was completely fractured or was removed during the bending check, the strain cycle curves were examined to ascertain its cycle life. If a connector did not fracture from the flange but a fatigue crack was present, its cycle life was taken as the total cycles applied to the specimen.

6. TEST RESULTS

The results of the fatigue study are summarized in this section. Each continuous composite beam except CC-1F, was subjected to at least the desired amount of cyclic loading. Beams CC-1F and CC-2F were designed for 2,000,000 cycles of load. Beams CC-3S and CC-4S were designed for 500,000 cycles of load. 1,907,000 cycles of load were applied to beam CC-1F and 2,079,000 cycles of load were applied to beam CC-2F. Beams CC-3S and CC-4S each had 500,000 cycles of load applied. The loads ranged from near zero to a maximum load as discussed in Section 4. It was observed during testing of beam CC-1F, that studs were failing in fatigue at about 500,000 cycles in the East span and that a continuous deterioration of studs in this span was occurring. To prevent complete failure of the beam in fatigue, a clamp was installed near the inflection point of the East span to delay the rate of failure of this span. This allowed additional cycles of load to be applied. However, the deterioration of the beam had progressed to the point where the fatigue test was stopped short of the desired number of cycles so that a static test of CC-1F to ultimate load could be safely carried out.

Deformation of the Continuous Beams

Deflection measurements under the load points, were obtained at intervals throughout the testing period. Figures 13 and 14 summarize the load-deflection characteristics of the East span of the four beams

tested. For beams CC-1F and CC-2F, the curves are plotted for the start of testing, for two intermediate cycle levels and at the end of testing. For beams CC-3S and CC-4S, the curves are also plotted for the start of testing, at one intermediate cycle level and at the end of testing. Also shown for comparative purposes, are the theoretical curves for the cases of complete interaction and no interaction. Two curves for the case of complete interaction are shown for beam CC-1F. The steeper curve assumes complete interaction throughout the beam (same as for beam CC-2F) and the other assumes complete interaction only in the regions containing studs.

The load-deflection curves for the West spans of the four continuous composite beams are similar to those shown in Figs. 13 and 14.

Load-rotation curves for the east end of each continuous beam are shown in Figs. 15 and 16. Also shown for comparative purposes are the theoretical curves for the cases of complete interaction and no interaction as previously explained. The load-rotation curves are also plotted for the same number of load applications as the load-deflection curves.

The measured load-rotation curves for the ends of the West spans of the four beams are similar to those shown in Figs. 15 and 16.

The use of lead shims at the interior supports of beams CC-2F, CC-3S and CC-4S and copper and steel shims at the exterior supports of all four beams, was discussed in Section 4. It was apparent after completion of the testing program that a small but varying amount of support settlement had occurred in all of the tests. The deflections of the supports were not measured in any of the tests. Some of the support settlement was inelastic and occurred during the initial zero to maximum static loading of each beam at the start of testing. For this reason the zero cycle curves in Figs. 13 to 16 are plotted so that the unloading curve obtained passes through the origin. Subsequent zero to maximum load-deflection and load-rotation curves obtained during the test program thus include only the effect of further inelastic support settlement due to squeezing of the lead at the interior support as fatigue testing continued.

Beam CC-1F had no lead shims at the interior support. Figure 13 shows that the increase in deflection of this beam with increasing cycles was relatively small. For beam CC-2F the Figure shows that the increase in deflection was larger because of the squeezing of the lead shims at the interior support. Because of the fewer cycles of load application to beams CC-3S and CC-4S, the increase in deflection is relatively small, as can be seen in Fig. 14.

Strain Measurements in the Continuous Beams

Strains measured with the electrical resistance strain gages and strains obtained from the mechanical strain gage points, were used to develop the distributions of strains throughout the depth of the continuous beams in both the positive and the negative moment regions. Typical strain distributions are shown in Fig. 17. This figure shows the strain distribution at section 1 (Refer to Fig. 7) of beams CC-1F and CC-2F for a static load of 60 kips. It can be seen that omitting connectors in the negative moment region of beam CC-1F apparently had little effect on the strains in the positive moment regions. A similar behavior was observed in Ref. 8. Figure 17 also shows the strain distribution at section 1 of beams CC-3S and CC-4S for a static load of 60 kips. These beams differed only in the amount of reinforcement and shear connection provided in the negative moment region. It is apparent from the figure that this difference had no significant effect on the strains in the positive moment regions.

Similar comparisons of strains are made in Fig. 18 for a typical section in the negative moment region of the four continuous beams. The comparison is again made for a static load of 60 kips. It is apparent from the figure that even though beam CC-1F had no shear connectors in the negative moment region, the slab and reinforcement had some effect on the strains in this region. Also the effect of the large amount of longitudinal reinforcement in beams CC-3S and CC-4S

can be observed by comparing the strain distribution for all four beams.

Figure 19(a) compares the location of the neutral axis as a function of cycle life for typical sections in the positive moment regions of beams CC-1F and CC-2F. Figure 19(b) makes a similar comparison for beams CC-3S and CC-4S. It can be observed that the number of applications of load had only a small effect on the flexural behavior in the positive moment regions of all four beams.

Figure 20 shows the location of the neutral axis as a function of the cycle life for typical sections in the negative moment regions. It is apparent from the figure that the slab had cracked in all four beams under the initial application of load and that additional applications of load had only a small effect on the stresses in the steel beams.

The measurements of strains on the top surface of the concrete slab at Sections 1 and 2 of beams CC-1F and CC-2F indicated that the full width was nearly effective. This can be seen from Fig. 21 where the strains are reasonably uniform across the width. The exception is at Section 1 of beam CC-1F where the strain at the edges of the slab tended to be somewhat below the strain over the steel beam as the number of load applications increased.

Strain Measurements Near Stud Connectors

As was noted earlier, electrical resistance strain gages were placed on the bottom of the upper beam flange directly adjacent to the stud shear connectors that were considered critical in each beam. Reference 3 provides considerable discussion on the use and interpretation of strain readings from these gages. Figure 8 summarized the location of the strain gage locations. Three areas were of interest: (1) over the exterior supports (2) in the positive moment region adjacent to the points of contraflexure and (3) in the negative moment regions.

Static tests were made at intervals during the progress of fatigue testing so that strain measurements could be made. The strains obtained at the maximum static load were plotted as a function of the applied cycles, and are shown in Figs. 22, 24, 25, 26 and 29.

Each figure shows schematically a portion of two steel beams below a strain versus cycle plot for certain studs on the steel beam. The studs are identified as follows:

(a) Open circles represent studs from which strain versus cycle data was obtained; studs which were examined visually following fatigue testing, or both.

(b) Closed circles represent studs for which the strain versus cycle curves are plotted immediately above.

(c) Circles with strokes through them represent studs which had failed during fatigue testing as evidenced by their separation from the steel beam either before or during the 45^{o} bending test described earlier.

(d) The circled numbers reference studs described above in (b), described elsewhere in the report and in Fig. 28.

Figure 22 illustrates the type of response observed over the exterior supports of beams CC-1F, CC-2F and CC-4S. All three beams indicated a similar behavior in this region. Connectors were observed to fail only in beams CC-3S and CC-4S. It is apparent from the figure that as fatigue loading was applied to the composite sections, the strains increased due to increasing flange distortion indicating that greater load was being carried by the connectors as bond was lost. The strains then leveled out after a few thousand cycles of load and remained reasonably uniform throughout the remaining portion of the test. The soundness of the connectors in beams CC-1F and CC-2F is illustrated in Fig. 23 where the photograph shows all to be sound even

after bending 45 degrees. It can be observed from Fig. 22 that connector failure in beams CC-3S and CC-4S was not apparent from the strain measurements near the studs. However after the slab was removed, the studs were easily removed from the beam during the bending test. This was expected in beam CC-4S since the studs in this region were subjected to a high range of shear stress in excess of the allowable stress range. (See Table 1) All studs in beam CC-4S were removed with one tap of a sledge hammer whereas the three failed studs in beam CC-3S were bent nearly 45^{o} before failure.

Figure 24 illustrates the type of response observed at the inflection point in the east span of all four beams. As was noted for the regions over the supports, an increase in strain was observed as the bond was broken and greater load was transferred to the connectors. In addition, the strains measured in beam CC-1F were nearly twice as great as the strains for beam CC-2F because no connectors were provided in the negative moment region of CC-1F and the force in the longitudinal reinforcing steel in that region was being carried by adjacent connectors in the positive moment region.

As the fatigue loading continued, the strains in beam CC-1F remained reasonably stable for at least 500,000 cycles. Thereafter, the strains began to decrease as a fatigue crack started to propagate through the base of the stud shear connector.[3] This decrease was

particularly severe in the East span of beam CC-1F and was nearly the same for all three sets of instrumented studs in this region, as can be seen from Figs. 24 and 26.

In beam CC-1F the failure of connectors near the point of contraflexure in the East span was rapid as observed in Fig. 24. After about 1,000,000 cycles, a clamp was installed in this region so that the shear was carried by friction as well. This increased the span stiffness and resulted in more uniform beam behavior. As a result, after 1,000,000 cycles the connectors in the West span started to fail at an accelerated rate as indicated in Fig. 25.

It can be observed from Figs. 24 and 25 that virtually all of the studs examined in the negative moment region and near the inflection points of beam CC-3S had failed. These studs were all removed easily during the bending test. This behavior was expected due to the higher than allowable stress range in the negative moment region. Evidently as studs in this region began to fracture, load was transferred to the studs near the inflection points accelerating their rate of failure.

The process of load transfer becomes even more apparent when similar studs in beam CC-4S are examined. The studs between the load points and the inflection points were considerably overstressed.

(See Table 1) Therefore a transfer of load to both of the exterior support regions and to the negative moment region would take place as studs began to fracture. Sufficient capacity existed in the negative moment region so that complete stud failure near the inflection points could be stopped. Since no excess capacity existed over the supports, load transfer probably accelerated the stud fracture that was observed in that region.

Figure 26 compares the behavior of the remaining two pairs of instrumented studs near the inflection points in both spans of beams CC-1F and CC-2F. It is apparent that all studs in beam CC-1F were subjected to about the same level of load and were failing at about the same rate. In comparison, all studs in beam CC-2F were subjected to a lower but nearly uniform level of load and no stud failures could be detected.

Photographs of the studs near the inflection points of beam CC-1F are shown in Fig. 27. The upper photo shows the East span. The inflection point passes through the two circular crates at the bottom of the photo which were left by the failure of studs 15 (left) and 16 (right). These studs remained in the portion of concrete slab which was removed. Studs 17 and 19 (left) and 18 and 20 (right) are shown beside their former positions after they were removed from the beam. These studs were easily removed by bending by hand. Since

these studs were observed to be nearly completely fractured from the beam after the slab was removed, it is probable that the high strain readings at the end of the test were caused by the dowelling of the failed stud in the rather deep crater that was taken from the beam flange. A similar view of the West span is shown in the lower photo. Beginning at the bottom of the photo the studs shown are numbers 9, 11, 13 (left) and 10, 12, 14 (right).

A typical view of the fracture surface of four studs is shown in Fig. 28. The fatigue fracture surfaces can easily be seen.

The response of studs in the negative moment region is illustrated in Fig. 29. A continuous increase in the apparent strain was noted for the first few hundred thousand cycles as the bond was broken and the slab cracking progressed. In beam CC-2F three of the 18 studs were observed to have fractured after the slab was removed and the studs bent 45 degrees. An examination of Fig. 29 shows that the fatigue cracking of studs on all beams occurred near the end of the applied cycles of loading and was not always easily apparent from the strain readings.

Slip Measurements

Slip measurements were taken at the exterior supports of each beam and at various locations in the negative moment region. These

measurements were not started in the negative moment region of beam CC-1F until about 1,000,000 cycles of loading.

Previous studies had indicated that the range of slip yielded some information on the fatigue failure of connectors.[3,5] Figure 30 is a bar graph indicating the range of slip and direction of the range of slip between 0 and 60 kips at various cycles of load application for beams CC-1F and CC-2F. It is apparent that after bond had broken in both beams the range of slip at the exterior supports changed very little. In the negative moment region of beam CC-1F, the range of slip was much greater than at the exterior supports and at least twice the range of slip observed in the negative moment region of beam CC-2F. The same is true also at the inflection points in both beams. This is in agreement with the observed levels of shear connector strain shown in Fig. 29. Since the range of slip readings were not taken at the inflection points of beam CC-1F until after obvious stud failures in that region, it is not known whether the large ranges of slip observed in beam CC-1F occurred after stud failure or was present from the beginning of the fatigue test.

The variation of total slip with applied cycles is shown in Fig. 31 for beam CC-2F. In general, the total slip increased as bond was destroyed. Large amounts of slip occurred in the negative moment region which was oppositely directed on either side of the center

support. This agrees with the observed cracking of the concrete slab which concentrated near the center support. (Discussed later in this report)

Cracking of Slabs in the Negative Moment Regions

All slabs were relatively free of cracks at the beginning of each test but cracked during the initial static loading of the beams. A few additional small cracks generally appeared during the fatigue tests, except in beam CC-1F where most of the cracking developed as fatigue testing progressed. The distribution of slab cracking is shown schematically in Fig. 32. Crack widths were measured on beam CC-3S, under a static load of 60 kips following the fatigue test, and are shown in Fig. 32 (c). The average crack width along a crack is shown in the Figure. Also the maximum width measured along a crack is shown in brackets. The average crack widths shown in Figs. 32(a) (b) and (c) were estimated, based on the known widths in beam CC-3S.

During the initial static loading of beam CC-1F to 60 kips relatively large cracks occurred about 8 and 18 inches on either side of the center support. Little or no cracking was observed elsewhere. This was expected since flexural conformance in this region due to bond would result in larger cracks near the center support. The cracks

were approximately perpendicular to the beam axis and were observed to increase in width as fatigue testing progressed. Additional smaller cracks also appeared throughout the rest of the negative moment region as fatigue testing progressed. Following the test it was observed that these cracks appeared at approximately 12 inch intervals near the inflection points to 6 inch intervals near the center support. Since the crack width did not vary appreciably through most of the negative moment region except over the support, this would indicate that the tensile force in the slab was reasonably uniform in this region. The appearance of many additional cracks during fatigue, would result from the decrease in flexural conformance in this region as bond was lost and as studs near the inflection points failed.

Beam CC-2F had connectors placed in the negative moment region except for a length of 22-in on either side of the interior support. The crack pattern was substantially different in this beam. Cracking was limited to a region of approximately 3'-0 either side of the support. The cracks in the regions with connectors were very small and remained small throughout the test. In the region without connectors, several large cracks formed with a predominant crack of large magnitude directly over the support.

As is apparent from Fig. 32, the crack widths in beams CC-3S

and CC-4S were substantially reduced with the increased area of longitudinal reinforcement. In beam CC-3S, cracks extended to 4 and 5 feet either side of the center support whereas in beam CC-4S, cracking was limited to a region only about 3 feet wide either side of the support.

Photographs of the crack patterns for beams CC-3S and CC-4S are shown in Fig. 33.

7. ANALYSIS OF TEST RESULTS

Stresses and Bending Moments in Continuous Composite Beams

The evaluation of the dead load stresses was based on computations using measured beam properties and dimensions and computed weights. Table 7 gives the computed dead load stresses at the top and bottom of the steel beam under the load points and at the center support.

Strains measured with electrical resistance strain gages were plotted in Figs. 17 and 18 for typical positive and negative moment cross-sections. Also shown for comparison are the computed strains based on measured section properties. The load level in all cases was 60 kips. It is evident that the presence or absence of connectors in the negative moment regions of beams CC-1F and CC-2F had little effect on the distribution of strains in the positive moment regions. Fairly good agreement also existed in all cases between computed and measured strains.

Figures 19 and 20 show that no significant shift in the neutral axis occurred with increasing applications of load. In addition they indicate that reasonably good agreement is obtained by assuming all beam sections, including the negative moment region of beam CC-1F, to have complete interaction. It is readily apparent

that the steel beam of CC-1F is interacting with the longitudinal reinforcement in the negative moment region. This is to be expected since considerable tensile force will be developed in the longitudinal steel due to rotation of the beam cross-sections at each inflection point. Since no shear transfer can take place between the slab and the beam after bond has been broken (except frictional forces), flexural conformance cannot exist in the negative moment region of beam CC-1F. It is shown later (see Fig. 37) that this was the case. It is also shown that a higher degree of flexural conformity was present in beam CC-2F but much less than the assumption of complete interaction would require.

Figures 34, 35 and 36 make a comparison of the theoretical and experimental bending moment distributions in the continuous beams. The theoretical bending moment curves are shown as dashed lines. The maximum values under the load points and over the center support have been shown in rectangular boxes. All values have been computed for a load of 60 kips, and are based on measured cross-section properties.

The experimental bending moment curves have been plotted as continuous lines. Maximum bending moments are shown corresponding to the beginning and end of the fatigue testing. The values of bending moment at the end of each fatigue test have been shown in parenthesis.

For beams CC-1F, CC-2F and CC-3S the change in bending moment distribution between the beginning and end of fatigue testing was relatively small. Because of this small difference only the distribution of moments at zero cycles has been plotted in Figs. 34 and 35. A larger difference occurred during the fatigue test of beam CC-4S, allowing both distributions of moment to be plotted in Fig. 36.

Figure 34 again confirms that beams CC-1F and CC-2F were both carrying load in a similar manner, even though no connectors were provided in the negative moment region of beam CC-1F. As discussed earlier, this behavior is a result of the considerable tensile forces induced in the longitudinal reinforcement throughout the negative moment region of beam CC-1F due to the curvatures in that region. Anchorage forces are in turn produced at the inflection points. Although similar static load behavior of the two beams is indicated in Fig. 34, the dynamic response of beam CC-1F was decidedly poorer than for beam CC-2F. It was difficult to maintain the maximum dynamic load during the test of beam CC-1F due to uneven deflection characteristics of each span, especially near 1,000,000 cycles of load application. This was undoubtedly due to the rapid deterioration of studs in the region of high anchorage stresses near each inflection point.

The distribution of bending moments in beams CC-3S and CC-4S were computed from the strain data obtained from gages on the steel beam as well as from the load cell which measured the center reaction. Figures 35(a) and 36(a) were plotted using strain data from the gaged sections while Figs. 35(b) and 36(b) were plotted using the load cell data. The excellent agreement between the two independent distributions of moment indicates that the moments shown in Fig. 34 will also be accurate.

A comparison of the theoretical and experimental bending moment curves for all four beams shows good agreement, in general, at zero cycles with a small loss of interaction at the end of the fatigue tests. The loss of interaction appeared to be the least in beams CC-1F and CC-2F and a maximum in beam CC-4S.

Slab Force in the Negative Moment Region

In composite beams, the degree of interaction is determined by the amount of slip between the concrete slab and the steel beam. Flexural conformance can be maintained only if sufficient shear connection is provided to reduce the slip to zero. Interaction and flexural conformance are of particular interest in the negative moment regions of continuous composite beams. To help evaluate the degree of interaction in beams CC-1F and CC-2F, the force in the slab at the inflection points and near the center support were

computed from the measured strains on the steel beams. Computations of the tensile force in the slab based on the strain data from the reinforcing steel over the support were considered unreliable because of the influence of slab cracking on these gages. Fig. 37 shows the computed slab forces at Sections 3 and 4 of beams CC-1F and CC-2F as a function of the applied cycles of load. Also shown for comparison is the theoretical slab force assuming (a) the slabs were uncracked and complete interaction; (b) the slabs were fully cracked and complete interaction; and (c) the slabs were cracked and there was no interaction, but the longitudinal reinforcement was carrying a tensile force computed from the average curvatures throughout the negative moment region. A similar comparison is made in Fig. 38 for the computed slab forces at the inflection points of beams CC-1F and CC-2F, Sections 2 and 5.

The force over the support of both beams showed a rapid decrease during the first 200,000 cycles of loading. This was likely due to the loss of interaction as bond was destroyed and the slab was cracked. In beam CC-1F, the initial slab force was about equal to the theoretical value for a cracked section with complete interaction. This rapidly decreased to a level slightly below the predicted force in the longitudinal reinforcement described above for no interaction. At the inflection points the slab force was virtually as predicted, at least up to the failure of connectors. Since frictional forces could account for the small difference near the support it is very apparent that without friction, the slab force would be uniform over the entire negative moment region.

The slab force in beam CC-2F maintained a level near the interior support which was greater than in beam CC-1F. Because of the presence of shear connectors, a higher initial slab force was observed until the slab was fully cracked. The slab force decreased in beam CC-2F in both spans at about the same rate. The force stabilized near the expected theoretical value for a cracked slab with complete interaction after about 200,000 cycles.

At the inflection points of beam CC-2F the slab force approached zero, which flexural conformance would require. It is obvious then that shear transfer is taking place between the slab in the negative moment region and the steel beam as a result of the stud shear connection. A similar behavior was observed in the negative moment regions of beams CC-3S and CC-4S. However the slab forces were substantially greater in these two beams because of the increased amounts of longitudinal reinforcing steel. The degree of interaction was also somewhat greater in these beams because of the greater number of shear connectors in the negative moment region.

The effect of stud failures near the inflection points of beam CC-1F on the slab forces can be observed in Figs. 37 and 38. Slab forces were rapidly changing at about 1,000,000 cycles. The clamp which was in place from 1,074,900 cycles to 1,375,500 cycles resulted in a readjustment of the slab forces so that they were again reasonably uniform.

It is apparent from the behavior of the test beams and a

comparison of Figs. 37 and 38 that shear connectors are required to resist the slab force in the negative moment region of all continuous composite beams with continuous longitudinal reinforcement. Stated in another manner, sufficient shear connection is required in the negative moment regions of continuous composite beams to reduce the slab force at the inflection points to zero. If connectors are not provided, the connectors in the positive moment regions, particularly those near the inflection points must carry this additional force, resulting in early fatigue failures of those connectors.

Forces on Stud Connectors

It was of interest to examine the forces to which the shear connectors were subjected during the progress of the tests. Of particular interest were those connectors at the ends of the beams, in the positive moment regions adjacent to the points of contraflexure and in the negative moment region.

As was observed in Fig. 37, bond failure between slab and beam took place in the negative moment region and the slab force necessarily had to be resisted by the connectors alone when they were present.

In the end portions of each beam, the bond failure was observed to start at the end of the member and progressed toward the

load points. In the positive moments adjacent to the points of contraflexure, bond failure progressed from the points of contraflexure toward the load points.

The average force per connector was taken as the compressive force in the slab at each strain gage location divided by the number of connectors between that location and the ends of the beam or the points of contraflexure, whichever was applicable.[1,5]

Table 8 summarizes the forces on the studs in the West spans of each beam at various cycles of load application. The forces in the East spans were similar. The applied load was 60^{k} for beams CC-1F, CC-2F and CC-3S, and 70^{k} for beam CC-4S. A comparison is made between the shear forces computed from strain data with the values of shear force computed according to elastic theory for horizontal shear. In general, the agreement could be considered good considering the assumptions made.

In beam CC-1F, no connectors were provided in the negative moment region to resist the slab force. Obviously, this force was resisted by the shear connectors in the positive moment regions adjacent to the points of contraflexure. Figures 24, 25 and 26 had indicated that the three pairs of studs adjacent to the points of contraflexure were carrying about the same load. Qualitative measure-

ments were not taken on other studs in these regions, so it was not known how many studs adjacent to the points of contraflexure actually resisted the slab force transmitted by the longitudinal slab steel in the negative moment region. If one assumes this force to be averaged over all the connectors between the load point and the point of contraflexure, the shear stress was from about 5.70 to 5.90 kips as shown in Table 8. If only half the connectors carried this load, they would be subjected to a shear of about 7 kips per stud.

Figure 39, compares the design cumulative resistance of the shear connectors in beams CC-1F and CC-2F with the force on the studs computed from the measured slab force at various locations along the beams. The comparison is made at 2,000,000 cycles at a load of 60 kips. It is apparent that connectors in beam CC-2F were subjected to forces that very closely correlated with their design resistance. The figure shows that in the negative moment region the tensile force in the slab was being adequately transferred into the beam by the shear connectors. At the points of contraflexure little slab force was present, confirming that the connectors in the negative moment region were effective. A similar behavior was observed in beams CC-3S and CC-4S.

In beam CC-1F, this was not the case. The slab force was approximately the same at the points of contraflexure as it was near the center support. This again confirms the previous discussion on the behavior of the reinforcing steel. It is apparent that the longitudinal slab steel is acting like tendons in an unbonded post-tensioned beam. Consequently, the studs near the points of contraflexure were subjected to shear forces considerably higher than those used in the designs. This contributed to the early failure of those shear connectors in beam CC-1F.

Fatigue Strength of Stud Shear Connectors

It is realized that the method of detecting connector failure is not exact but is believed to give conservative results. As was noted when discussing the test procedure, if a connector was found to be completely fractured after the slab was removed, or was knocked off the beam during the bending check, the strain data from the flange distortion gage under that connector was used to evaluate its cycle life.

Table 9 summarizes all test data to show the cycle life for the connectors in five regions of interest for each test beam. Also shown is the average stress on the connectors in a given region during the indicated cycle life. Failures were observed in all four test beams.

The test data summarized in Table 9 was compared with the S-N curve developed in Ref. 5. The comparison is shown in Fig. 40. Each point plotted represents the average stress versus observed cycle life for 6 to 24 studs. Where no failures were observed the points were plotted as runouts (arrow). As was noted in Refs. 1 and 5, push-out tests provide a lower bound of the fatigue strength. Since the S-N curve shown in Fig. 10 of Ref. 5 was based on the pushout tests, these beams test results were expected to exhibit slightly greater cycle lives. Most of the test results shown in Fig. 40 verify this behavior since they lie between the mean curve and the upper limit of dispersion. Except for one point, representing failures in the East interior positive moment region of beam CC-1F, each failure point lying below the mean curve in Fig. 40 represented failures detected by the bending test. No failures were apparent from the flange distortion gage readings for these studs. Thus, these points represent a conservative estimate of cycle life.

Comparison of Beam Performance

The four continuous composite beams in this study provide several direct comparisons of beam performance. For example, beams CC-1F and CC-2F differed only in that shear connectors were provided in the negative moment region of beam CC-2F. In all other respects, they were identical as their slabs were cast at the same time, the number of shear connectors and their spacing was the same in the posi-

tive moment regions, and the longitudinal reinforcement was the same throughout the beam length.

Beams CC-3S and CC-4S differed from beam CC-2F in that substantially more longitudinal reinforcement was placed in their negative moment regions. Also, the spacing of shear connectors in their positive and negative moment regions differed as they were designed using different criteria.

Hence there were two major variables to be evaluated: (1) the placement of connectors in the negative moment region and (2) effect of increasing the amount of longitudinal steel in the negative moment region.

The placement of connectors in the negative moment regions of beams CC-2F, CC-3S and CC-4S, provided better flexural conformance, better dynamic response of the beam, and more uniform beam behavior. In general, the performance of beam CC-1F was poor. Premature fatigue failures were observed near the points of contraflexure and the general response of the beam to cyclic loading was very poor. The two spans of this beam were observed to behave differently under dynamic load. Since the dynamic behavior of CC-2F was considerably improved, this was undoubtedly due to the presence of shear connectors in the negative moment region of beam CC-2F.

Also, the slab cracking of beams CC-1F and CC-2F differed. In beam CC-1F, the cracks were about equal width throughout the negative moment region confirming that the force in the longitudinal reinforcement was reasonably uniform throughout the negative moment region. Although beam CC-2F had connectors designed to transmit the force in the longitudinal reinforcement, they were not placed continuous throughout the negative moment region because only a few were required and also because it was desirable to shift them toward the points of contraflexure in order to prevent a fatigue failure in the beam flange over the center support. As a result, large cracks occurred in the length in which the connectors were omitted. As the slab force was transferred to the connectors, the crack width decreased somewhat as additional smaller cracks appeared closer to the inflection points. In both beams CC-1F and CC-2F, the maximum crack widths exceeded the limits suggested in Refs. 13 for cracks in reinforced concrete bridges at the service load level.

Beams CC-3S and CC-4S had substantially more longitudinal reinforcement in the negative moment region. This additional reinforcement greatly increased the flexural conformance of the composite beams. In addition, slab cracking behavior was greatly improved over beams CC-1F and CC-2F. There was not a great deal of difference in the behavior of beams CC-3S and CC-4S. This was true for dynamic re-

sponse of the beams, flexural conformance and crack width and distribution. Hence the larger increase in longitudinal reinforcement in beam CC-4S provided virtually no improvement in behavior over beam CC-3S.

Comparison of Test Results with Design Recommendations

Reference 1 had suggested that shear connectors were needed in the negative moment region to provide resistance to the range of shear to which they are subjected. Also, elastic theory assuming complete interaction was recommended to evaluate the horizontal shear resisted by the shear connection.

This study has confirmed these recommendations. It was shown clearly that shear connectors are required in the negative moment regions of continuous longitudinal reinforcement steel. When they were omitted, the response of the structure was poor and fatigue failure of connectors adjacent to the points of contraflexure was observed at a substantially lower number of cycles than that assumed in the design.

This study also confirmed that elastic theory could be used to evaluate the horizontal shear transferred by the shear connectors. Only the cracked section of the concrete slab was observed to be effective. The statical moment of the composite section need only consider

the longitudinal reinforcing steel in the slab. The slab was observed to crack under first application of the working load in all four beams. The maximum force developed by the slab rapidly decreased to the cracked section value as bond was destroyed.

Also, all longitudinal reinforcing steel in the slab cross-section was observed to be effective in these tests. It would appear then that all longitudinal reinforcement should be taken into account when ascertaining the magnitude of the slab force which must be resisted, at least up to the width to depth ratio used in this study.

In general, this study has confirmed the design recommendations given in Refs. 1 and 5.

Variables Requiring Further Study

This study has also indicated that additional work is needed on continuous composite beams. Attention should be directed to a detailed study of continuous beam behavior and to the development of a design procedure for continuous composite beams.

Areas requiring further analytical and experimental study are as follows:

(1) Spacing of shear connectors in the negative moment region. The purpose of this study is twofold. Because shear connectors de-

Make clear this is title, not a sentence

crease the fatigue strength of the tension flange of the beam, it is desirable to place the connectors in the regions closer to the inflection points as was done in beam CC-2F. It is necessary to evaluate to what degree this spreading is effective and how much is permissible. In addition to this, the number and spacing of shear connectors affects the width and distribution of slab cracks. An increased number of connectors over what is required will promote better flexural conformity. But this will induce larger cracks near the center support and smaller cracks near the inflection points. On the other hand the minimum number of connectors required will result in poorer flexural conformity but will induce a larger number of cracks with a smaller average crack width. Since the bending moments in the negative moment regions of beams CC-2F, CC-3S and CC-4S differed by only about 30% some indication of this behavior was obtained from this test program.

(2) Amount of longitudinal reinforcement in the negative moment region. A comparison of the four beams tested in this program showed clearly that beams CC-1F and CC-2F did not have adequate longitudinal reinforcement in the negative moment region to help limit crack width and improve flexural behavior. It was also evident that even though beam CC-4S had over twice as much reinforcement as CC-3S and nearly eight times that of beams CC-1F and CC-2F, its flexural behavior did not greatly differ from that of beam CC-3S. This test program has thus shown the ideal amount of negative reinforcement to lie somewhere

between the amounts provided in beams CC-2F and CC-3S. Spreading of connectors over the support will likely influence the choice of reinforcement and their interaction should be explored. The later distribution of the reinforcing steel needs further study to determine whether more should be concentrated over the steel beam. This would undoubtedly also affect the number and placement of connectors as well as slab cracking.

(3) Effective width in negative moment regions. Although it appeared that the full slab width was effective in each beam tested, further consideration should be given to the evaluation of the effective width of the negative moment region. Since the width to thickness ratio of the slabs used in these tests was only 10, it is not known what limits should be used.

(4) Other variables such as the influence of coverplates in the negative moment region and the use of prestressed longitudinal negative reinforcement should be studied.

8. SUMMARY

The results of fatigue tests of four continuous composite steel-concrete beams has been presented in this report. Each beam had two equal spans of 25 feet and consisted of a 60 inch wide by 6 inch reinforced concrete slab connected to a 21WF62 A36 steel beam with 3/4 inch diameter by 4 inch high headed steel stud shear connectors. Two beams were designed for 2,000,000 cycles of load application; two were designed for 500,000 cycles of load. A pulsating concentrated load was applied to each span by two Amsler jacks. The load varied from near zero to a maximum load which was approximately the service load for each beam. The loading rate was constant for all beams at 250 cycles of zero to maximum load per minute.

Two beams were designed according to the current AASHO Bridge Design Specifications except for the shear connection which was designed in accordance with the procedure recommended in Ref. 5. The shear connectors were left out of the negative moment region of one of the beams so that a comparison of the fatigue behavior of the two beams could be made.

The other two beams were also designed in accordance with the AASHO Specifications and the recommendations of Ref. 5. However, each beam had substantially greater amounts of longitudinal reinforcement in the negative moment region.

The basic variables investigated in this test program were then:

(1) The effect of stud shear connectors in the negative moment region on the fatigue behavior, and

(2) The effect of increased amounts of longitudinal reinforcing steel in the negative moment regions.

The following conclusions were drawn from an analysis of the test results:

(1) Shear connectors are required in the negative moment regions of continuous composite beams which have continuous longitudinal slab reinforcement. The amount of shear connection required depends upon the percentage of longitudinal reinforcing steel in that region but should not be less than the amount recommended in Ref. 5 . If connectors are omitted from the negative moment regions of continuous composite regions, the connectors in the adjacent positive moment regions are required to resist the tensile forces which will exist in the reinforcing steel in the negative moment region.

(2) Increased percentages of longitudinal reinforcement in the negative moment regions of continuous composite beams, over that presently allowed by the AASHO Specifications, appears desirable in order to control the number and widths of slab cracks as well as to improve interaction and flexural conformance in that region. It was evident

from the test results that this will also improve the deflection characteristics and overall structural behavior of the continuous composite beam.

(3) Further study is required to evaluate the effect of stud placement, coverplates and prestressing in the negative moment regions of continuous composite beams, as well as to determine the optimum reinforcement required and investigate crack control procedures. Following this additional study a design procedure should be developed for the design of continuous composite girders for fatigue loading.

9. ACKNOWLEDGMENTS

The study described in this report was part of an investigation on composite beams that was conducted at Fritz Engineering Laboratory, Department of Civil Engineering, Lehigh University. L. S. Beedle is Acting Chairman of the Department and Director of the Laboratory. The project was financed by the New York Department of Public Works, the Department of Commerce - Bureau of Public Roads, Nelson Stud Division of Gregory Industries, Inc., KSM Products Division of Omark Industries Inc., Tru-Weld Division of Tru-Fit Screw Products Inc., and Lehigh University.

The writers are particularly indebted to R. G. Slutter for his advice and help in the planning and conduct of these tests. Sincere thanks are also due Noriaki Yoshida and James O. Armacost III for assistance in the conduct of several of the tests and for aid in reducing and analyzing the test data; to Messrs. K. R. Harpel and C. F. Hittinger and their staff at the Fritz Laboratory for their work in preparing the test set-up and instrumentation; to R. N. Sopko and his staff for preparing, drawing and providing the photographic coverage; and to Mrs. D. Eversley for typing the manuscript.

10. TABLES AND FIGURES

TABLE 1

SUMMARY OF DESIGN STRESSES

TEST BEAM NO.	LOADS		FLEXURAL STRESS (DL + LL)								FATIGUE LIFE	STUD STRESS (LL)		
			AT LOAD POINTS				AT CENTER SUPPORT							
	LIVE LOAD	DEAD LOAD	W BTM	W TOP	REINF	CONC	W BTM	W TOP	REINF	CONC		EXT. POS MOM	INT. POS MOM	NEG MOM
	K	K/FT	KSI	KSI	KSI	KSI	KSI	KSI	KSI	KSI	10^6 CYC	KSI	KSI	KSI
CC-1F	60	0.44	+20.7	-3.3	-5.5	-0.8	-19.2	+19.2	0**	0	2.0	4.4	4.4	-
CC-2F	60	0.44	+20.1	-3.3	-5.4	-0.7	-18.8	+15.3 x	+17.2	0	2.0	4.4	4.4	4.4
CC-3S	60	0.44	+18.9	-2.9	-5.0	-0.6	-21.1	+11.7	+21.8	0	0.5	5.4	5.2	6.2*
CC-4S	70	0.44	+22.0	-3.4	-5.9	-0.8	-21.8	+ 7.8	+24.6	0	0.5	6.1*	6.4*	4.3

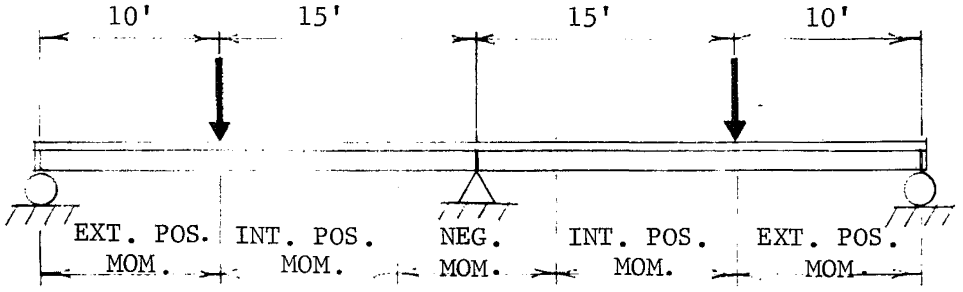

* ALLOW STRESS: 4.4 KSI (2 x 10^6 CYC.) OR 5.94 KSI (0.5 x 10^6 CYC.) REF. 1

** STRESS IN REINFORCEMENT WAS NEGLECTED.

x STRESS ADJACENT TO NEAREST STUD: 10.6 KSI

TABLE 2

MILL TEST REPORT FOR 21W62

Yield Point (KSI)	Tensile Strength (KSI)	Elongation 8-in. %	Chemical Analysis			
			C	Mn	P	S
41.9	67.2	30	0.19	0.70	0.010	0.029

TABLE 3

MATERIAL PROPERTIES OF STEEL

Type of Specimen	No. of Tests	Yield Point (KSI) **		Static Yield Stress (KSI)		Tensile Strength (KSI)	
		Mean	Std. Dev.	Mean	Std. Dev.	Mean	Std. Dev.
Web * (21W62)	12	37.3	2.24	35.0	2.19	62.1	2.26
Flange * (21W62)	12	36.4	0.81	34.3	0.85	61.6	0.87
No. 4 Bar	2	50.1	-	47.9	-	78.4	-
No. 6 Bar	2	45.1	-	43.0	-	75.2	-
No. 7 Bar	2	46.7	-	44.4	-	78.2	-
3/4-in. Studs "A"	5	54.9	-	-	-	70.4	1.86
3/4-in. Studs "B"	5	62.3	-	-	-	73.3	1.76

* Average Modulus of Elasticity $E = 30.1 \times 10^3$ (ksi)

Average Strain Hardening Modulus $E_c = 0.685 \times 10^3$ (ksi)

** Yield Point applies to 21W62 only. Other values refer to yield strength at 2% offset.

TABLE 4

RESULTS OF CONCRETE CYLINDER TESTS

Beam	Location	MOIST CURED							DRY CURED			
		No Of Tests	Age (Days)	Splitting Tensile Strength T(psi)		Compressive Strength f'_c (psi)		Modulus Of Elasticity E_c ($x10^6$ksi)	No. Of Tests	Age (Days)	Compressive Strength f'_c(psi)	
				Mean	Std. Dev	Mean	Std. Dev				Mean	Std.Dev.
CC-1F And CC-2F	Positive Moment	4	28	550	28.1	5164	462.7	3.85	12	35 to 84	5602	319.9
CC-1F And CC-2F	Negative Moment	6	28	564	68.0	5247	213.2	3.85	9	37 to 78	5611	98.8
CC-3S And CC-4S	Pos. & Neg. Moment	7	28	432	2.55	3581	116.0	3.57	9	93	3964	131.1

TABLE 5

PROPERTIES OF 21W62 BEAMS

BEAM	AREA*	DEPTH	FLANGE		WEB THICKNESS	MOMENT OF INERTIA*
			WIDTH	THICKNESS		
	in^2	in	in	in	in	in^4
CC-1F	18.848	21.092	8.360	0.604	0.440	1348
CC-2F	18.348	20.984	8.301	0.581	0.439	1287
CC-3S	17.705	21.031	8.312	0.564	0.435	1271
CC-4S	17.700	21.063	8.312	0.570	0.430	1281
21W62**	18.23	20.99	8.250	0.625	0.400	1327

* BASED ON RECTANGULAR ELEMENTS - FILLETS NEGLECTED

** FROM AISC MANUAL OF STEEL CONSTRUCTION

TABLE 6

PROPERTIES OF COMPOSITE BEAMS

BEAM	POS. MOMENT REGIONS		NEG. MOMENT REGIONS	
	Moment of Inertia	Position of Neutral Axis From Bottom	Moment of Inertia	Position of Neutral Axis From Bottom
	in^4	in	in^4	in
CC-1F	3661	19.35	1348	10.50
CC-2F	3600	19.35	1662	11.90
CC-3S	3584	19.45	2198	14.25
CC-4S	3594	19.45	2851	16.90

TABLE 7

DEAD LOAD STRESSES IN W BEAM

TEST BEAM No.	DEAD LOAD	FLEXURAL STRESS (D.L.)			
		AT LOAD POINTS		AT CENTER SUPPORT	
		W BTM	W TOP	W BTM	W TOP
	K/FT	KSI	KSI	KSI	KSI
CC-1F	0.44	+1.77	-1.77	-3.20	+3.20
CC-2F	0.44	+1.86	-1.86	-3.35	+3.35
CC-3S	0.44	+1.88	-1.88	-3.49	+3.49
CC-4S	0.44	+1.86	-1.86	-3.33	+3.33

TABLE 8

TYPICAL FORCES ON STUD SHEAR CONNECTORS

LOCATION	CC-1F			CC-2F			CC-3S			CC-4S		
	Cycles	Test	Theor.	Cycles	Test	Theor.	Cycles	Test	Theor.	Cycles	Test	Theor.
	x 10^6	Kips	Kips	x 10^6	Kips	Kips	x 10^6	Kips	Kips	x 10^6	kips	Kips
END OF BEAM - POSITIVE MOMENT	0	4.50	4.40	0	4.47	4.40	0	5.44	5.40	0	6.08	6.10
	0.539	4.44	4.40	0.597	4.61	4.40	0.310	5.00	5.40	0.348	5.80	6.10
	1.075	4.47	4.40	0.979	4.49	4.40	0.500	4.84	5.40	0.500	5.90	6.10
	1.376	4.51	4.40	1.335	4.51	4.40						
	1.907	4.44	4.40	2.079	4.55	4.40						
INTERIOR POSITIVE MOMENT	0	5.82	5.40*	0	5.27	4.40	0	5.85	5.20	0	7.08	6.40
	0.539	5.70	5.40	0.597	5.32	4.40	0.310	5.38	5.20	0.348	6.75	6.40
	1.075	5.94	5.40	0.979	5.20	4.40	0.500	5.19	5.20	0.500	6.86	6.40
	1.376	5.72	5.40	1.335	5.20	4.40						
	1.907	5.68	5.40	2.079	5.57	4.40						
NEGATIVE MOMENT				0.	5.11	4.40	0	6.67	6.20	0	3.46	4.30
				0.597	3.32	4.40	0.310	4.96	6.20	0.348	3.95	4.30
				0.979	3.19	4.40	0.500	5.44	6.20	0.500	3.20	4.30
				1.335	3.10	4.40						
				2.079	2.12	4.40						

* Force from longitudinal reinforcement in negative moment region included and distributed over all studs in the interior positive moment region.

TABLE 9

SUMMARY OF CONNECTOR CYCLE LIVES

LOCATION	CC-1F			CC-2F			CC-3S			CC-4S		
	Cycle Life	Stress Range	Fail Ratio*	Cycle Life	Stress Range	Fail Ratio*	Cycle Life	Stress Range	Fail Ratio	Cycle Life	Stress Range	Fail Ratio*
	x 10^6	ksi		x 10^6	ksi		x 10^6	ksi		x 10^6	ksi	
W. END POS. MOM.	2.00+	10.15	0	2.00+	10.30	0	0.50	11.65	0.38	0.50	13.40	1.00
E. END POS. MOM.	2.00+	10.75	0	2.00+	10.00	0	-	11.40	-	0.50	13.50	-
W. INTERIOR POS. MOM.	1.00	13.01**	1.00	2.00	11.80	0.17	0.50	13.00	1.00	0.50+	15.50	0
E. INTERIOR POS. MOM.	0.50	12.72**	1.00	2.00+	10.90	0	0.50	12.70	1.00	0.50+	14.75	0
NEGATIVE MOMENT	-	-	-	2.00	9.60	0.17	0.50	12.80	0.83	0.50+	8.00	0

* Ratio of number of studs failed to number of studs examined.

** The force in the negative reinforcement was distributed over all the studs in the interior positive moment regions. Distribution of force over ½ the studs would increase the stress ranges to 15.33 and 14.70 ksi respectively for the W. and E. interior positive moment regions.

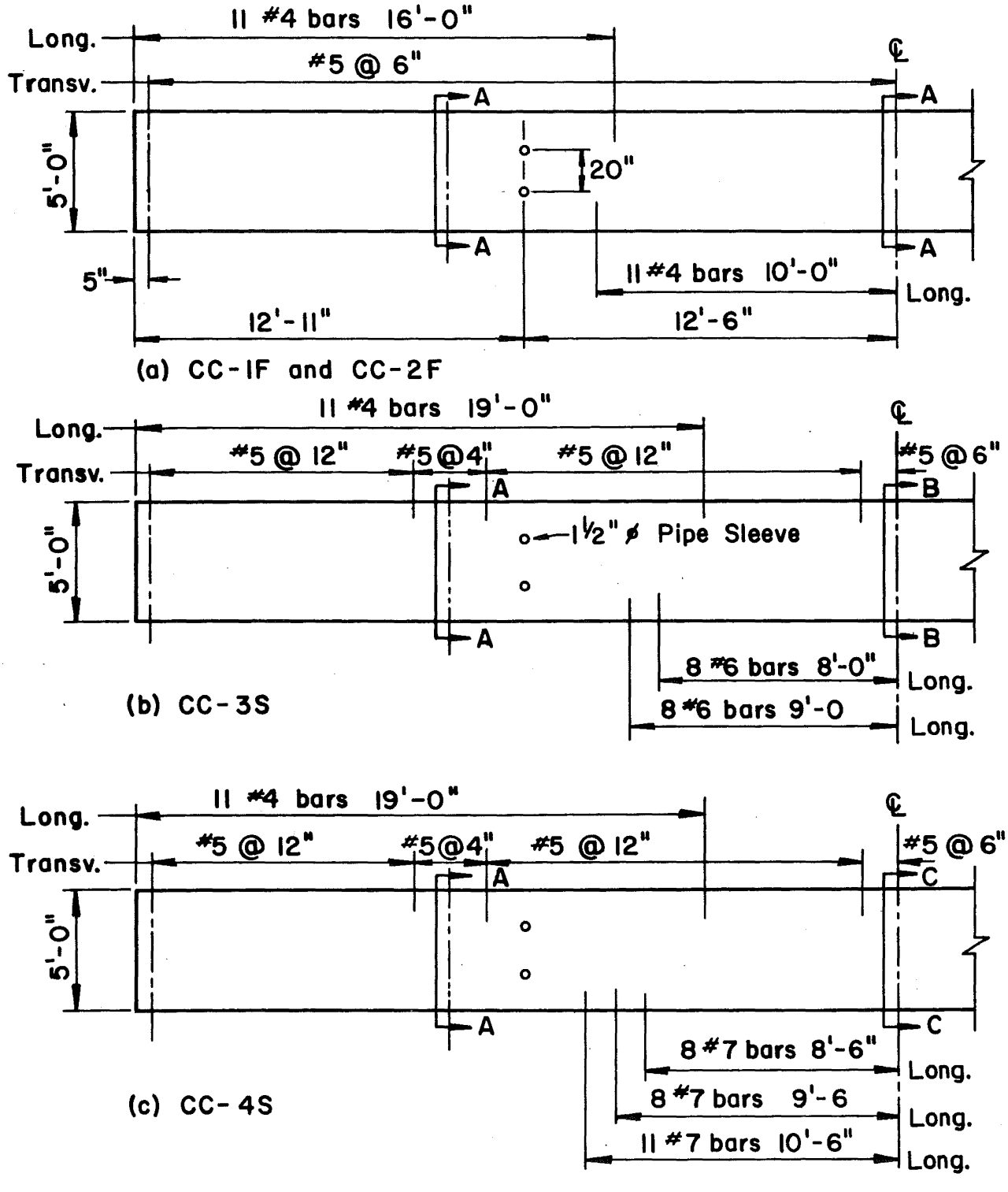

Sections A, B and C are Shown on Fig. 2

Fig. 1 Details of Composite Beams

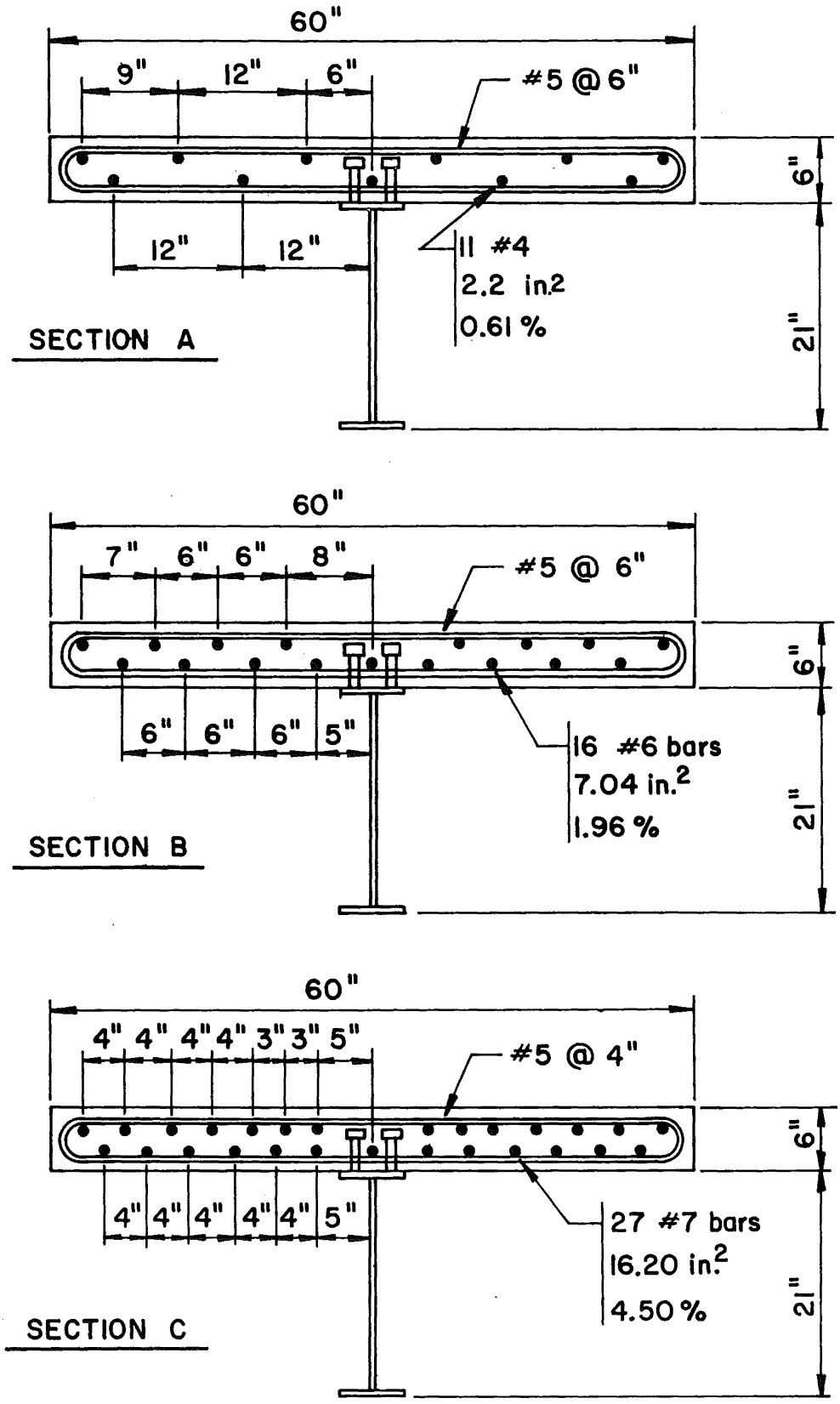

Fig. 2 Typical Beam Cross-Section

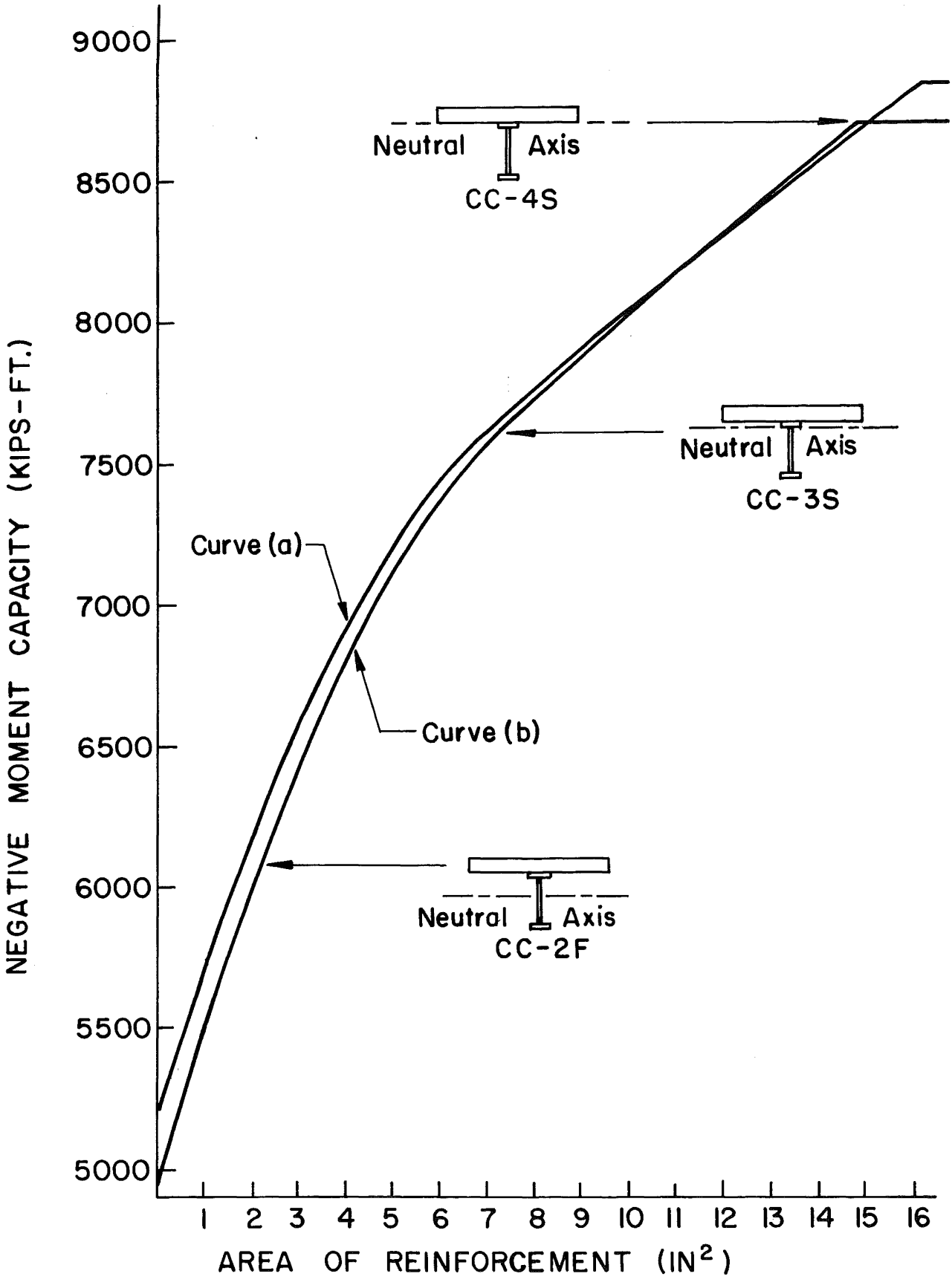

Fig. 3 Negative Moment Capacity vs. Area of Negative Reinforcement

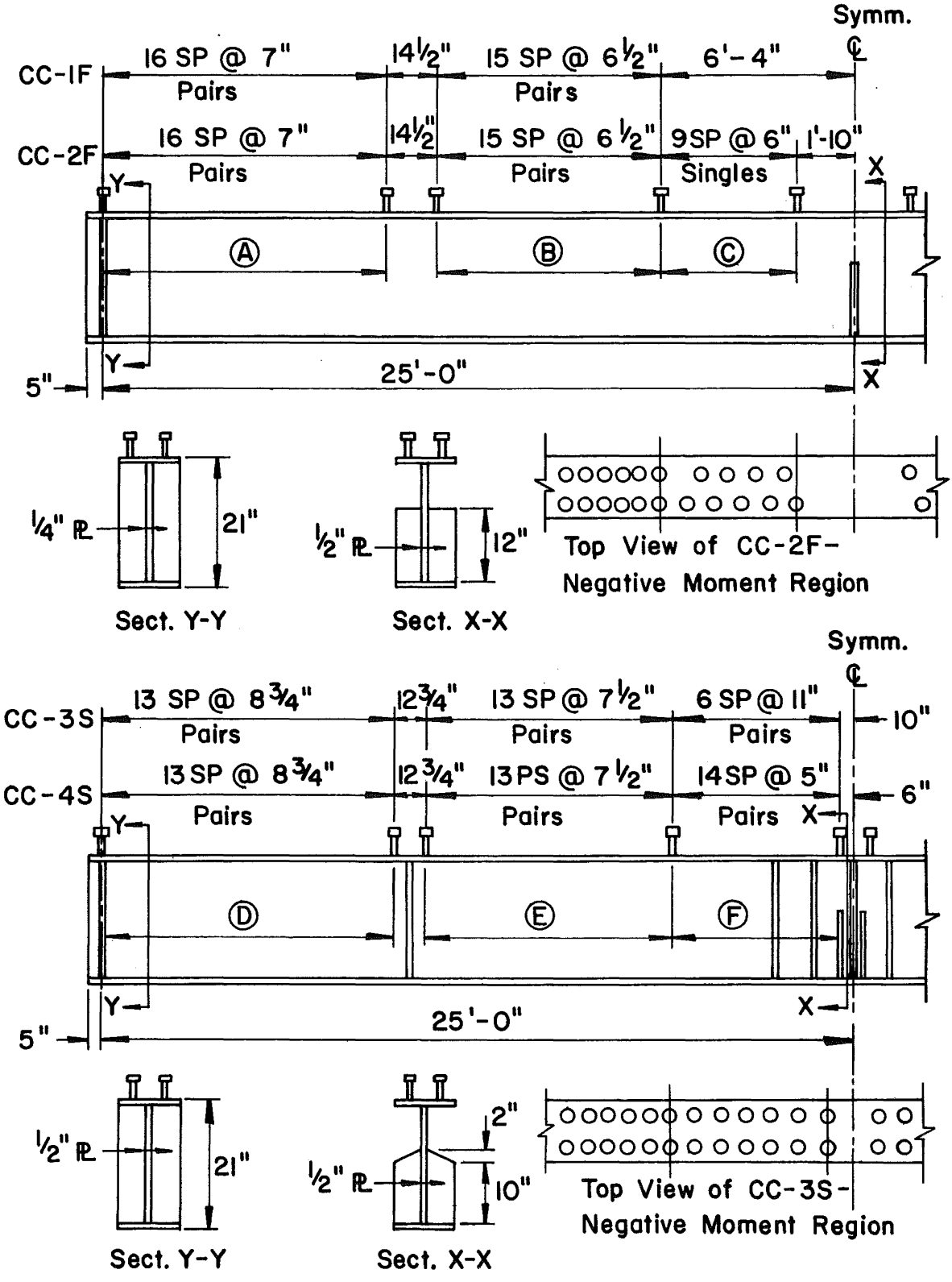

Fig. 4 Details of the Steel Beams

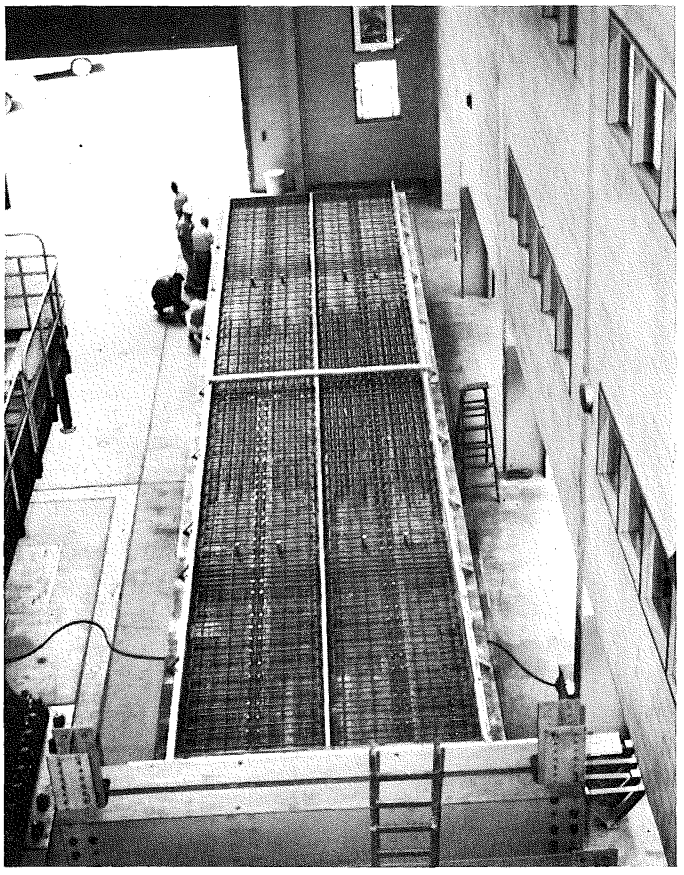

Fig. 5 Construction of Composite Beams

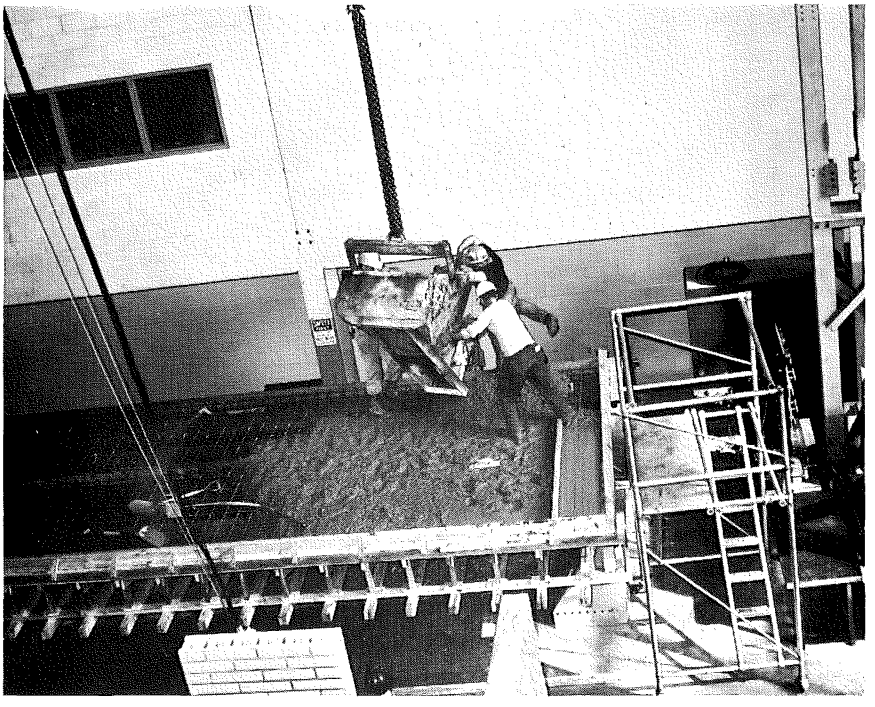

Fig. 6 Casting Concrete Slabs

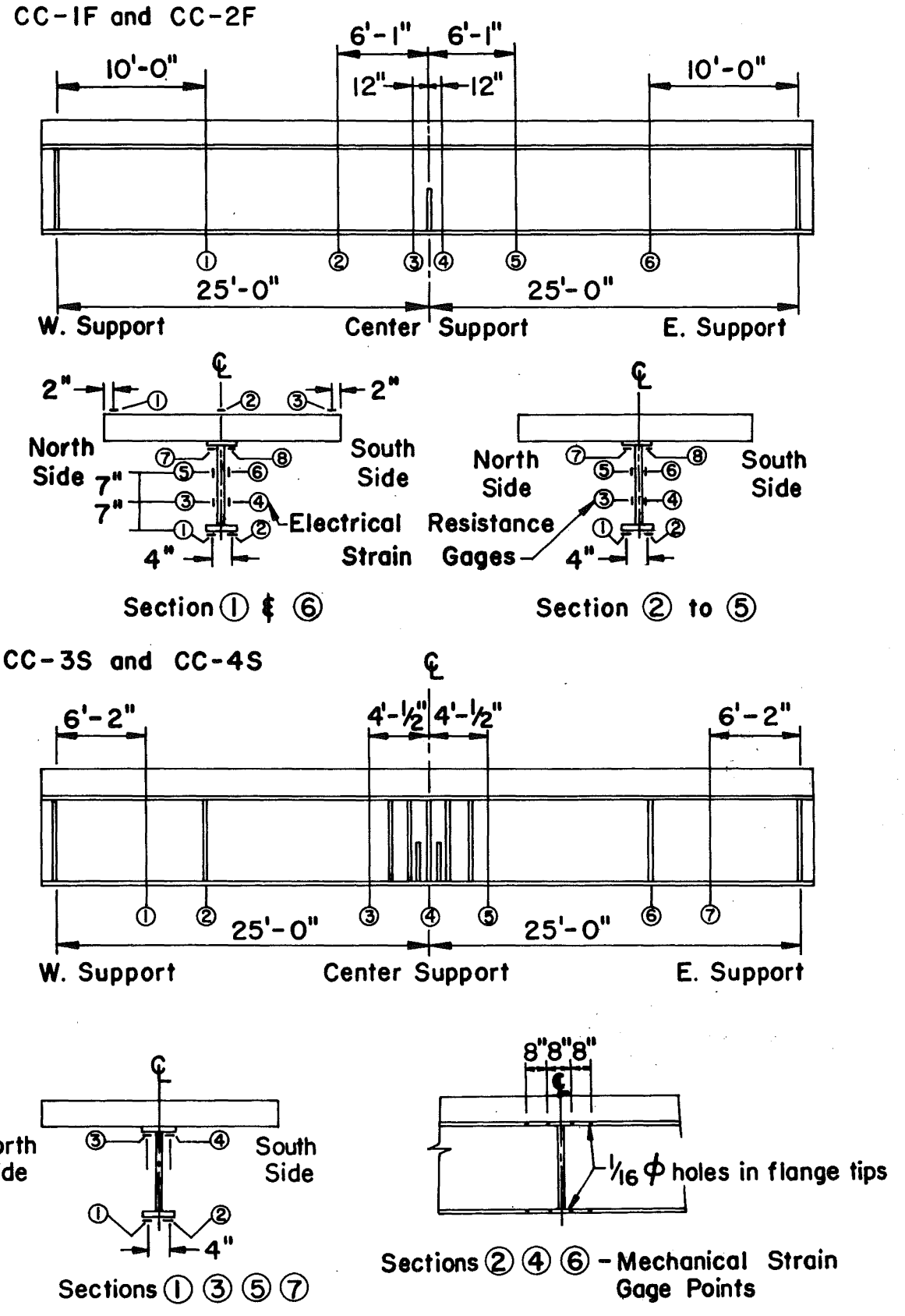

Fig. 7 Strain Gage Locations on 21W62 and Concrete Slab

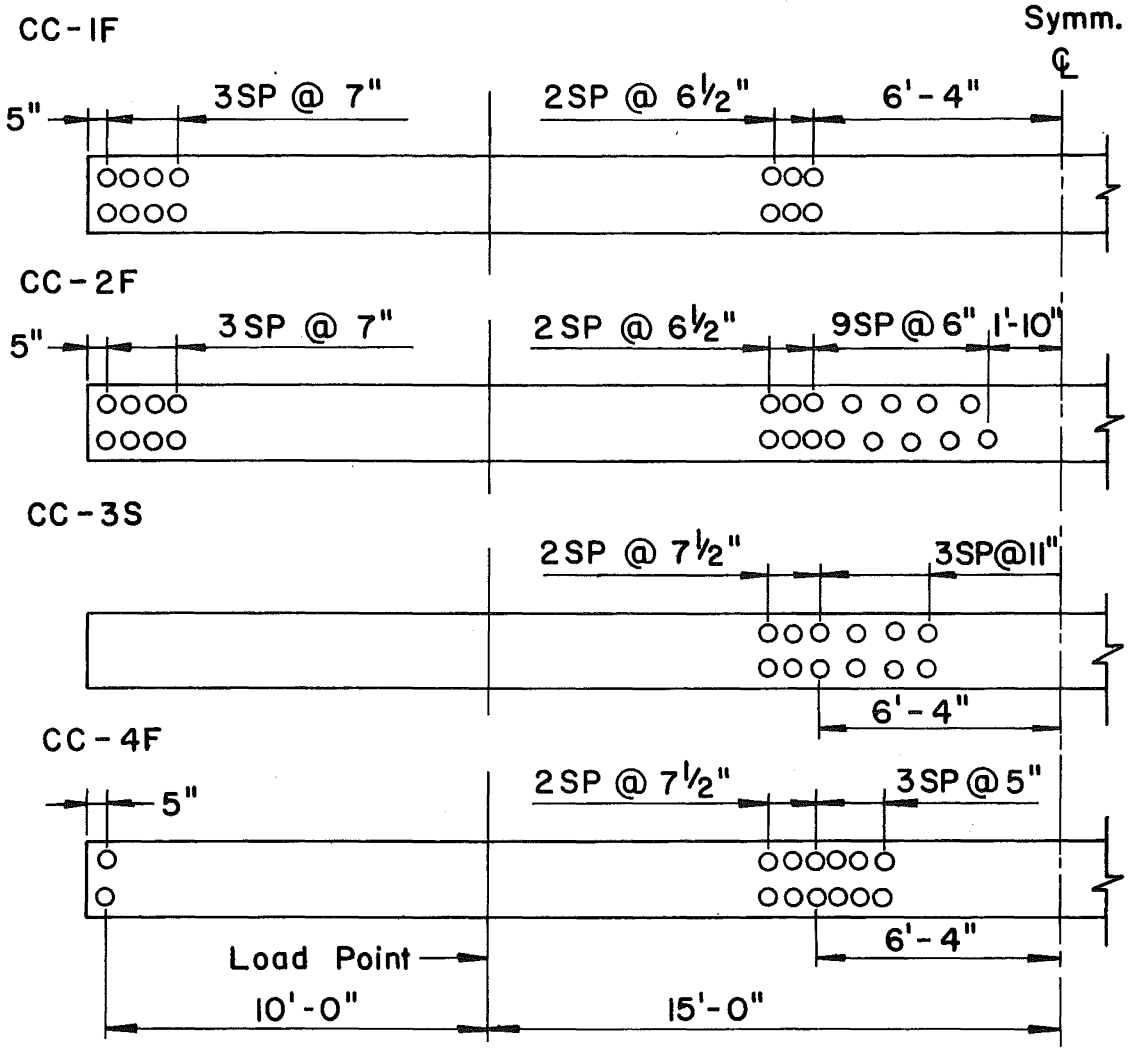

(a) Location of Gaged Studs

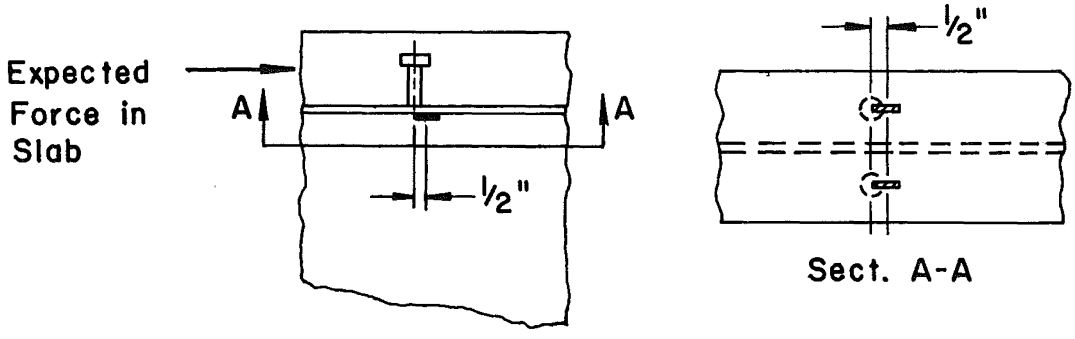

(b) Relative Position of Stud and Gage

Fig. 8 Location of Strain Gages under Studs

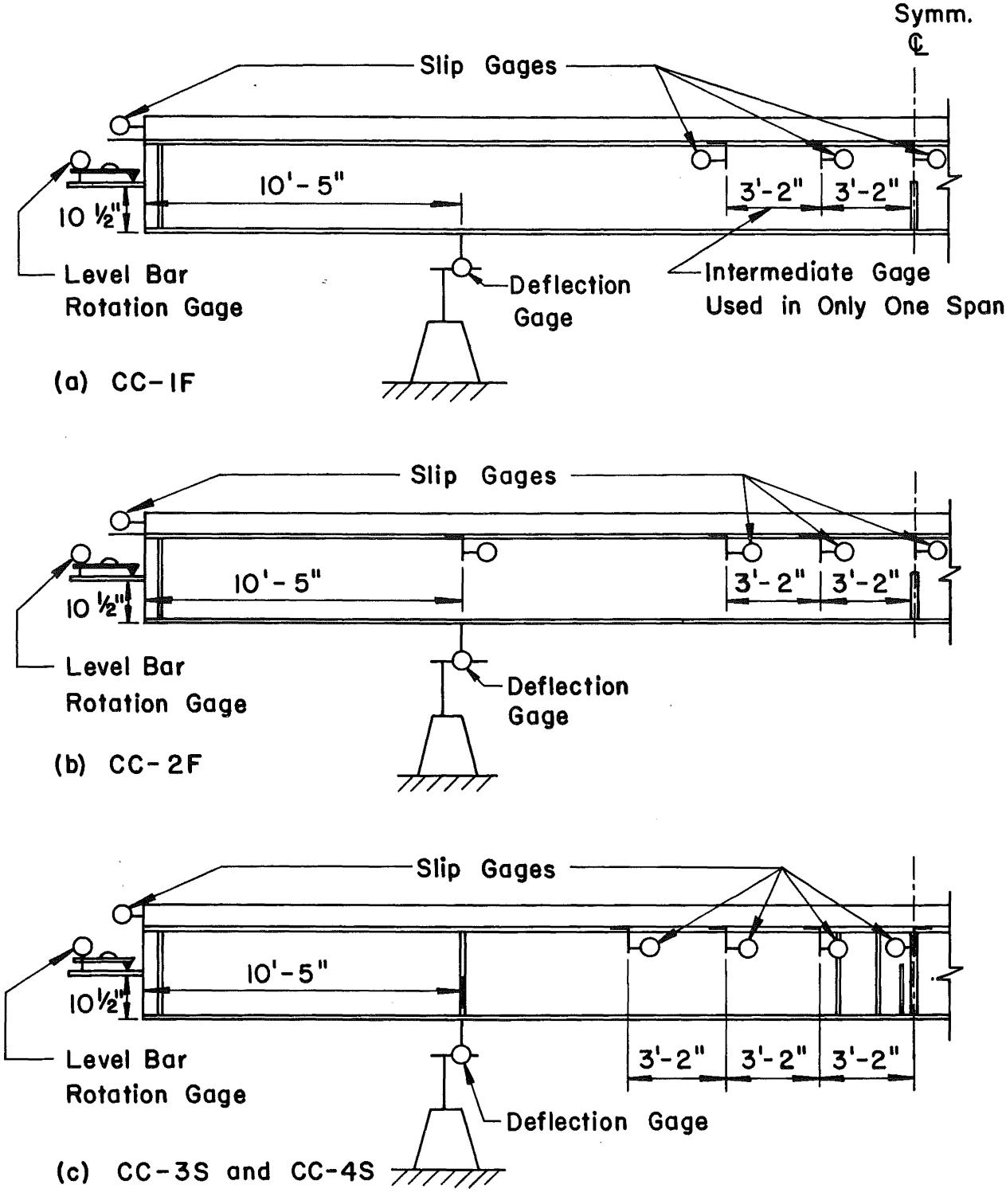

Fig. 9 Locations of Deflection, Rotation, and Slip Gages

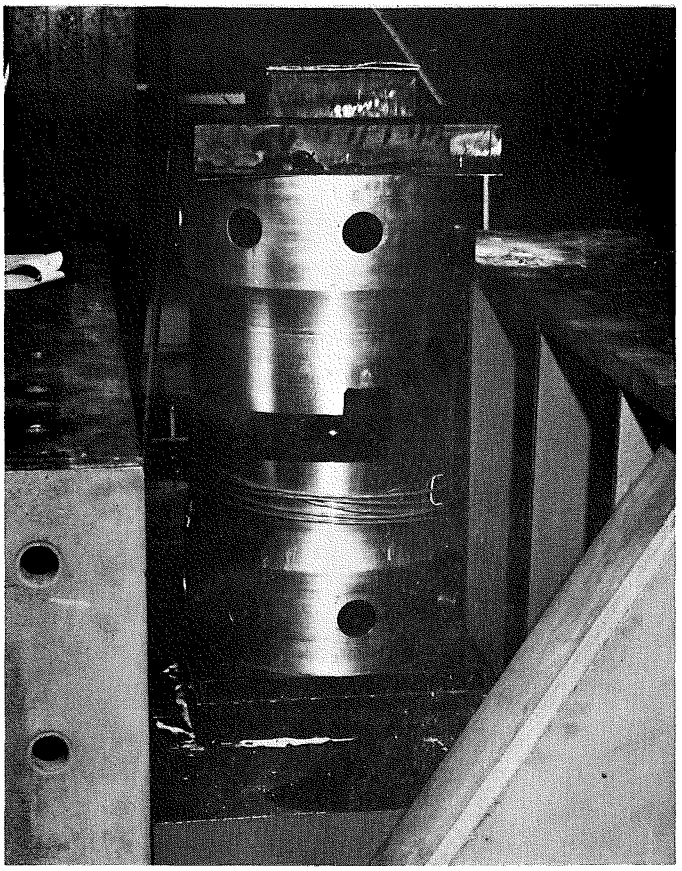

Fig. 10 Compression Dynamometer

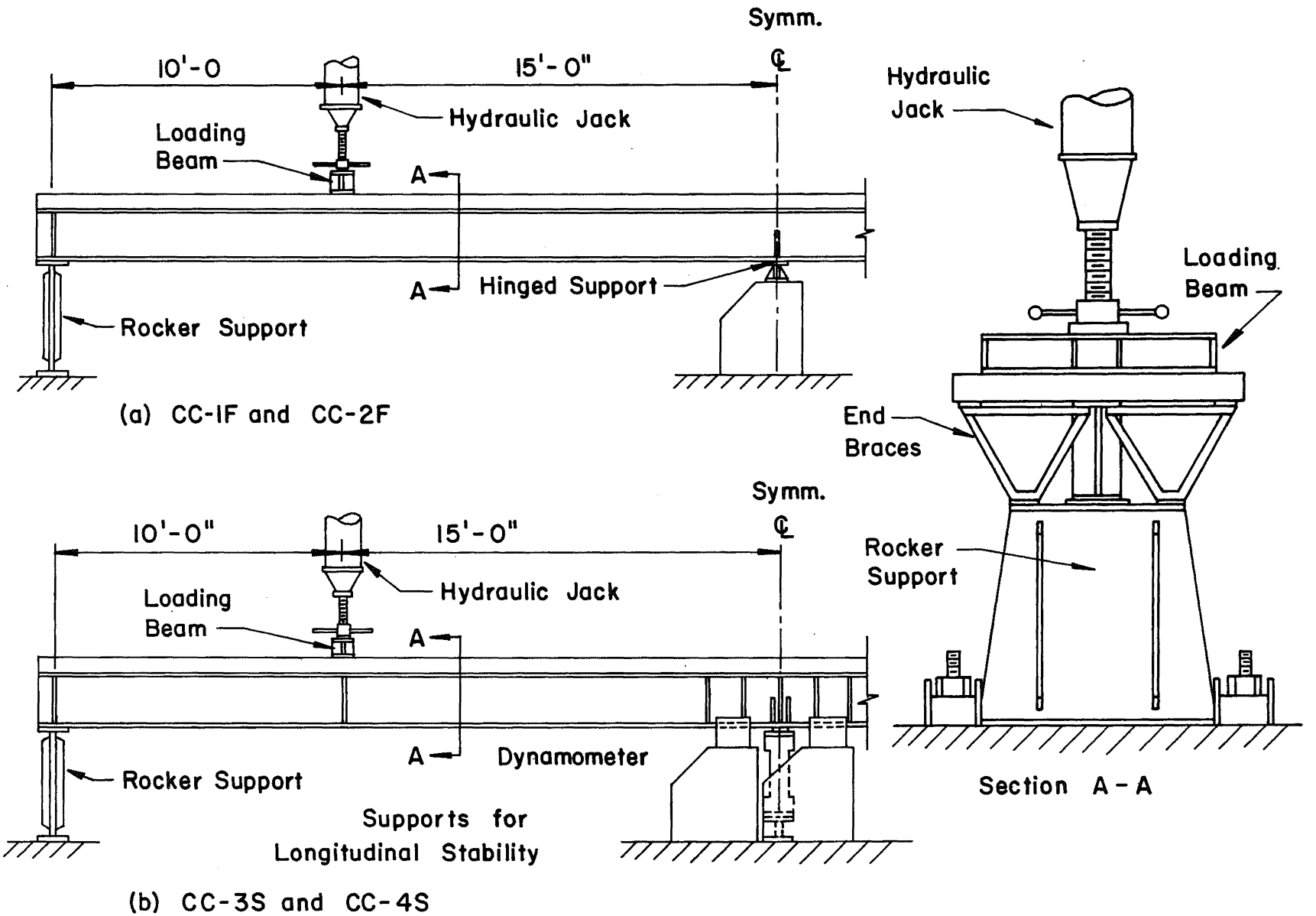

Fig. 11 Test Set-up

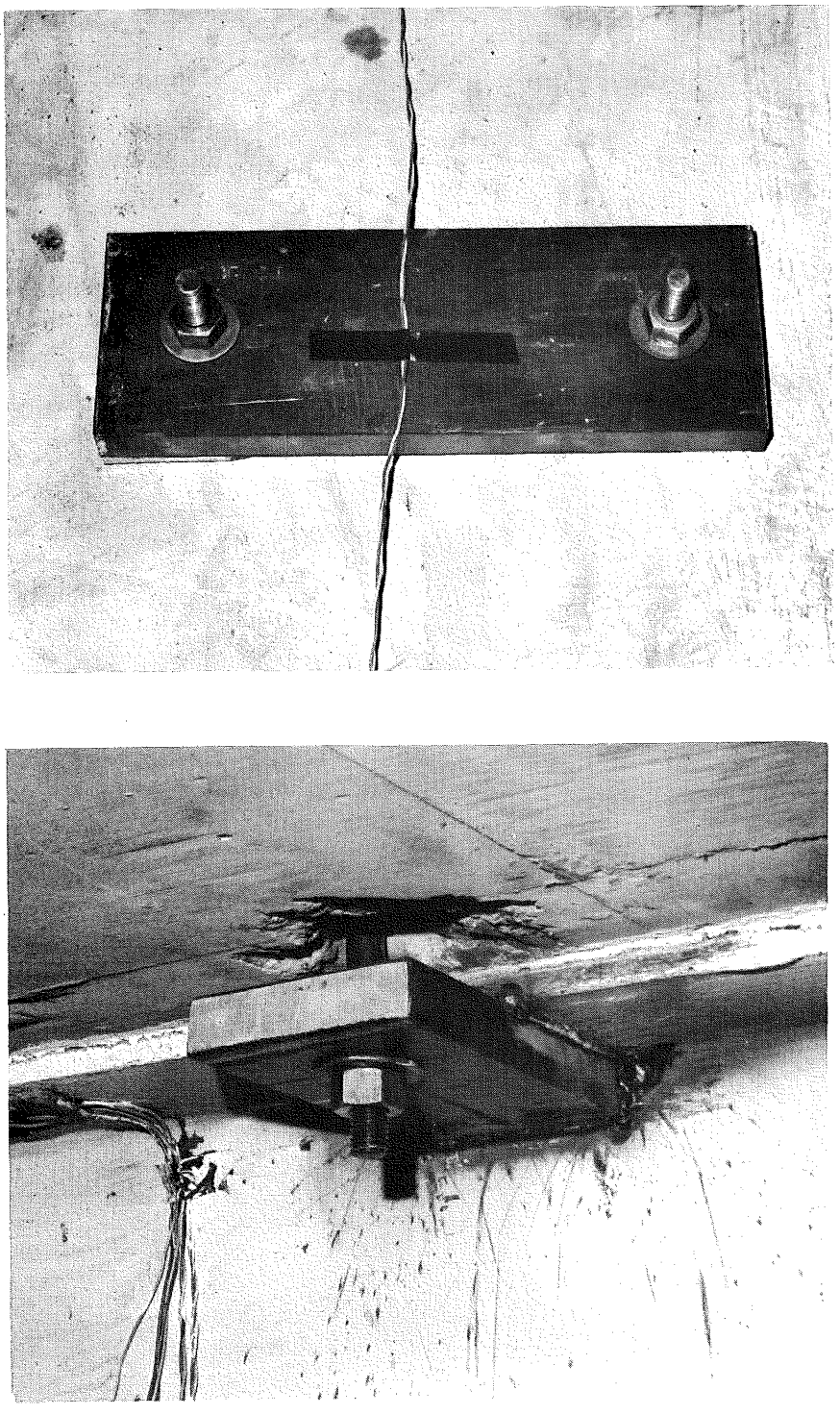

Fig. 12 Clamp Used in Test of Beam CC-1F

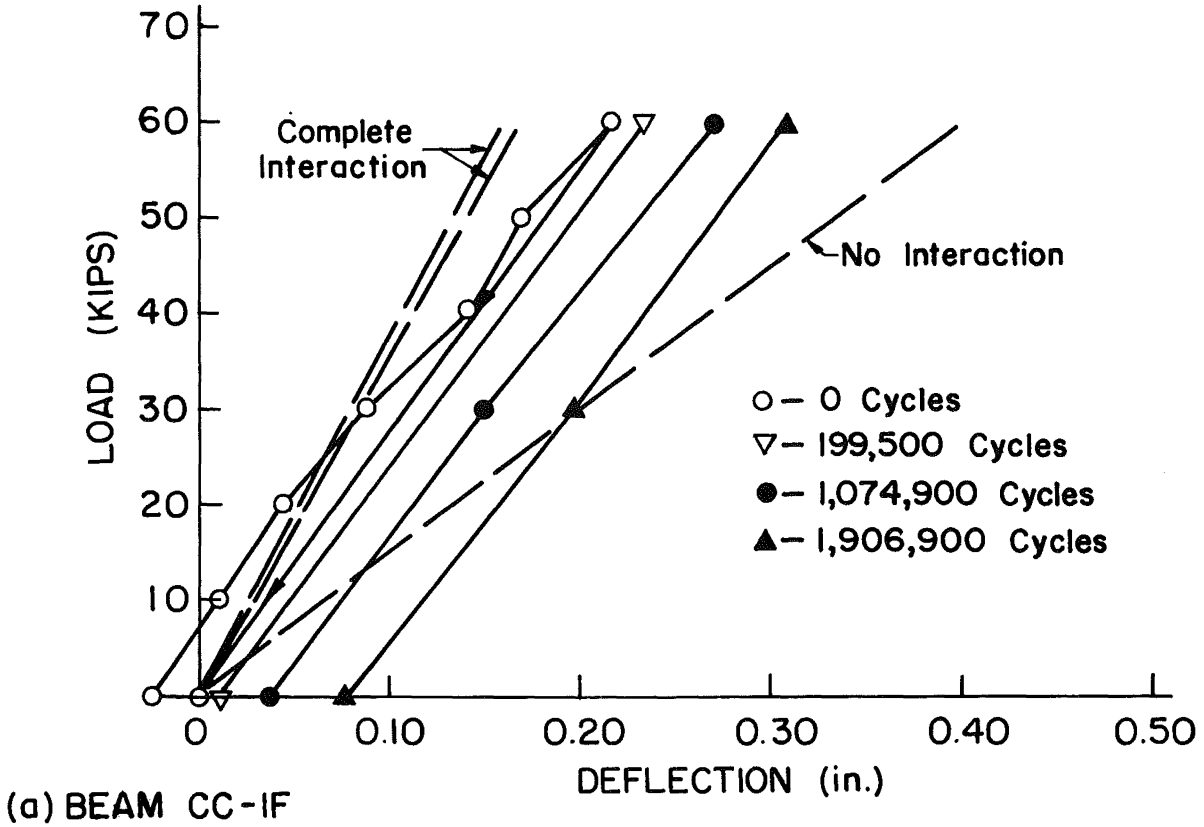

(a) BEAM CC-1F

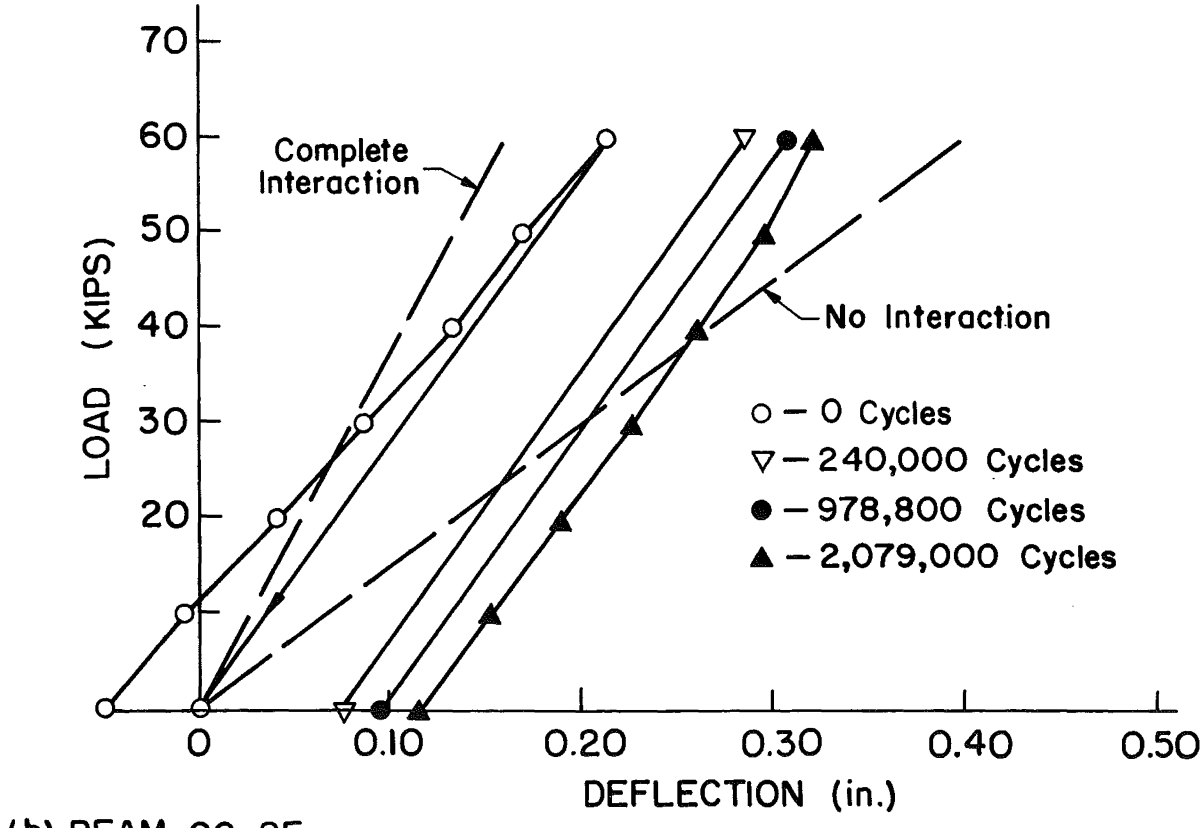

(b) BEAM CC-2F

Fig. 13 Load-Deflection Curves - Beams CC-1F and CC-2F

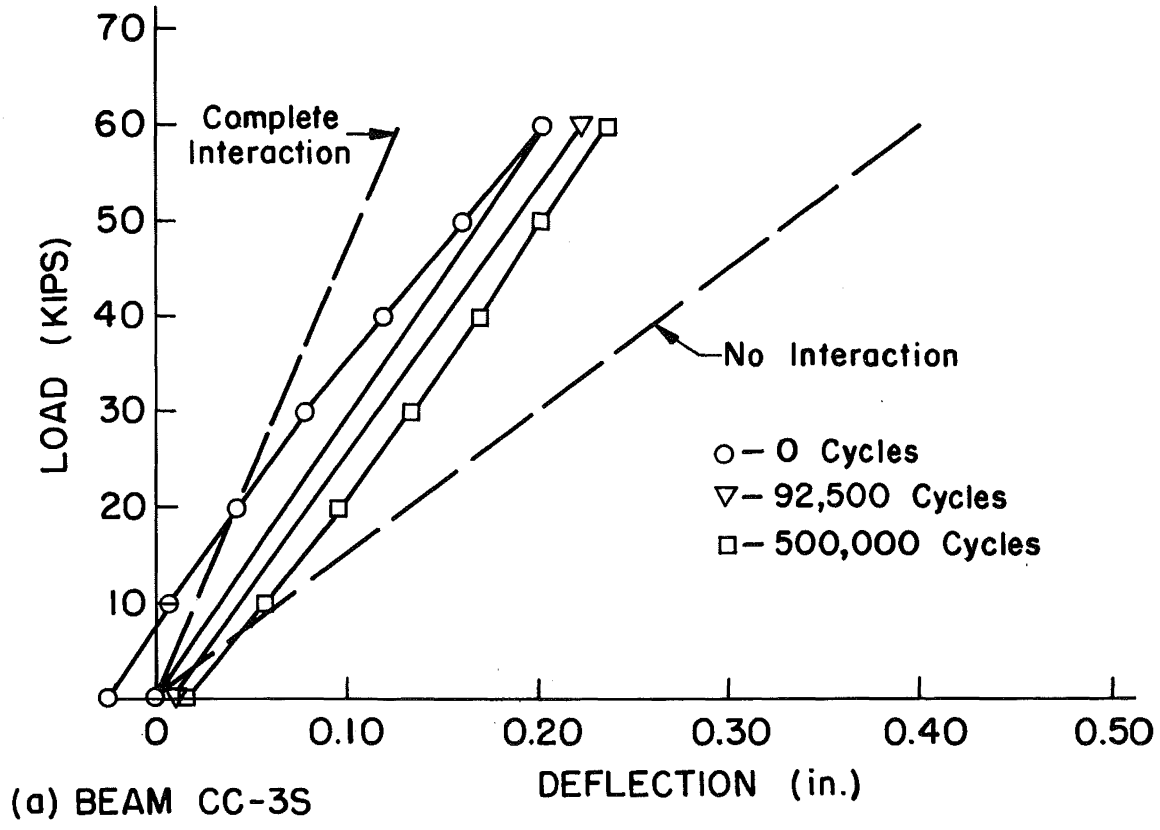

(a) BEAM CC-3S

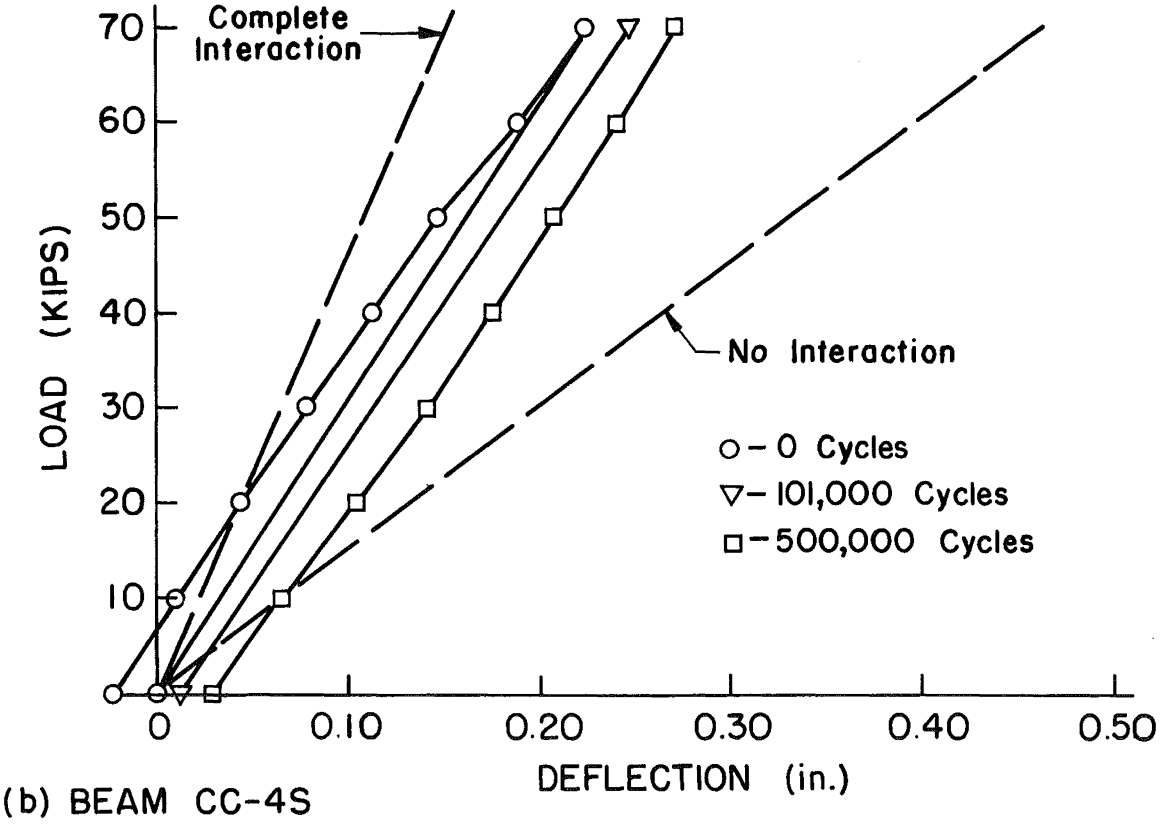

(b) BEAM CC-4S

Fig. 14 Load vs. Deflection Curves CC-3S and CC-4S

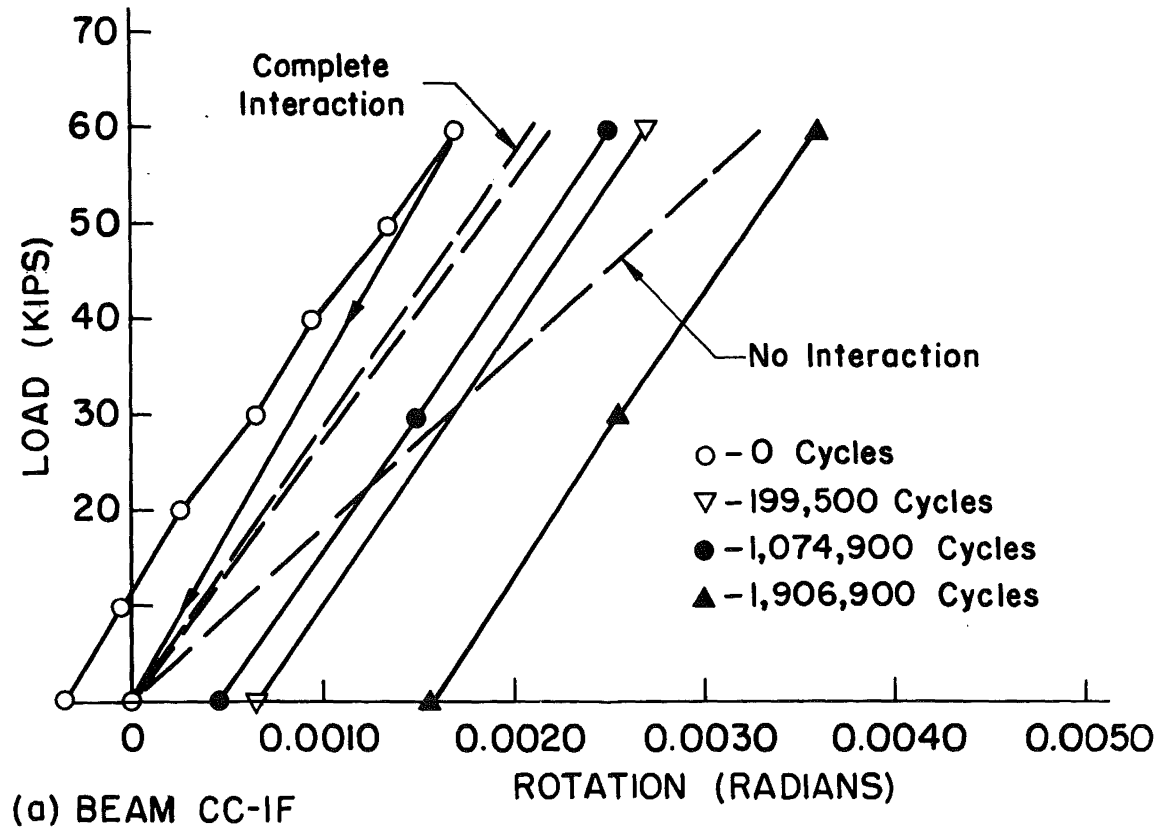

(a) BEAM CC-1F

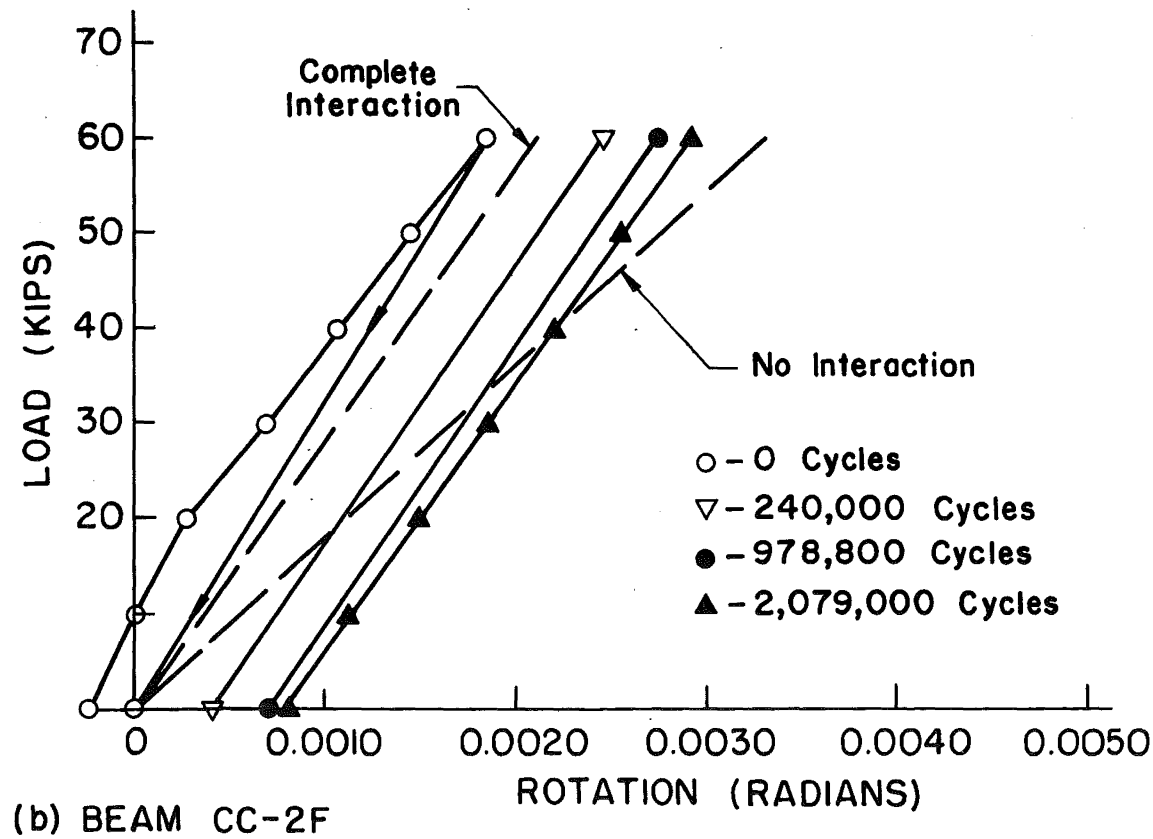

(b) BEAM CC-2F

Fig. 15 Load vs. Rotation Curves CC-1F and CC-2F

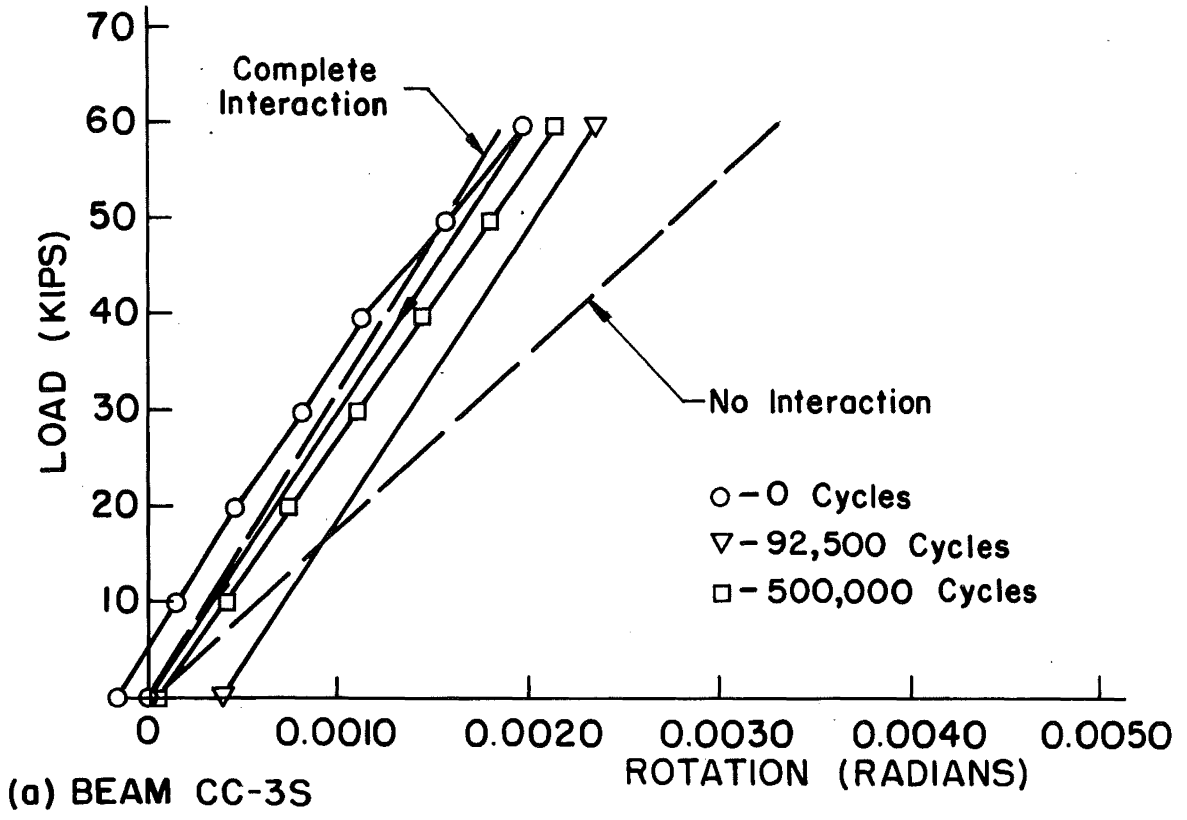

(a) BEAM CC-3S

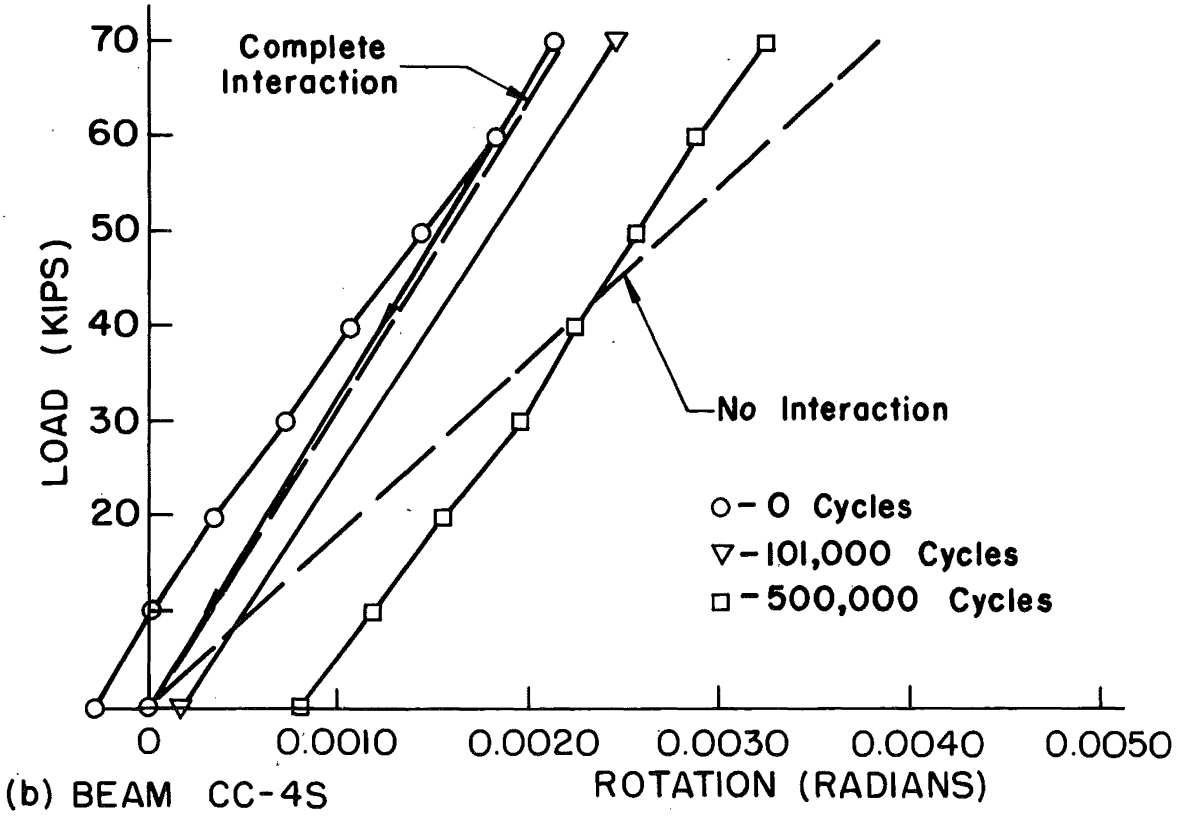

(b) BEAM CC-4S

Fig. 16 Load vs. Rotation Curves CC-3S and CC-4S

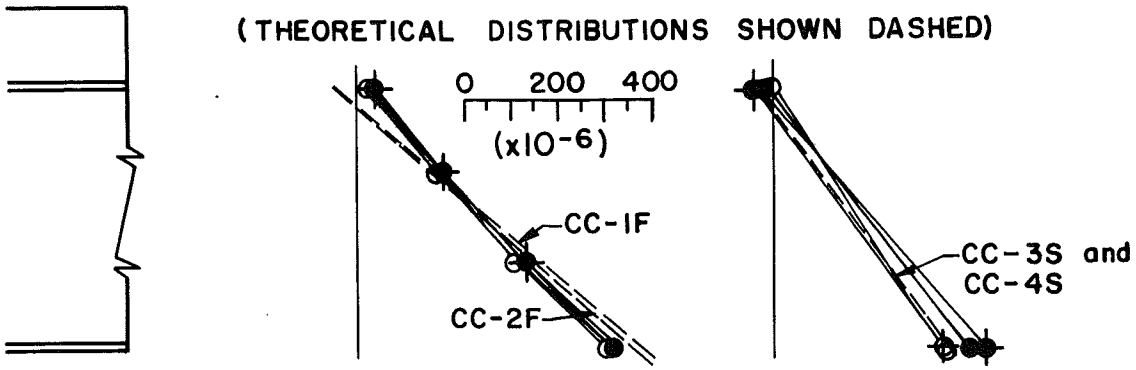

SECTION ①

CC-1F
- ○ -0 CYCLES
- ⊕ -1,906,900 CYCLES

CC-2F
- ● -0 CYCLES
- ✦ -2,079,000 CYCLES

SECTION ①

CC-3S
- ○ -0 CYCLES
- ⊕ -500,000 CYCLES

CC-4S
- ● -0 CYCLES
- ✦ -500,000 CYCLES

Fig. 17 Typical Strain Distribution in Positive Moment Regions

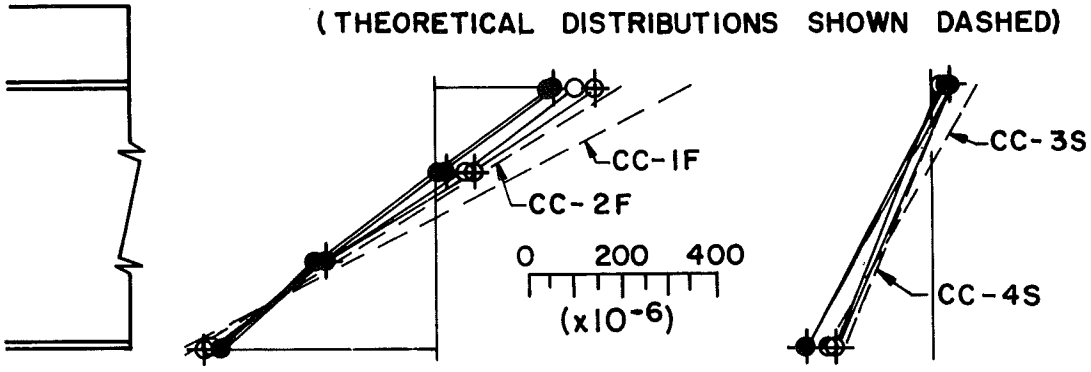

SECTION ③

CC-1F
- ○ -0 CYCLES
- ⊕ -1,906,900 CYCLES

CC-2F
- ● -0 CYCLES
- ✦ -2,079,000 CYCLES

SECTION ③

CC-3S
- ○ -0 CYCLES
- ⊕ -500,000 CYCLES

CC-4S
- ● -0 CYCLES
- ✦ -500,000 CYCLES

Fig. 18 Typical Strain Distribution in Negative Moment Regions

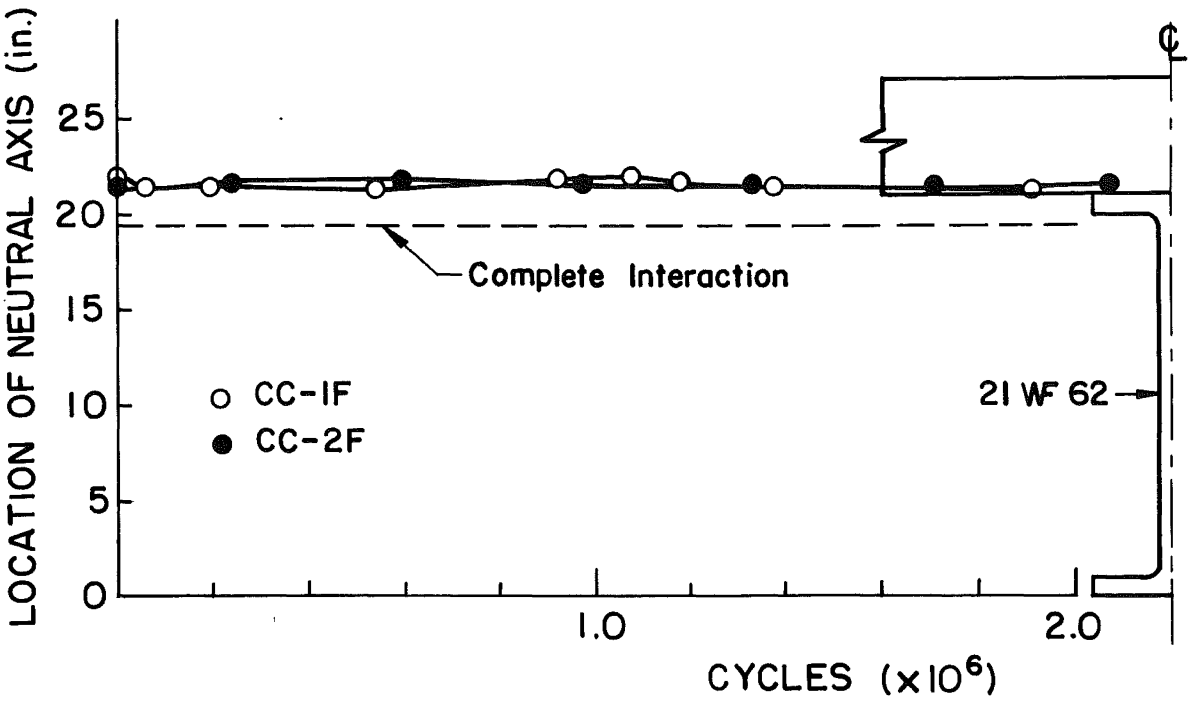

(a) BEAMS CC-1F and CC-2F (SECTION 1)

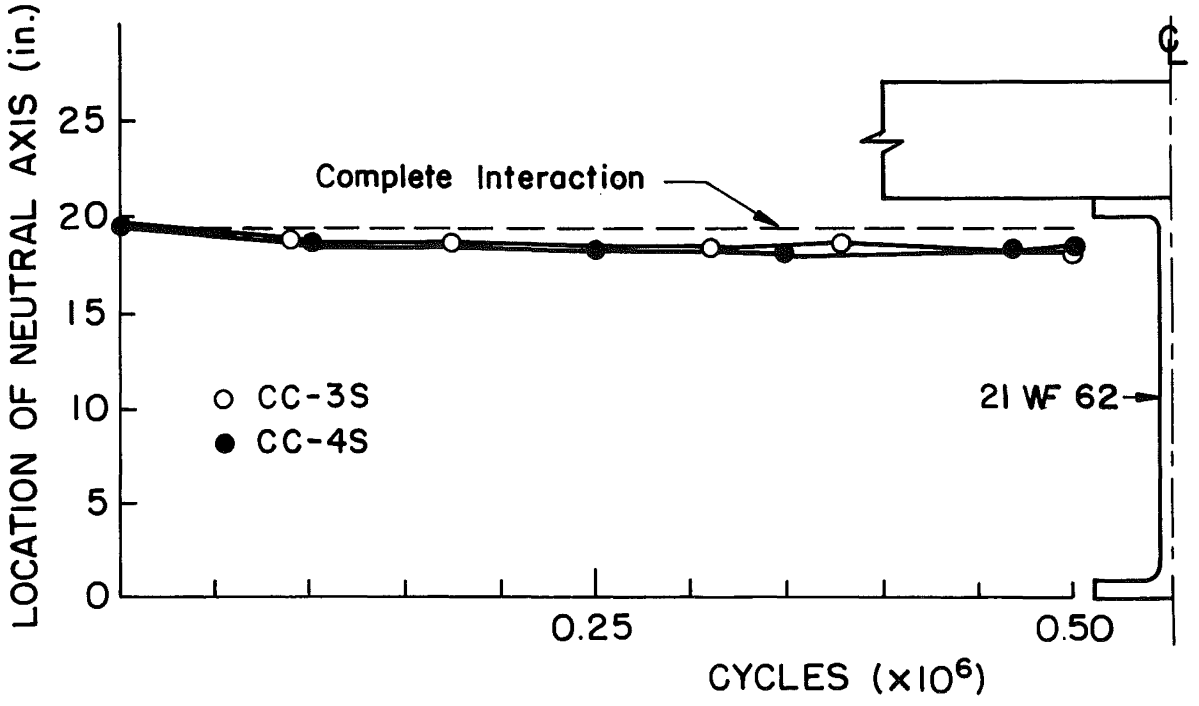

(b) BEAMS CC-3S and CC-4S (SECTION 1)

Fig. 19 Location of Neutral Axis Positive Moment Regions (Typical)

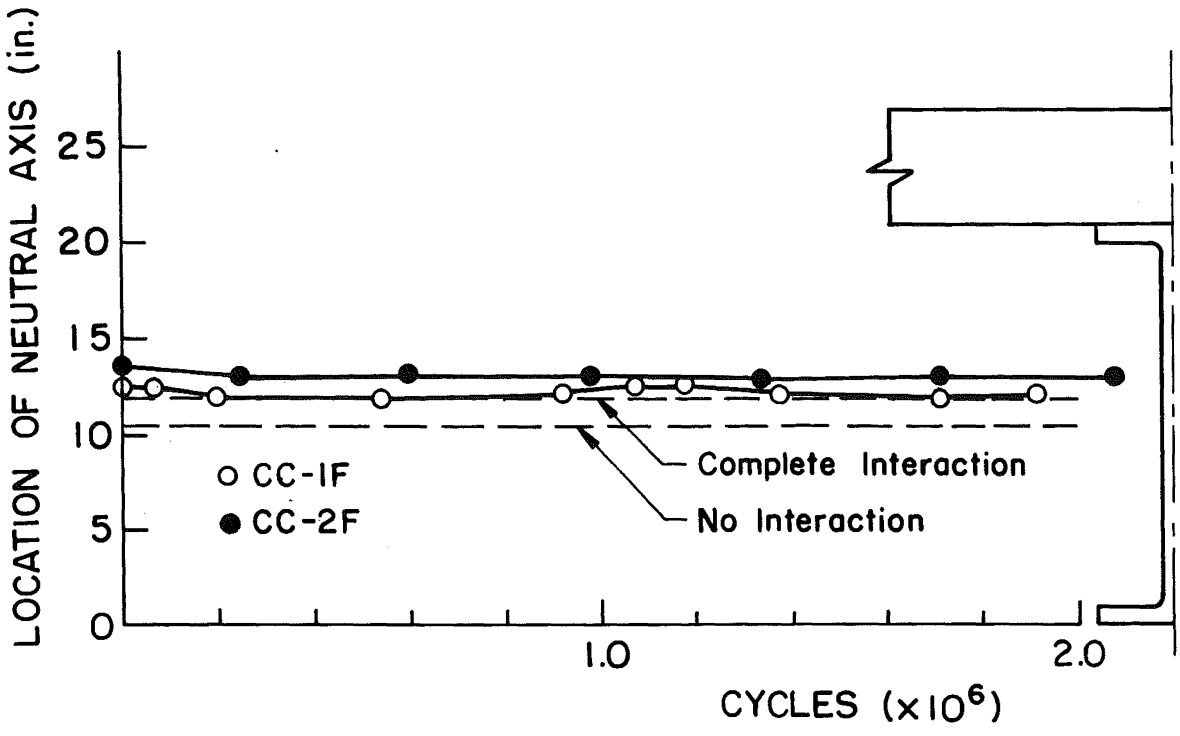

(a) BEAMS CC-1F and CC-2F (SECTION 3)

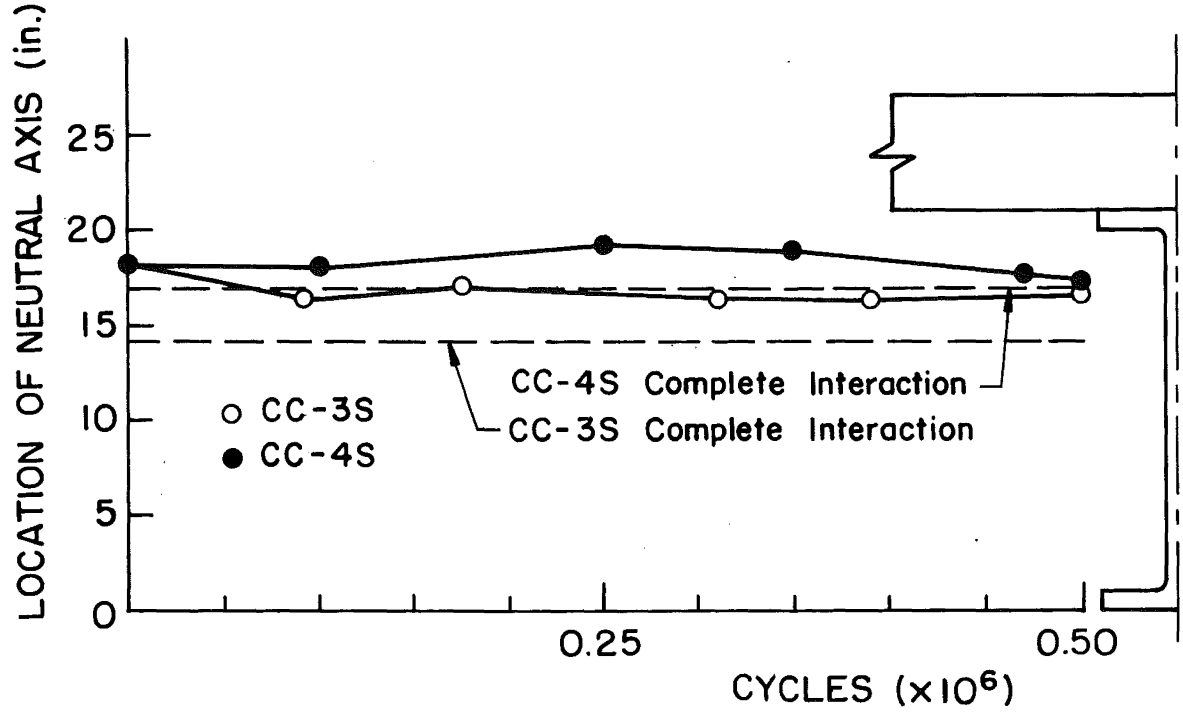

(b) BEAM CC-3S and CC-4S (SECTION 3)

Fig. 20 Location of Neutral Axis in Negative Moment Regions (Typical)

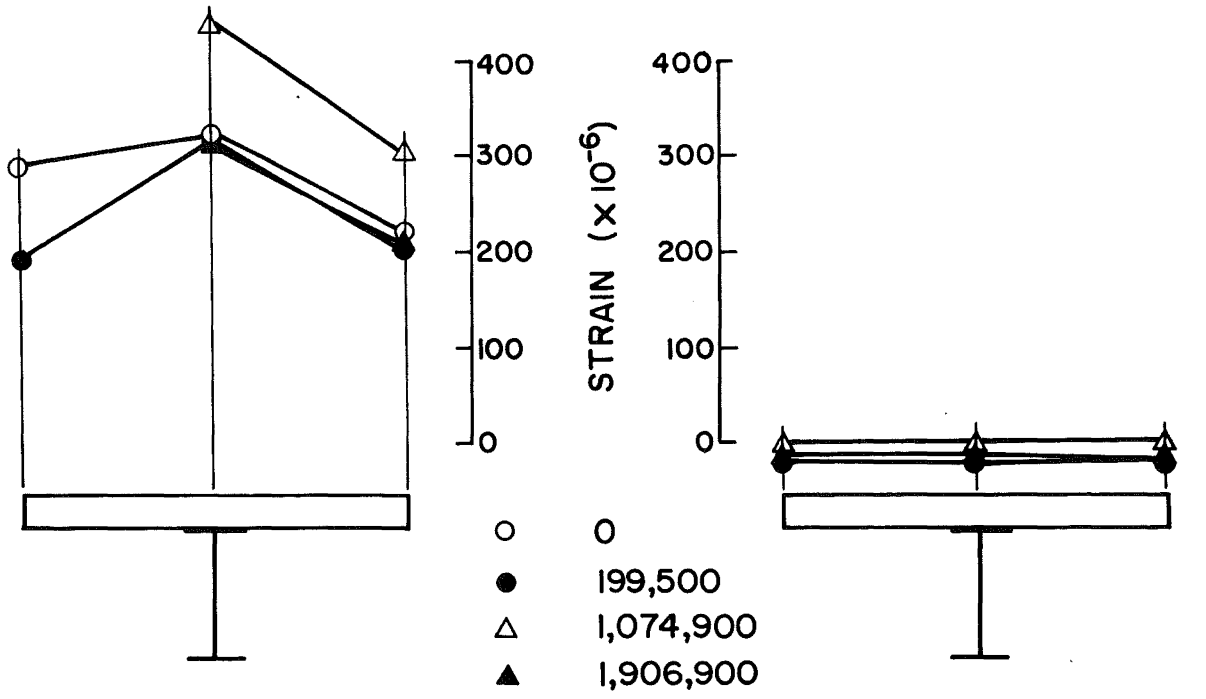

(a) BEAM CC-1F (SECTION 1)

(b) BEAM CC-1F (SECTION 2)

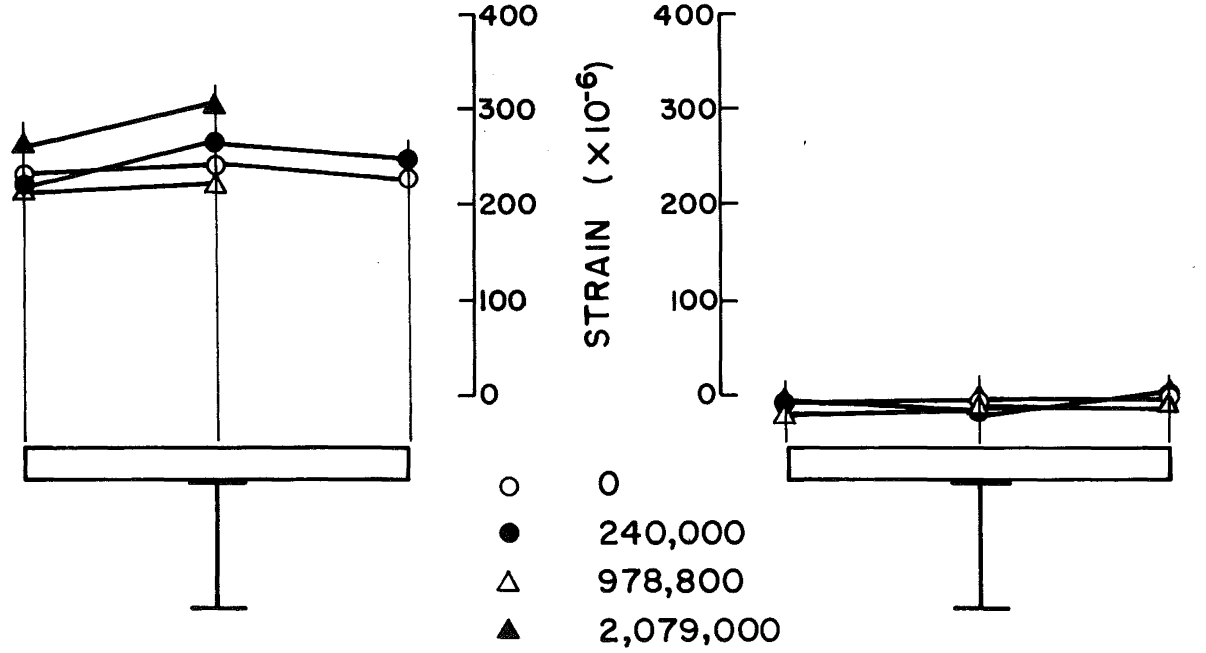

(c) BEAM CC-2F (SECTION 1)

(d) BEAM CC-2F (SECTION 2)

(See Fig. 7 for section locations)

Fig. 21 Strain Distribution Across Slab

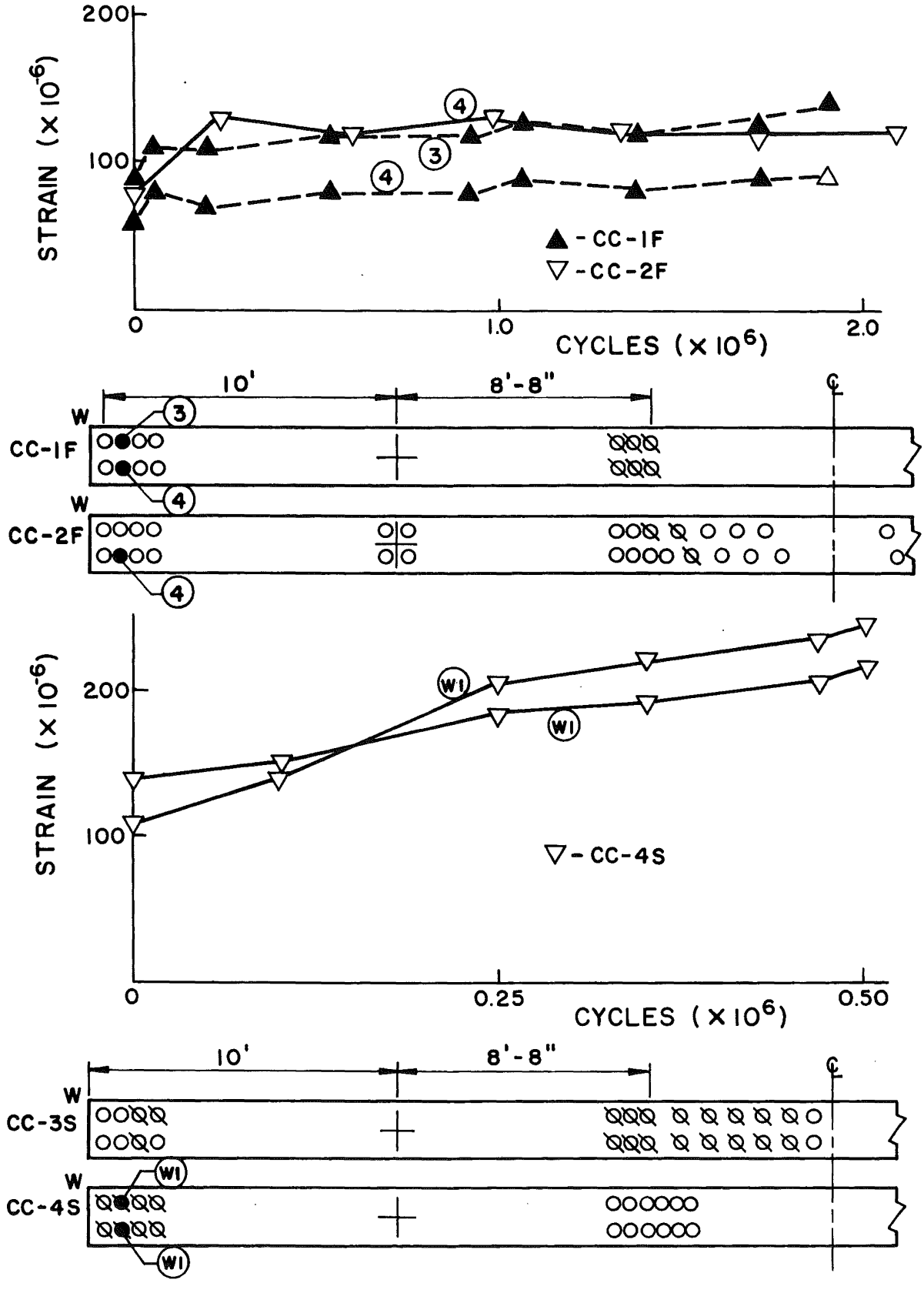

Fig. 22 Typical Local Strain Readings vs. Cycles at Ends of Beams

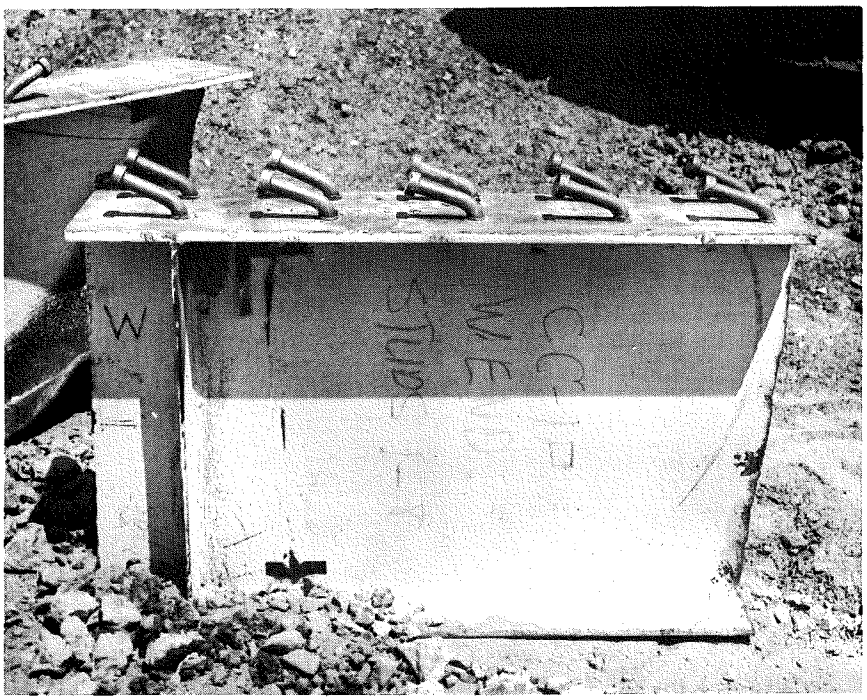

Fig. 23 Studs at End of Beam CC-1F after Fatigue Tests

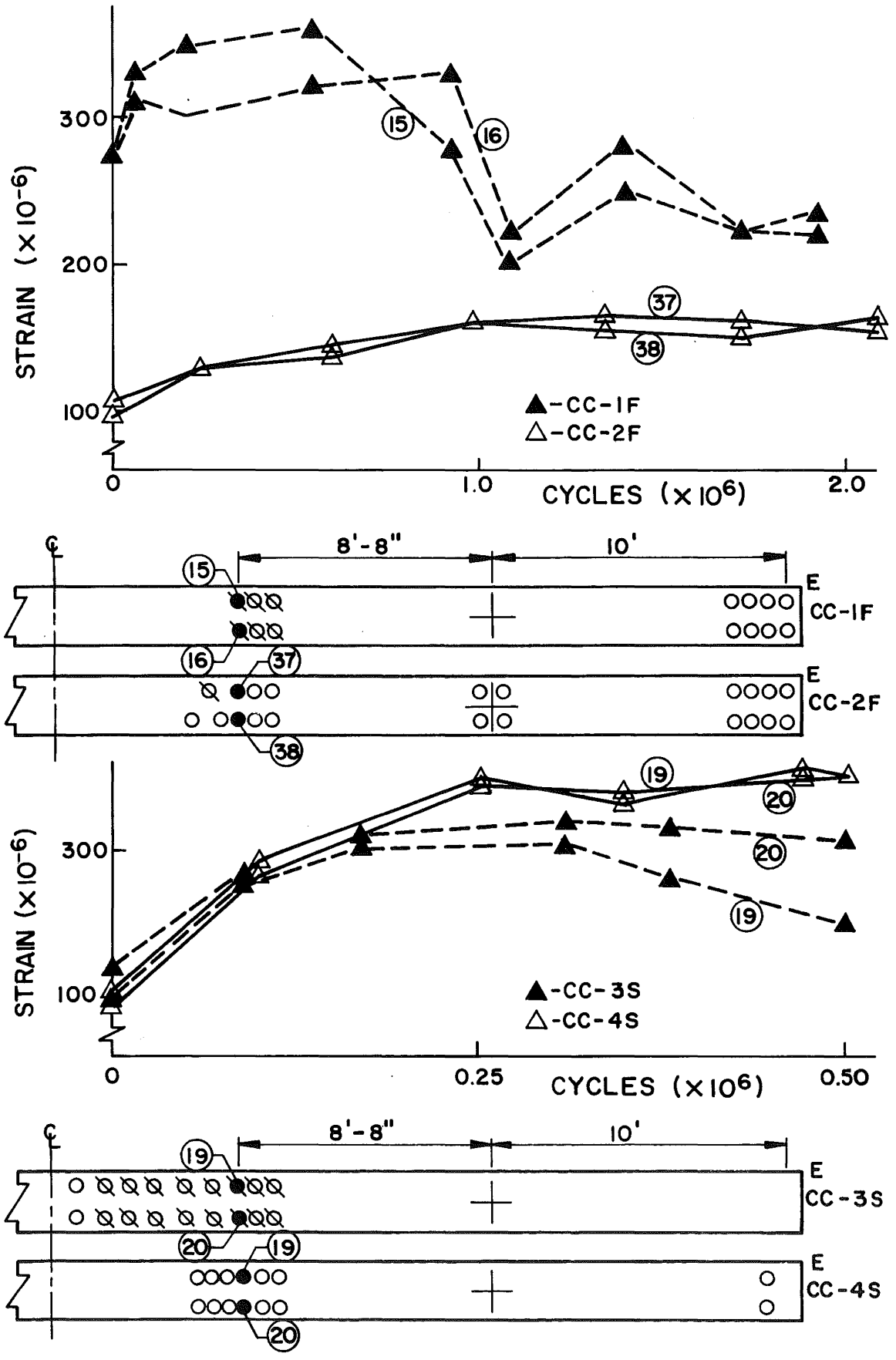

Fig. 24 Typical Local Strain Readings vs. Cycles at Inflection Point in East Spans of Beams

324-24

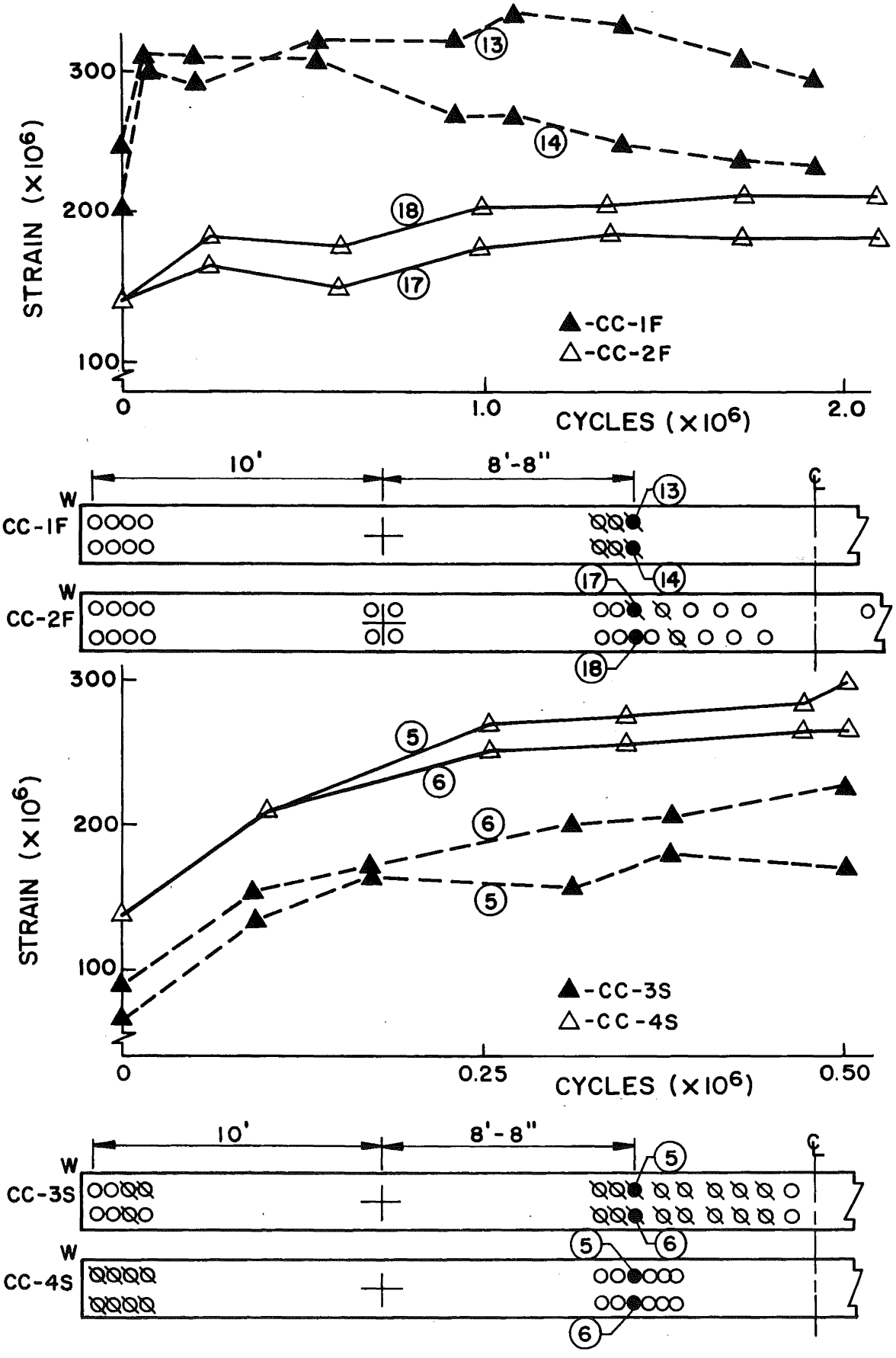

Fig. 25 Typical Local Strain Readings vs. Cycles at Inflection Point in West Spans of Beams

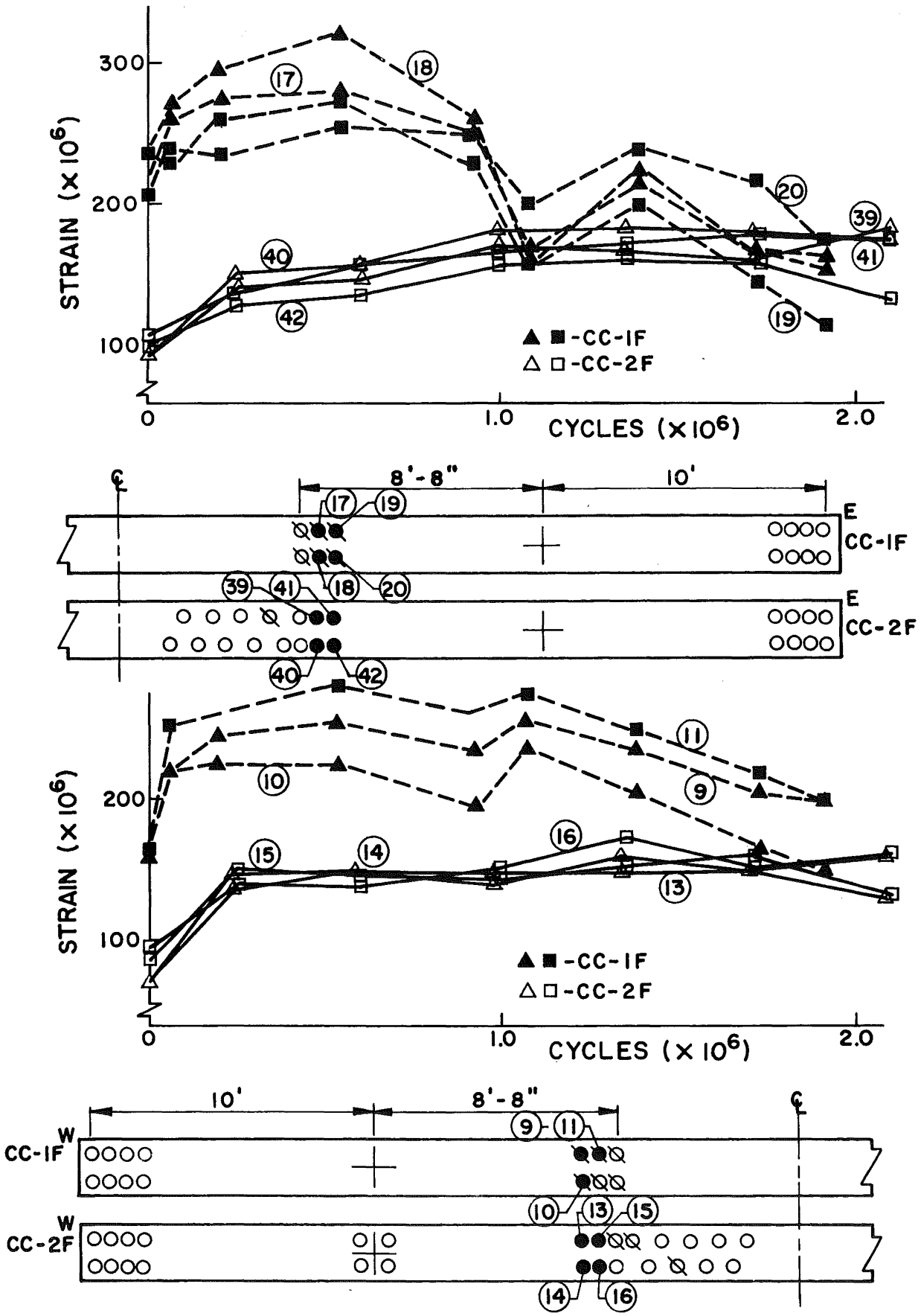

Fig. 26 Comparison of Local Strain Readings at Inflection Point of CC-1F and CC-2F

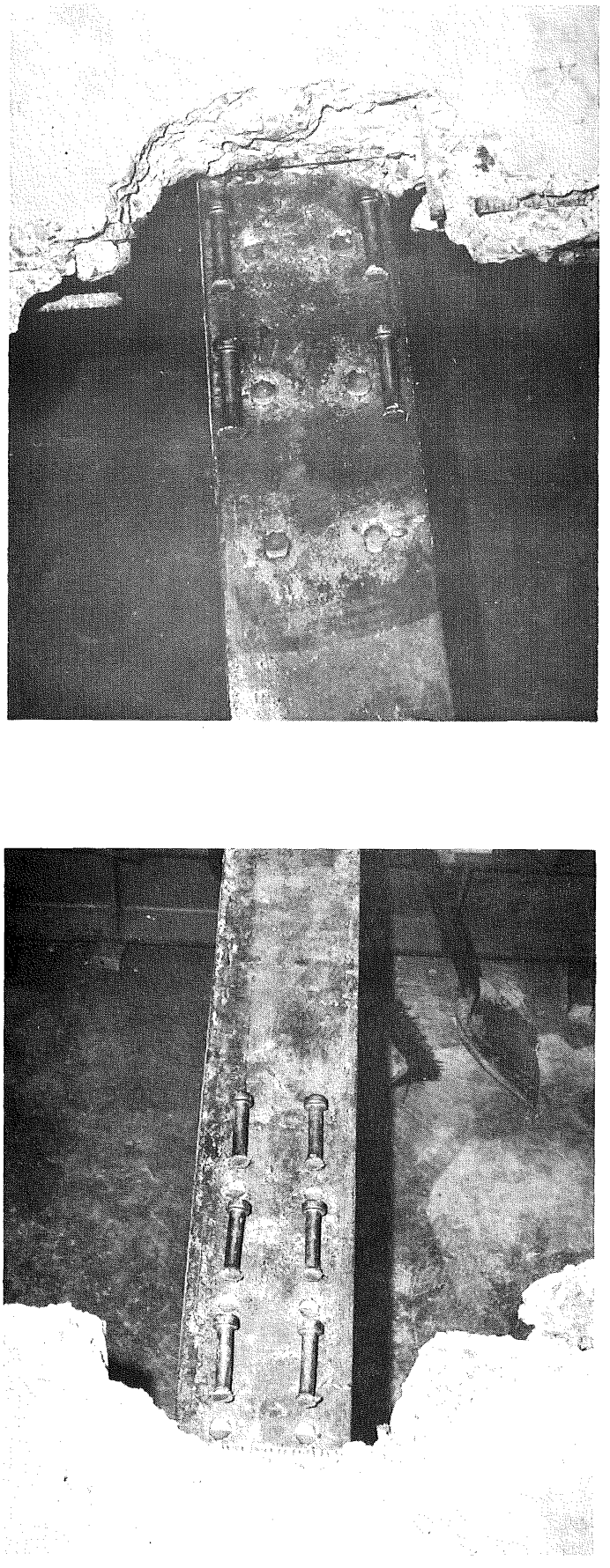

Fig. 27 Studs at the E. and W. Inflection Points of Beam CC-1F after Fatigue Testing

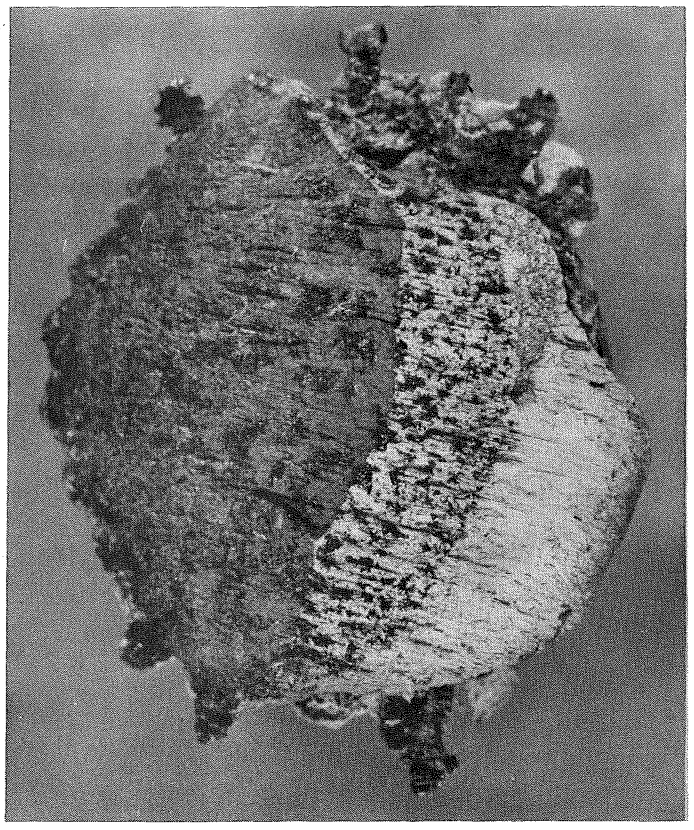

Stud 13

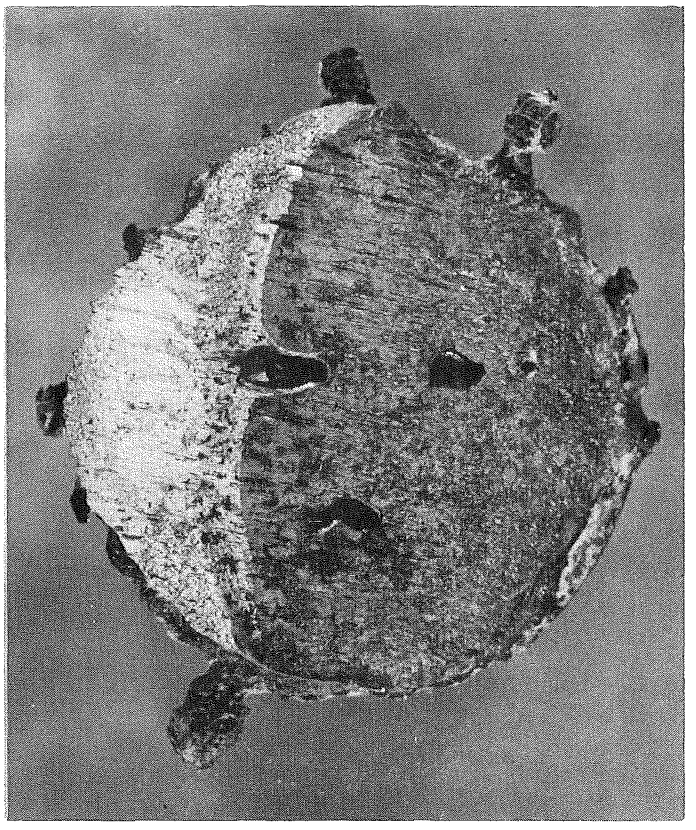

Stud 14

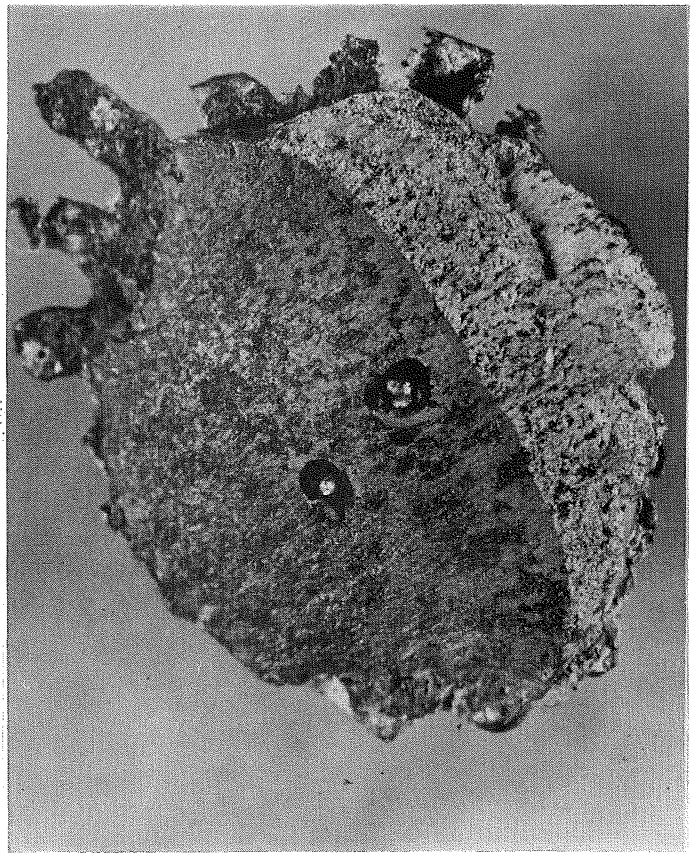

Stud 17

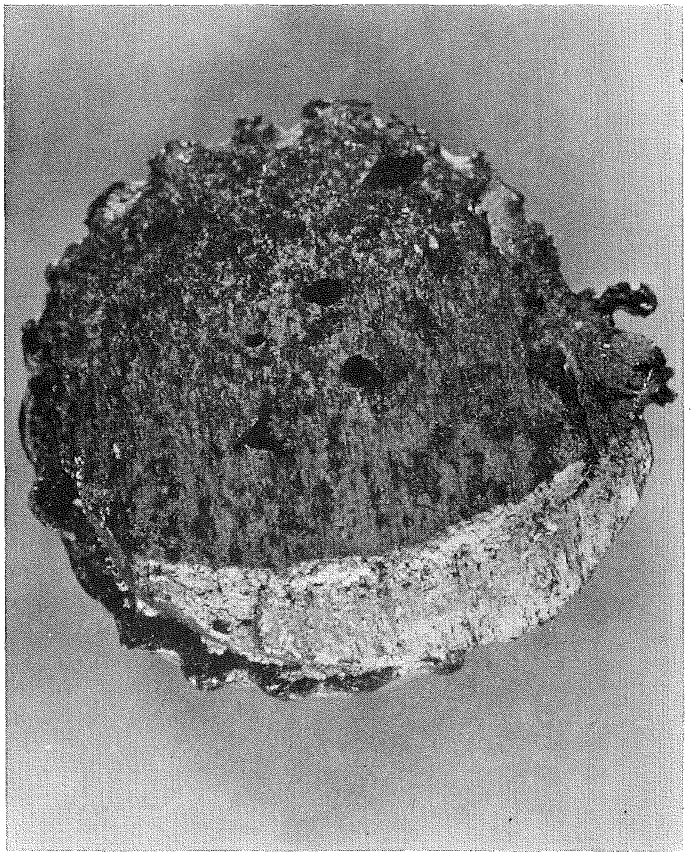

Stud 18

Fig. 28 Fracture Surfaces of Typical Studs on Beam CC-1F

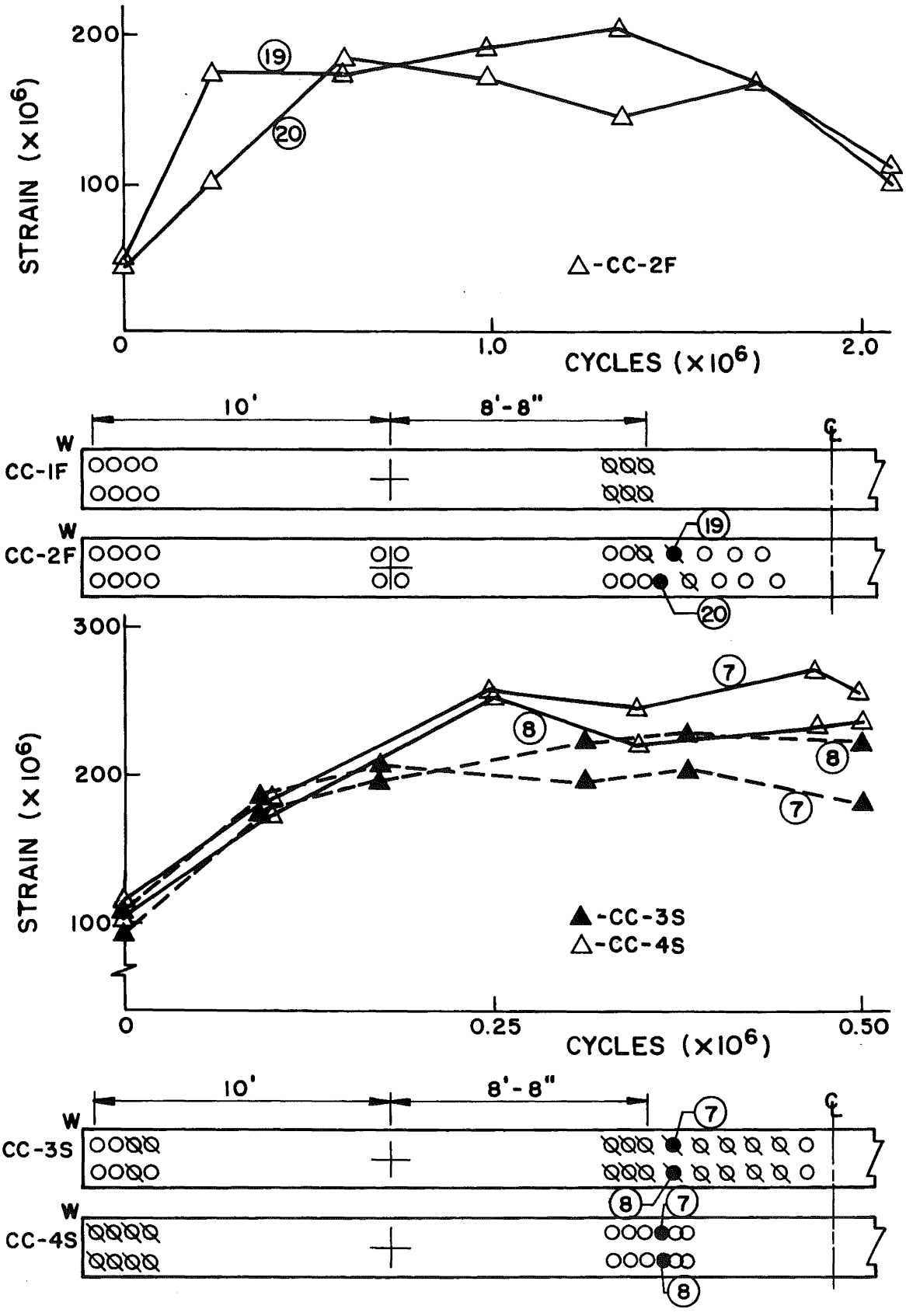

Fig. 29 Typical Local Strain Readings vs. Cycles in Negative Moment Regions

324-29

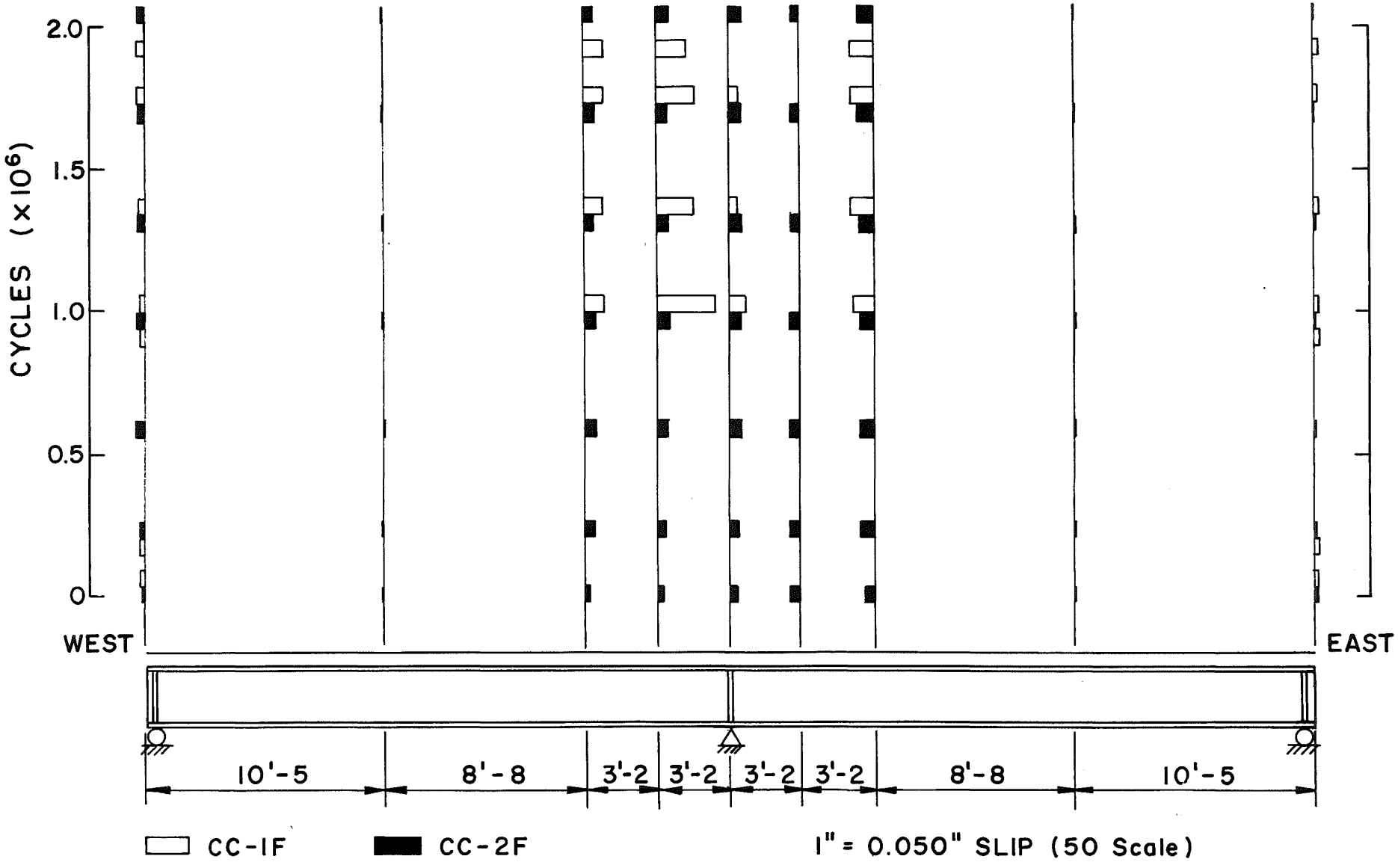

Fig. 30 Range of Slip vs. Cycles for Beams CC-1F and CC-2F

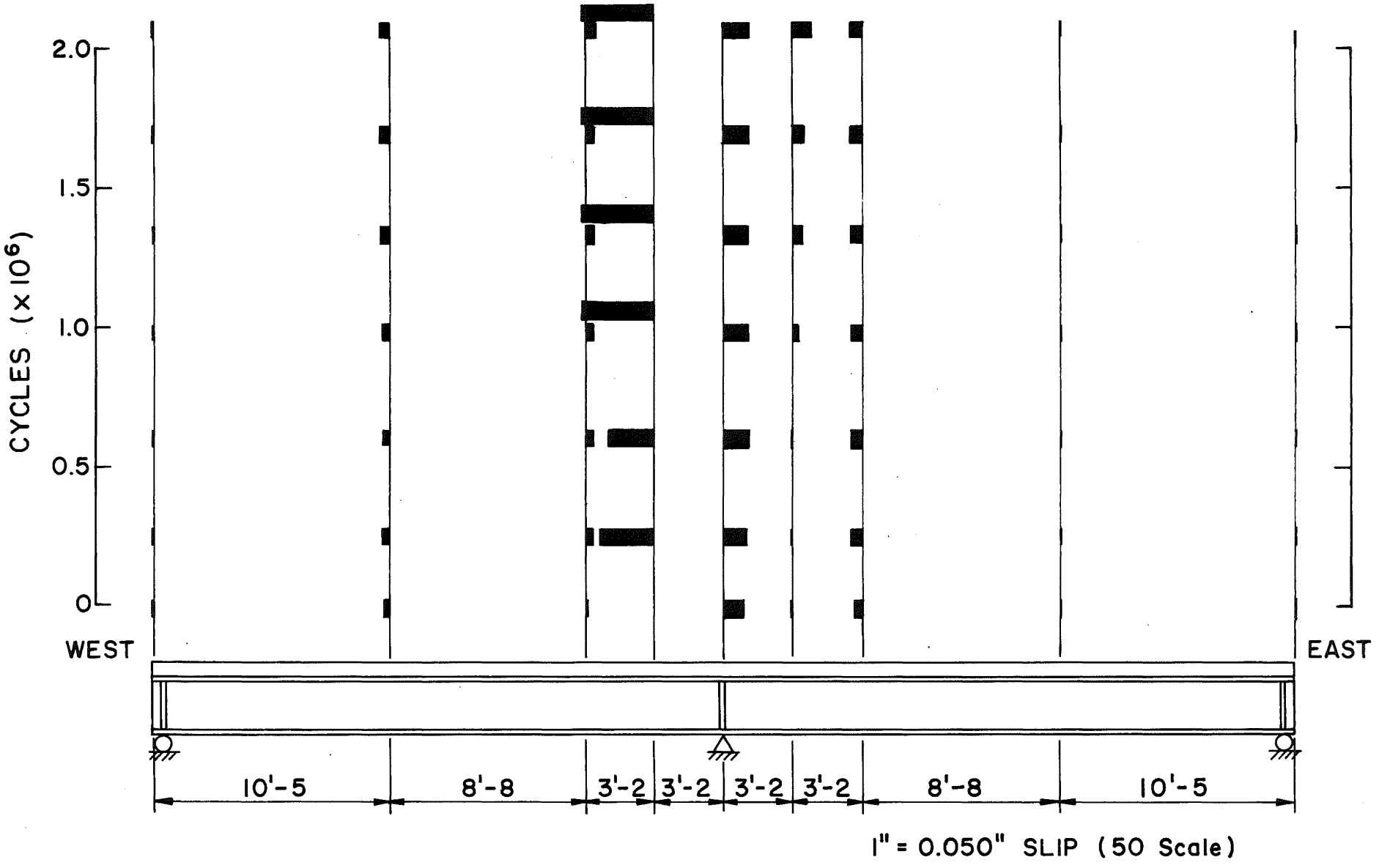

Fig. 31 Maximum Slip vs. Cycles for Beam CC-2F

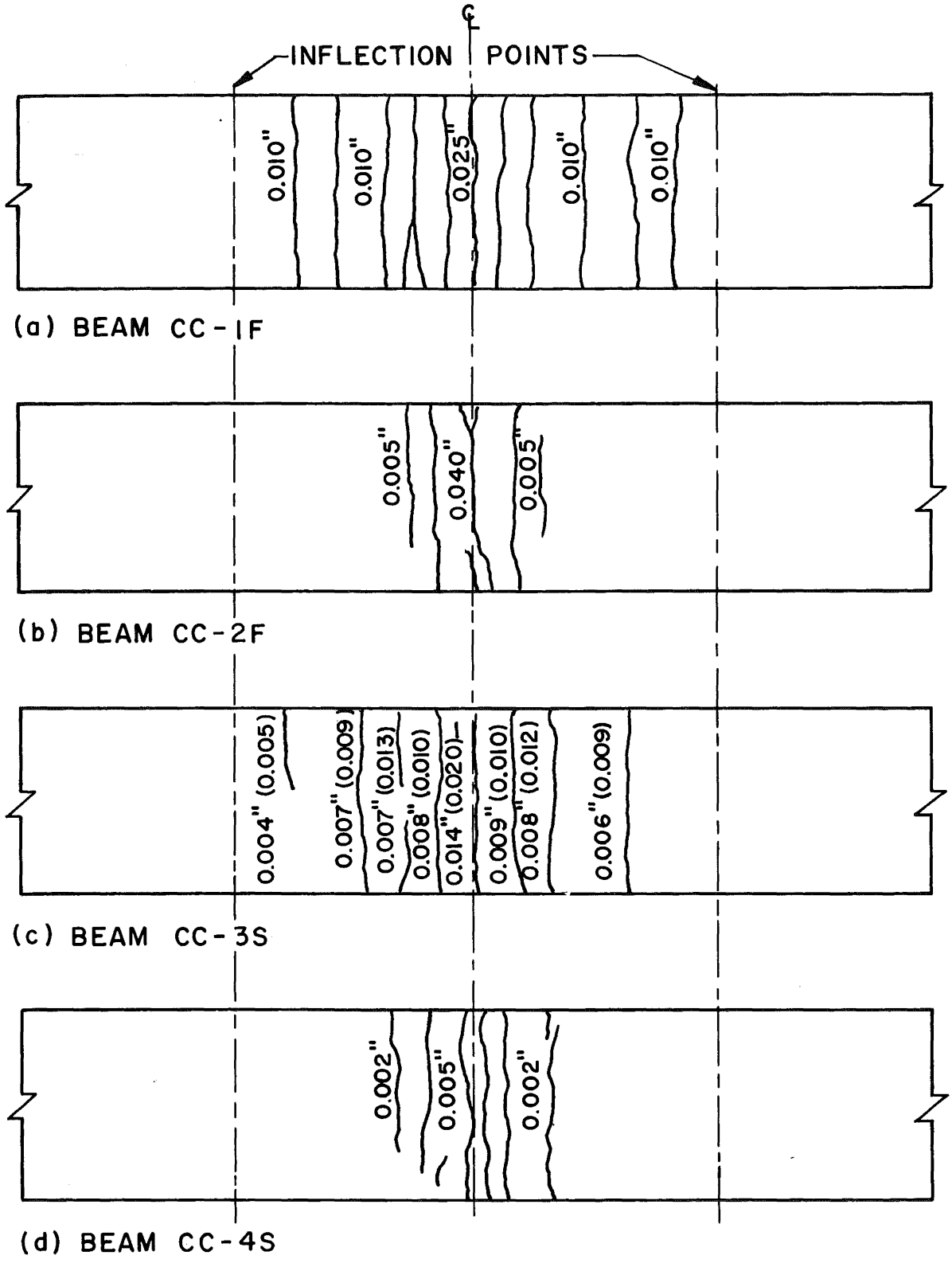

Fig. 32 Distribution of Slab Cracking in Negative Moment Regions of Beams

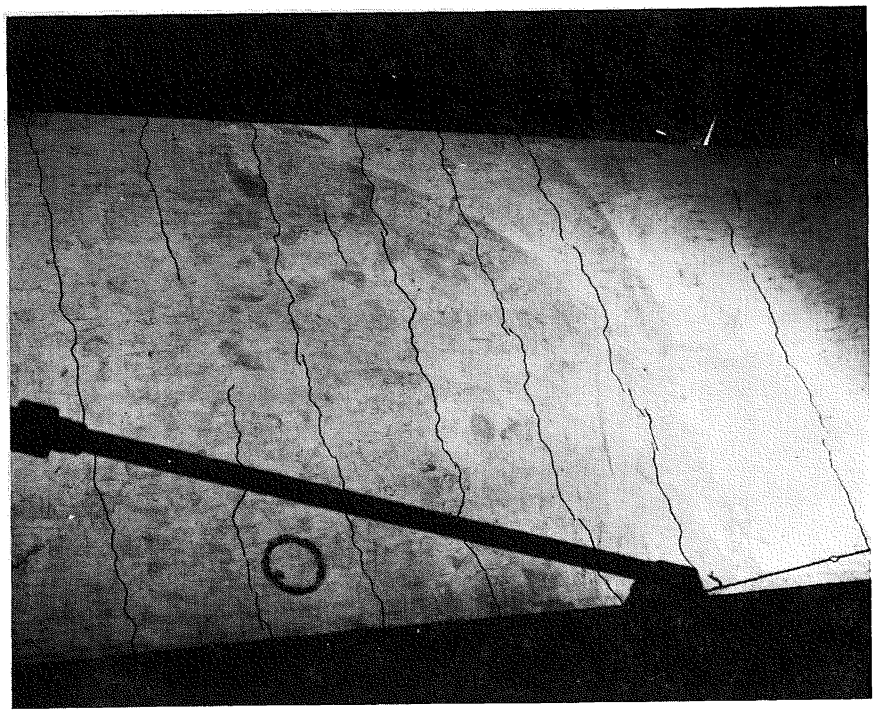

CC-3S

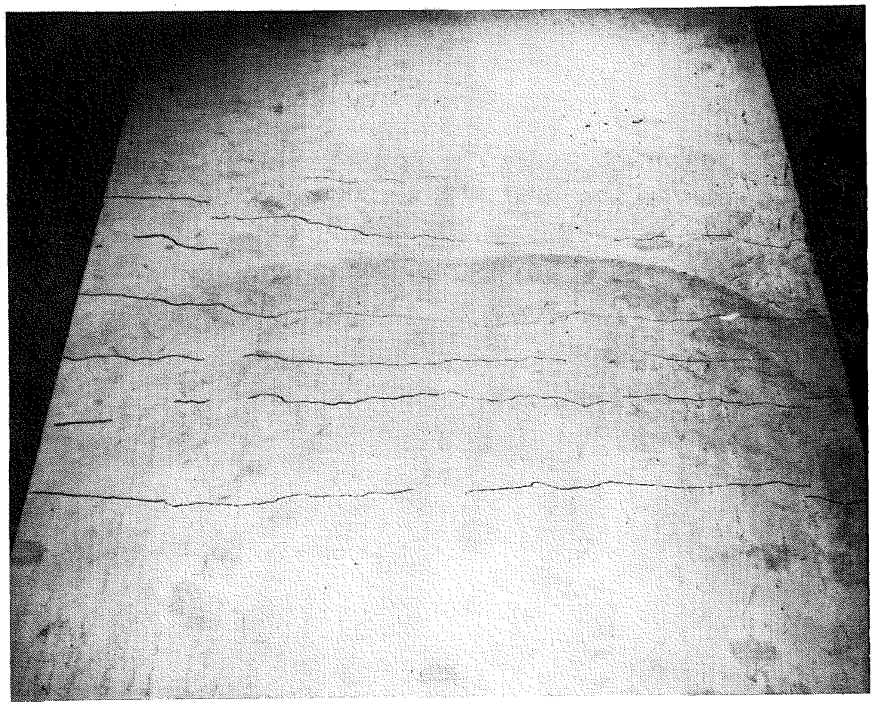

CC-4S

Fig. 33 Crack Patterns at the End of Fatigue Tests of Fatigue Tests of Beams CC-3S and CC-4S

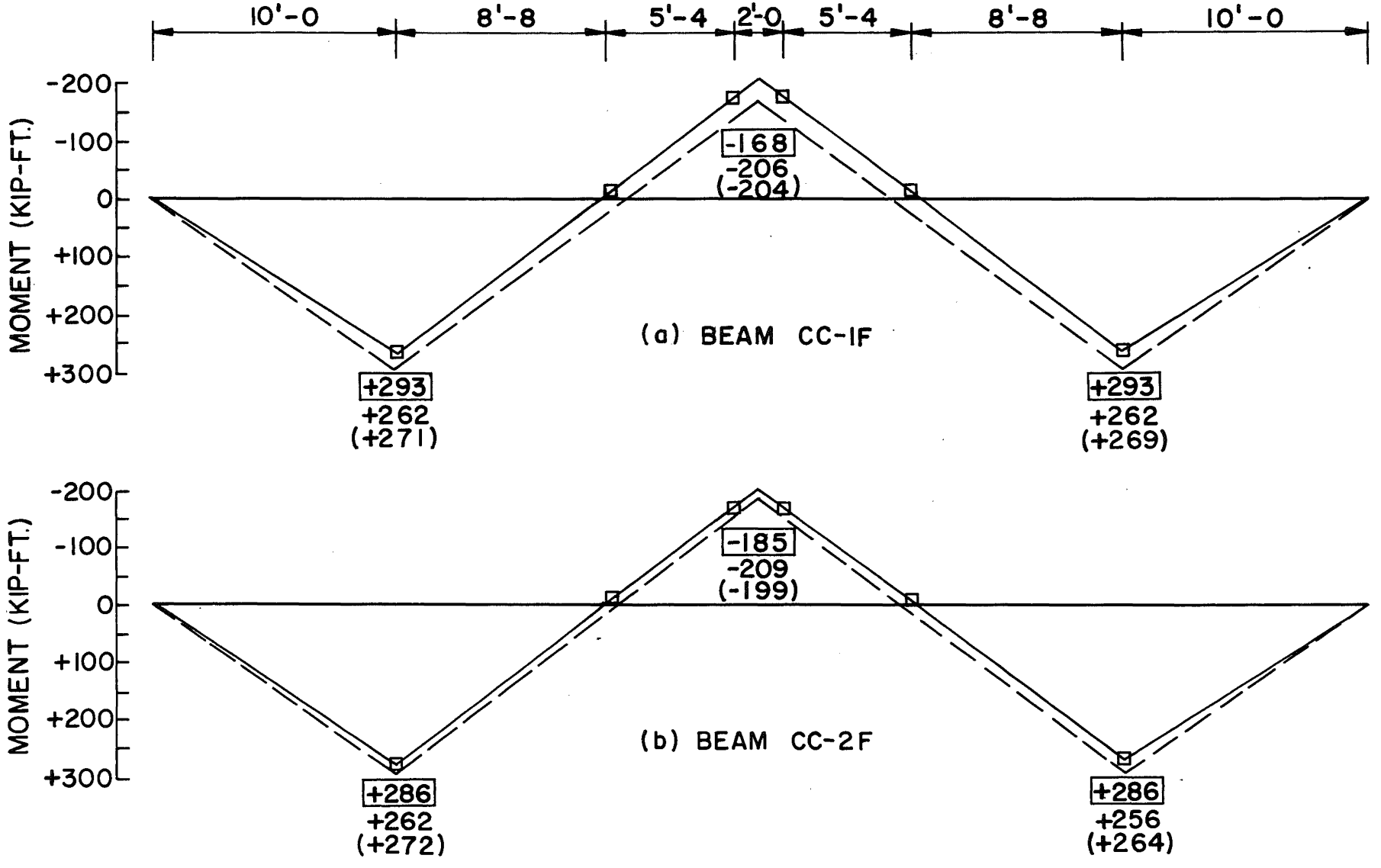

Fig. 34 Comparison of Computed and Measured Bending Moments for Beams CC-1F and CC-2F

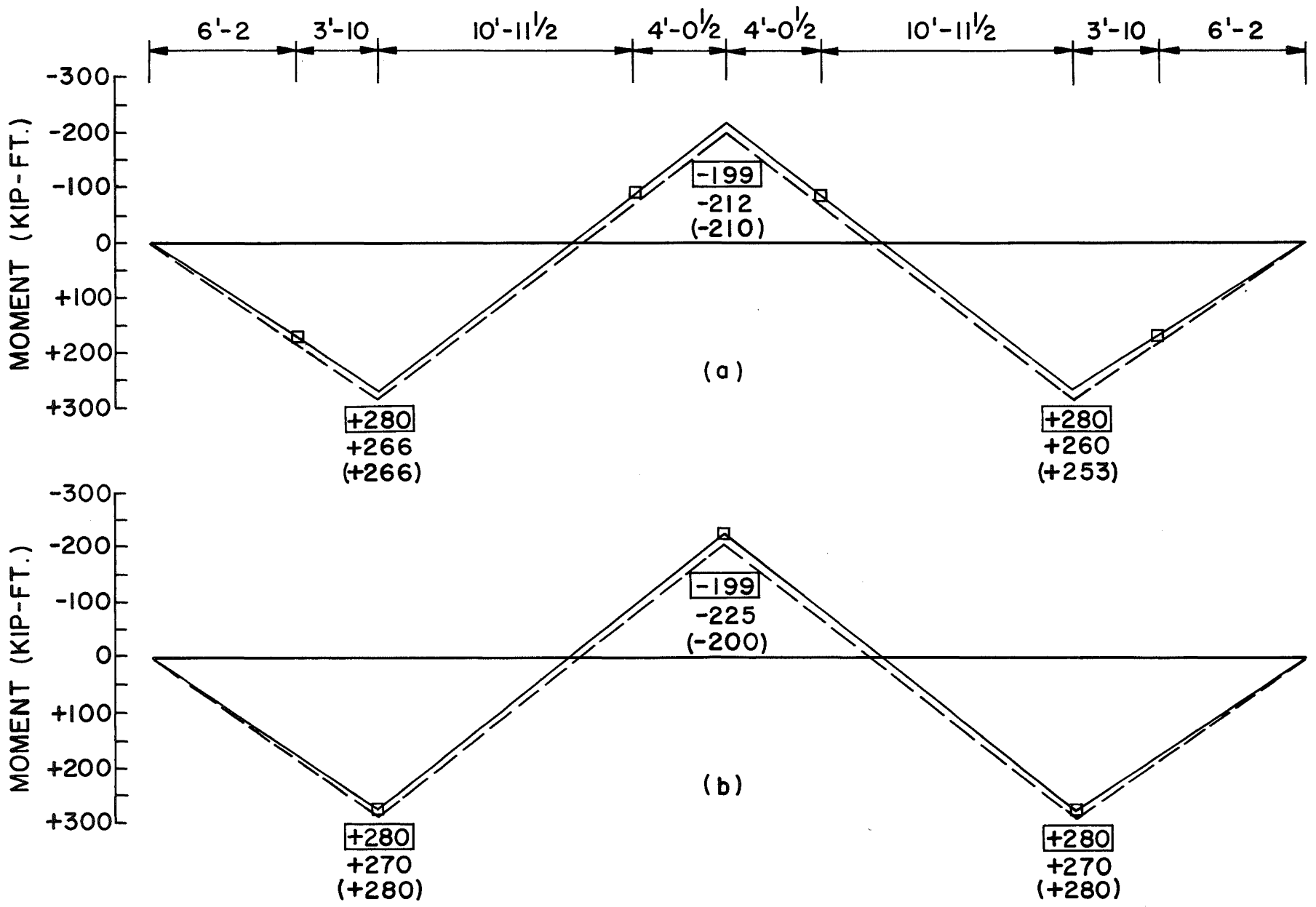

Fig. 35 Comparison of Computed and Measured Bending Moments for Beam CC-3S

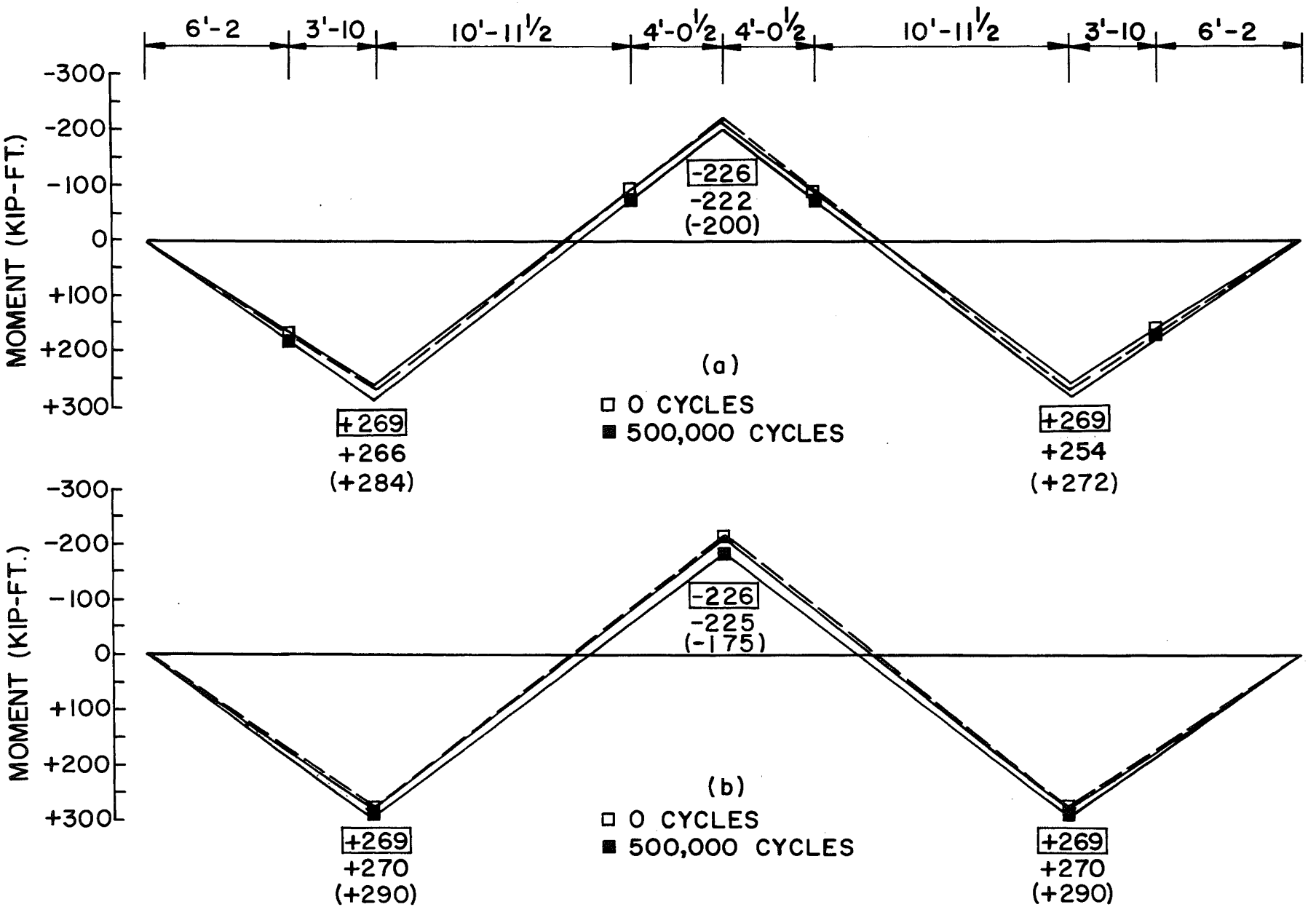

Fig. 36 Comparison of Computed and Measured Bending Moments for Beam CC-4S

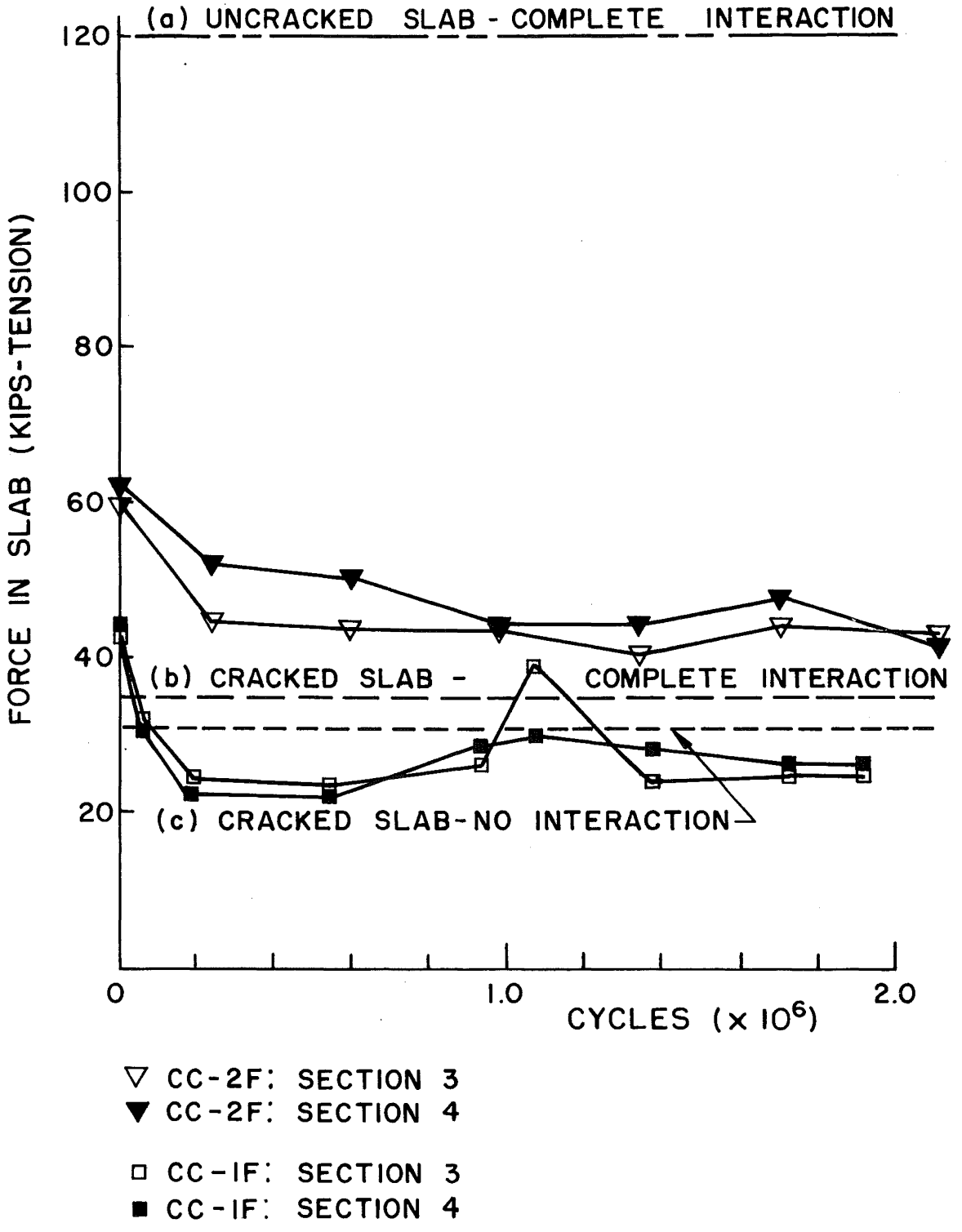

Fig. 37 Slab Force Near Center Support of Beams CC-1F and CC-2F

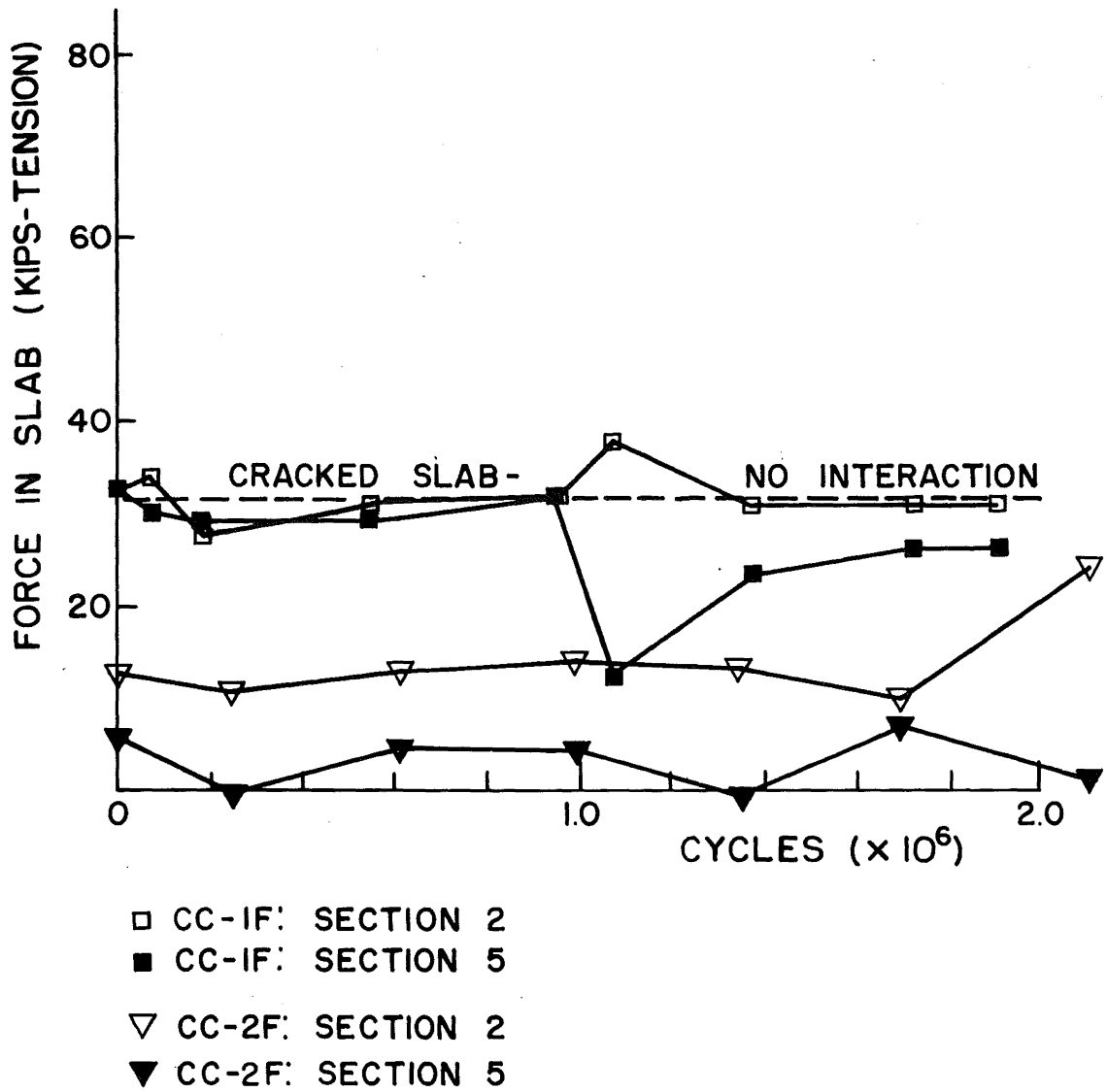

Fig. 38 Slab Force at Inflection Points of Beams CC-1F and CC-2F

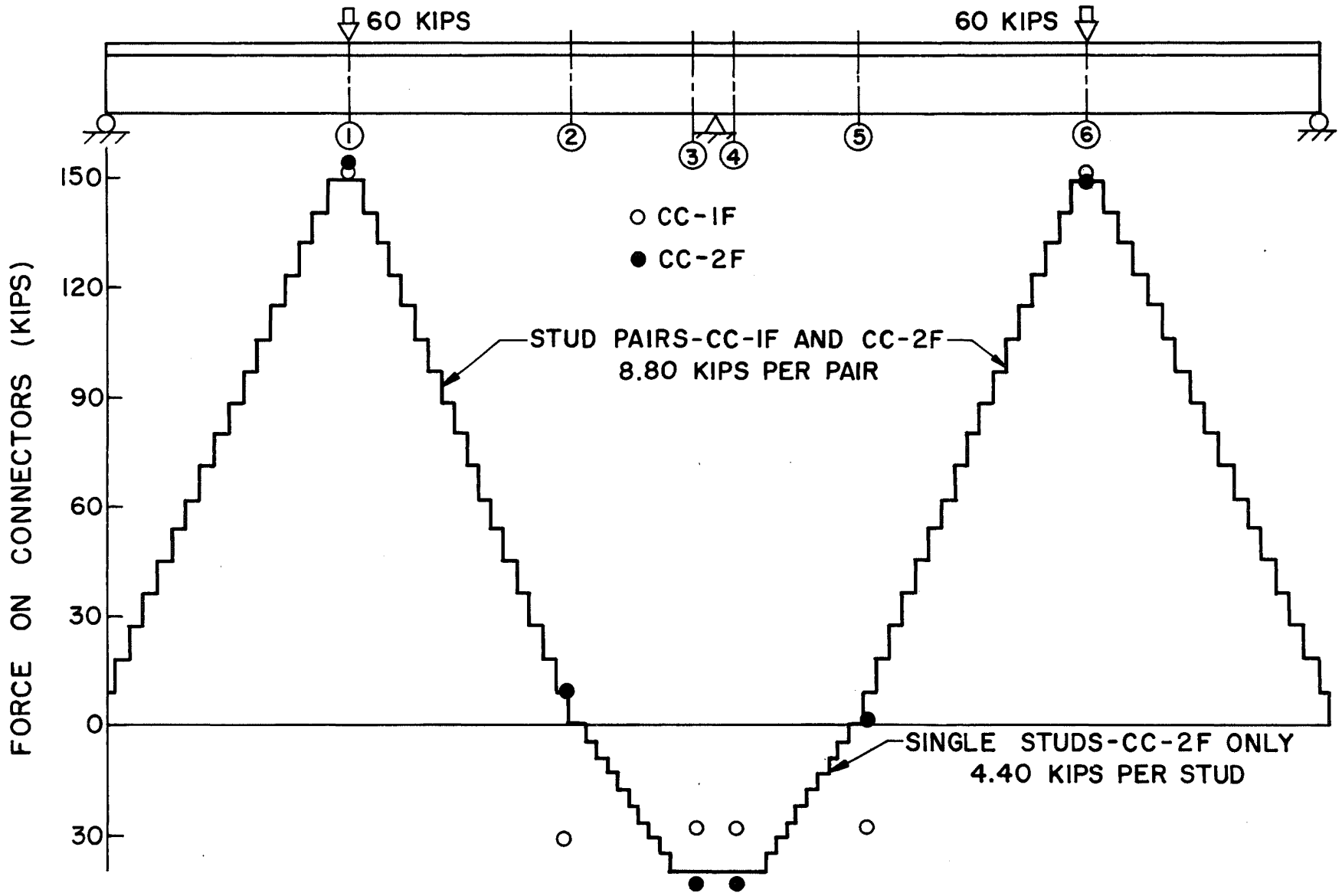

Fig. 39 Cumulative Resistance of Stud Shear Connectors on Beams CC-1F and CC-2F at 2,000,000 Cycles

324.39

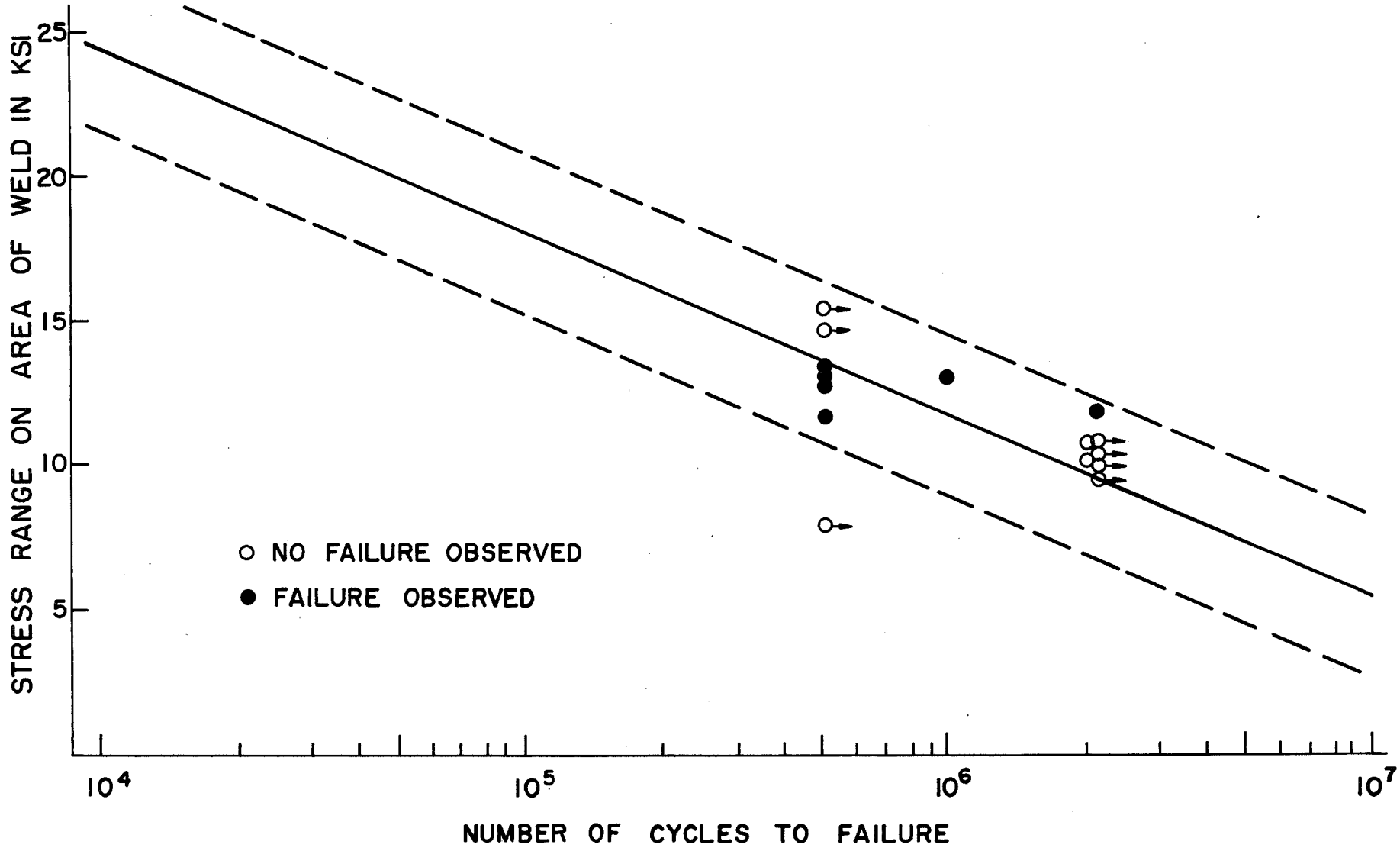

Fig. 40 Semi-Log Plot Stress Range vs. Cycle Life for all Beams

11. REFERENCES

1. Slutter, R. G., and Fisher, J. W.
   A PROPOSED PROCEDURE FOR THE DESIGN OF SHEAR CONNECTORS IN COMPOSITE BEAMS, Fritz Engineering Laboratory Report No. 316.4, March 1966

2. Toprac, A. A.
   FATIGUE STRENGTH OF 3/4-INCH STUD SHEAR CONNECTORS, Highway Research Record No. 103, Highway Research Board, 1965 pp. 53 - 77

3. King, D. C., Slutter, R. G., and Driscoll, G. C.
   FATIGUE STRENGTH OF ½-INCH DIAMETER STUD SHEAR CONNECTORS, Highway Research Record No. 103, Highway Research Board, 1965 pp. 78 - 106

4. Siess, C. P., Viest, I. M., and Newmark, N. M.
   STUDIES OF SLAB AND BEAM HIGHWAY BRIDGES, PART III, SMALL SCALE TESTS OF SHEAR CONNECTORS AND COMPOSITE T-BEAMS, University of Illinois, Engineering Experiment Station, Bulletin No. 396, Urbana, Illinois. 1952

5. Slutter, R. G., and Fisher J. W.
   FATIGUE STRENGTH OF SHEAR CONNECTORS, Highway Research Record No. 147, Highway Research Board, 1966, pp. 65 - 88

6. STANDARD SPECIFICATIONS FOR HIGHWAY BRIDGES, Ninth Edition by American Association of State Highway Officials, Washington, D.C. 1966

7. Viest, I. M., Fountain, R. S., and Siess, C. P.
   DEVELOPMENT OF THE NEW AASHO SPECIFICATIONS FOR COMPOSITE STEEL AND CONCRETE BRIDGES, Highway Research Board, Bulletin 174, 1958

8. Siess, C. P., and Viest, I. M.
   STUDIES OF SLAB AND BEAM HIGHWAY BRIDGES: V: TESTS OF CONTINUOUS RIGHT I-BEAM BRIDGES, Bulletin No. 416, University of Illinois Engineering Experiment Station, 1953

9. Slutter, R. G., and Driscoll, G. C.
   FLEXURAL STRENGTH OF STEEL-CONCRETE COMPOSITE BEAMS, Journal of the Structural Division ASCE, Vol. 91, No. ST2, April 1965

10. Barnard, P. R., and Johnson, R. P.
PLASTIC BEHAVIOR OF CONTINUOUS COMPOSITE BEAMS, Proceedings, Institution of Civil Engineers, Vol. 32, October 1965, pp. 161 - 179

11. Johnson, R. P., VanDalen, K., and Kemp, A. R.
ULTIMATE STRENGTH OF CONTINUOUS COMPOSITE BEAMS, Progress Report, British Constructional Steelwork Association Conference, September 1966

12. Appendix C-Welding and Inspection of Stud Shear Connectors.
RECOMMENDATIONS FOR THE DESIGN AND CONSTRUCTION OF COMPOSITE BEAMS AND GIRDERS FOR BUILDINGS. Report of the Joint ASCE-ACI Committee on Composite Construction, 1966

13. U.S. Department of Commerce - Bureau of Public Roads.
TENTATIVE CRITERIA FOR ULTIMATE STRENGTH DESIGN OF REINFORCED CONCRETE HIGHWAY BRIDGES, 1966

14. Daniels, J. H., and Fisher, J. W.
STATIC BEHAVIOR OF CONTINUOUS COMPOSITE BEAMS, Fritz Engineering Laboratory Report 324.2, in preparation.